THE ROLE OF THE hGRB14 ADAPTOR PROTEIN BPS DOMAIN IN INSULIN SIGNALING

BY

SHERRIE KELLY

A Thesis
Submitted to the Faculty of Graduate Studies
In Partial Fulfillment of the Requirements for the Degree of

MASTER OF SCIENCE

Department of Biochemistry and Medical Genetics
University of Manitoba
Winnipeg, Manitoba

THE UNIVERSITY OF MANITOBA

FACULTY OF GRADUATE STUDIES

*****

COPYRIGHT PERMISSION PAGE

The Role of the hGrb14 Adaptor Protein BPS Domain in Insulin Signaling

BY

Sherrie Kelly

A Thesis/Practicum submitted to the Faculty of Graduate Studies of The University of Manitoba in partial fulfillment of the requirements of the degree of

MASTER OF SCIENCE

TABLE OF CONTENTS

LIST OF FIGURES

LIST OF TABLES

LIST OF ABBREVIATIONS

3-AT	3-Amino-1,2,4-triazole
aa	Amino acid(s)
Ab	Antibody
AD	Activating domain
BD	Binding domain
β-ME	Beta-mercaptoethanol
BSA	Bovine serum albumin
bp	Base pair(s)
CIP	Calf-intestinal alkaline phosphatase
dATP	Deoxyadenosine triphosphate
dCTP	Deoxycytosine triphosphate
dGTP	Deoxyguanosine triphosphate
dNTP	Deoxynucleotide triphosphate
dTTP	Deoxythymidine triphosphate
ddH_2O	double distilled water
DNA	Deoxyribonucleic acid
E. coli	*Escherichia coli*
EDTA	Ethylene diaminetetraacetic acid
EtBr	Ethidium bromide
F	FLAG epitope tag
FCS	Fetal calf serum
g	Earth's gravitational constant
Grb	Growth factor receptor bound
IR	Insulin receptor
GAL4	Galactose 4
GAL4AD	GAL4 Activation Domain
GAL4bD	GAL4 Binding Domain
HIS	Histidine
hGrb14	human (*Homo sapien*) Growth factor receptor bound 14
LB	Luria Bertani
LEU	Leucine
LiAc	Lithium acetate
MCS	Multiple cloning site
mGrb14	mouse (*Mus musculus*) Growth factor receptor bound 14
ONPG	Ortho-nitrophenyl β-D-galactopyranoside
PBS	Phosphate buffered saline
PCR	Polymerase chain reaction
pTyr	phosphorylated Tyrosine
rGrb14	rat (*Rattus norvegicus*) Growth factor receptor bound 14
RPM	Revolutions per minute
S. cerevisiae	*Saccharomyces cerevisiae*
SC-	Synthetic complete omission media

TRP	Tryptophan
TBS-T	Tris-HCl buffered saline-tween-20
X-gal	5-Bromo-4-chloro-3-indolyl-β-D-galactopyranoside

ACKNOWLEDGMENTS

From the onset, I have felt very fortunate to study in Dr. Barbara Triggs-Raine's laboratory, Barb, as she insisted I call her from day one. The experience has been invaluable, I learnt about the intricacies of a biochemistry and medical genetics laboratory while being encouraged to explore other avenues of science. I would like to express my sincere gratitude to Barb for providing the opportunity to learn and develop as a scientist in her lab. Thank you for your constant support, guidance, and encouragement. I could always count on a smile from you when I walked into your office and you always made me feel like a priority in your busy schedule.

I would like to thank the members of the Triggs lab, both past and present; Tammy, Rick, Tim, Brandy, Ketan, and Dianna, for sharing your time and knowledge and for providing training in the theoretical and technical aspects of research. Thanks for your genuine concern for the success of my research project. Thanks Rick for teaching me about the protein world. A warm thank you to Tammy for sharing in the journey toward our MSc. degrees, for being such a great workout partner, and for your friendship, which I will always cherish. Thank you to the members of the lab for your support in and outside the lab, it has been a privilege to know you.

Thank you to committee members, Dr. Grant Hatch and Dr. Gilbert Arthur, for their guidance and interest in the success of my project. Thanks to Dr. Dan Gietz and lab for assistance with the yeast two-hybrid system. I'd also like to thank the students, faculty and staff of the Biochemistry and Medical Genetics department for sharing their knowledge and resources.

Thank you to my parents, Josie and Gary Kelly who have taught me the meaning of hard work and dedication, and taught me to take pride in everything I do. Thank you for cultivating the belief that I could do anything I set my mind to and for believing in me and supporting me unconditionally.

To Nick, my boyfriend, my soul mate, thank you for your everlasting support, I am blessed to have the chance to share my dreams with yours. You've made the goals I'm striving towards seem more meaningful and the successes more rewarding. You have shown me what *really matters* in life. Your strength, perseverance, and inner beauty are an awesome inspiration.

I have learnt that I have much more to learn and look forward to continuing my studies. I was given the opportunity to attend the Canadian Bioinformatics Workshop during my MSc studentship, which has been a jumping off point for my future research career in Bioinformatics and Proteomics.

Wishing you all the happiness and peace, I feel in my heart.
Best regards,
Sherrie

Funding for this research has been provided by an MHRC studentship.

ABSTRACT

Human Growth factor receptor bound 14 (hGrb14) belongs to the Grb7 protein family, which is comprised of Grb7, Grb10, and Grb14. These proteins share common structural features including a conserved proline-rich N-terminal sequence, a central PH (Pleckstrin Homology) domain, a newly described intermediate BPS (between PH and SH2) domain, and a C-terminal SH2 (Src Homology 2) domain. The presence of SH2 and PH domains and the apparent absence of catalytic domains in these proteins led to their classification as adaptor proteins. These proteins may function in connecting signaling molecules to receptors or to other molecules in the signaling pathway. Indeed we, and others, have identified hGrb10 and hGrb14 as binding partners of the insulin receptor (IR), but the role of these proteins in insulin signaling is unknown. The SH2 domain of hGrb14 plays a role in this interaction, but the involvement of the newly described BPS domain in the interaction with the IR remains to be elucidated. In order to determine if the BPS and SH2 domains work independently or in concert, and how they affect insulin signaling, we created wild-type and mutant, full-length and sub-domain hGrb14 constructs. These were tested for interaction with insulin receptor using the yeast-two-hybrid system and cell culture based studies. The BPS plus SH2 domain fusion protein had a seven fold greater binding affinity to the IR than the SH2 domain alone, indicating that the BPS domain plays an important role in the ability of hGrb14 to bind to the IR. We identified a key residue in the BPS domain (R387Q) that when mutated significantly reduced the ability of hGrb14 to bind the IR. Mutation of the BPS domain residue, R387Q, and the SH2 domain residue, R466Q, abrogated the hGrb14-IR interaction in the yeast two-hybrid system and in cell culture.

1. INTRODUCTION

1.1. Diabetes mellitus

Diabetes mellitus is a chronic metabolic disorder affecting approximately 5% of the world population [1]. This condition is characterized by high levels of blood glucose which can lead to severe complications including heart disease, kidney failure, blindness, stroke, neuropathy, hypertension, hypertriglyceridemia, ketoacidosis, and even premature death [2]. The prevalence of diabetes, along with its associated pathologies, makes this disorder a major health concern. Diabetics have either a deficiency in insulin production, called type 1 or Insulin Dependent Diabetes mellitus [IDDM] or a reduced effectiveness of insulin activity at its receptor sites, referred to as type 2 or Non-Insulin Dependent Diabetes mellitus [NIDDM]. The latter accounts for the majority of diabetic cases and is therefore a major focus of research.

Type 1 diabetes is the most severe form of the disease and accounts for 5-10% of cases. Although its occurrence is common in childhood, it may also occur in adults. In this form of the disease, there is an insulin deficiency due to the destruction of insulin producing pancreatic β-cells, which can be caused by genetic, autoimmune, and/or environmental factors. Type 2 diabetes, a more clinically heterogeneous form of the disease, accounts for 90-95% of diabetic cases. This condition is often called adult onset diabetes, as symptoms generally appear at approximately 40 years of age [3]. Type 2 diabetes, characterized by an endogenous resistance to the actions of insulin is thought to result from the development of post-receptor signalling defect(s). This polygenic, multifactorial disease is associated with several factors including diet, weight, physical activity, and age. In both forms of diabetes treatment is aimed at regulating blood glucose levels by controlling diet. The administration of exogenous insulin is most often

used to moderate glucose levels in the case of type 1 diabetes, while drugs that potentiate the secretion or action of insulin are used in the case of type 2 diabetes.

1.2. Insulin

Insulin is synthesized by pancreatic β-cells as a long single-chain molecule (preproinsulin). This is then cleaved and folded (proinsulin), and lastly the connecting C peptide is removed to yield the 51-amino acid double-chain polypeptide that is released into the bloodstream [4]. In response to high blood glucose levels, insulin is released from the pancreas into the bloodstream where it is bound by receptors on insulin sensitive tissues including skeletal muscle, adipose, and liver tissue. When bound to its cell surface receptor, insulin mediates actions such as glucose uptake, inhibition of hepatic gluconeogenesis, as well as stimulation of glycogen synthesis and lipogenesis [5]. Overall, insulin has effects on protein and fat metabolism, as well as on protein, RNA, and DNA synthesis, acting therefore to regulate metabolic homeostasis, cell growth, and death. Clearly, when normal insulin function is compromised, many important anabolic and catabolic cellular functions are disrupted.

1.3. Insulin receptor

The insulin receptor is a 480 kDa heterotetrameric glycoprotein composed of α and β subunits that are linked by disulfide bonds (Fig. 1)[6]. The IR differs from most other tyrosine kinase receptors because it exists in the dimeric state in the absence of ligand. The structure of the receptor consists of two extracellular α-subunits linked by disulphide bonds to two β-subunits. The IR β-subunits are composed of a small extracellular region, a transmembrane domain,

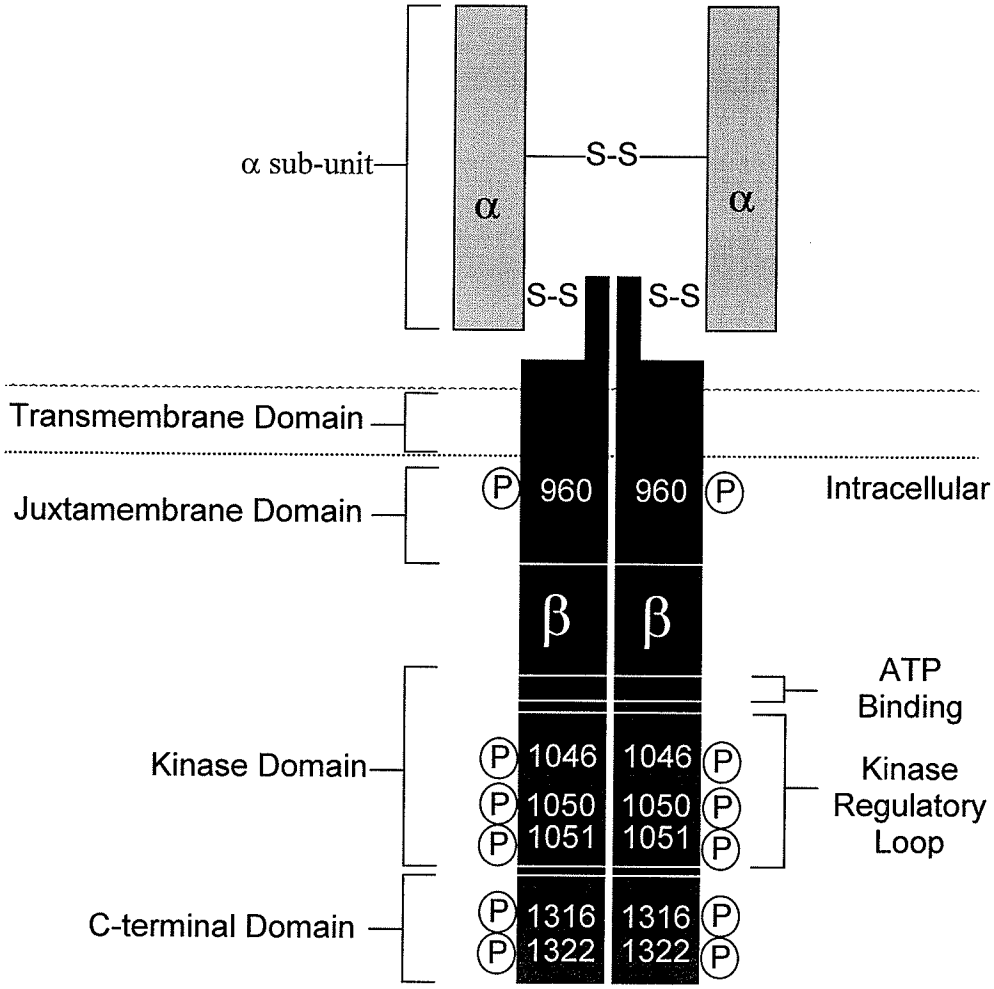

Figure 1. Diagram of the structure of the IR. The IR is a heterotetrameric protein consisting of two α-subunits (grey) covalently linked by disulphide bonds (S-S) to each other and to two β-subunits (black). The β-subunits consist of a small extracellular region and an intracellular region, which is divided into transmembrane, juxtamembrane, kinase, and C-terminal domains. Several tyrosine residues undergo autophosphorylation, including: Y960, Y1046, Y1050, Y1051, Y1316, and Y1322.

and a cytoplasmic domain that contains four functional regions: the juxtamembrane region, the kinase catalytic region, a central regulatory loop, and a C-terminal region. The gene encoding the IR is located on chromosome 19 [7], and is widely expressed in mammalian tissues, however, the receptor is most prevalent in tissues instrumental in glucose metabolism, namely the liver, kidney, skeletal muscle, and fat tissues [8]. Upon insulin stimulation, the IR becomes autophosphorylated on β-subunit tyrosine residues in the juxtamembrane region (Tyr953 and Tyr960), in the kinase regulatory loop (Tyr1046, Tyr1050, and Tyr1051), and in the C-terminal region (Tyr1316 and Tyr1322). Once phosphorylated, the IR activates several complex signaling pathways.

1.4. Insulin signaling pathway

To understand the mechanism by which insulin controls glucose metabolism, as well as the pathogenesis of type 2 diabetes, it is critical to understand the signaling pathways downstream of the IR. Upon insulin binding, the IR becomes autophosphorylated on tyrosine residues within its kinase domain. The activated receptor recruits and phosphorylates downstream signaling proteins resulting in the initiation of a signal transduction cascade [8]. The ultimate outcome of insulin signaling in the cell depends on which effector molecules are expressed and recruited to the active receptor and which pathways are activated as a result [9]. The recruitment and activation of many signaling proteins is mediated by their Src homology (SH2) domains [10]. The activated tyrosine kinase domain of the IR recruits SH2 domain-containing proteins including the IR substrate (IRS) and the Src-homology-collagen-like protein (Shc) (Fig. 2). Activated IRS and Shc in turn activate the SH2 domain-containing adaptor protein Grb2. Grb2 is constitutively bound

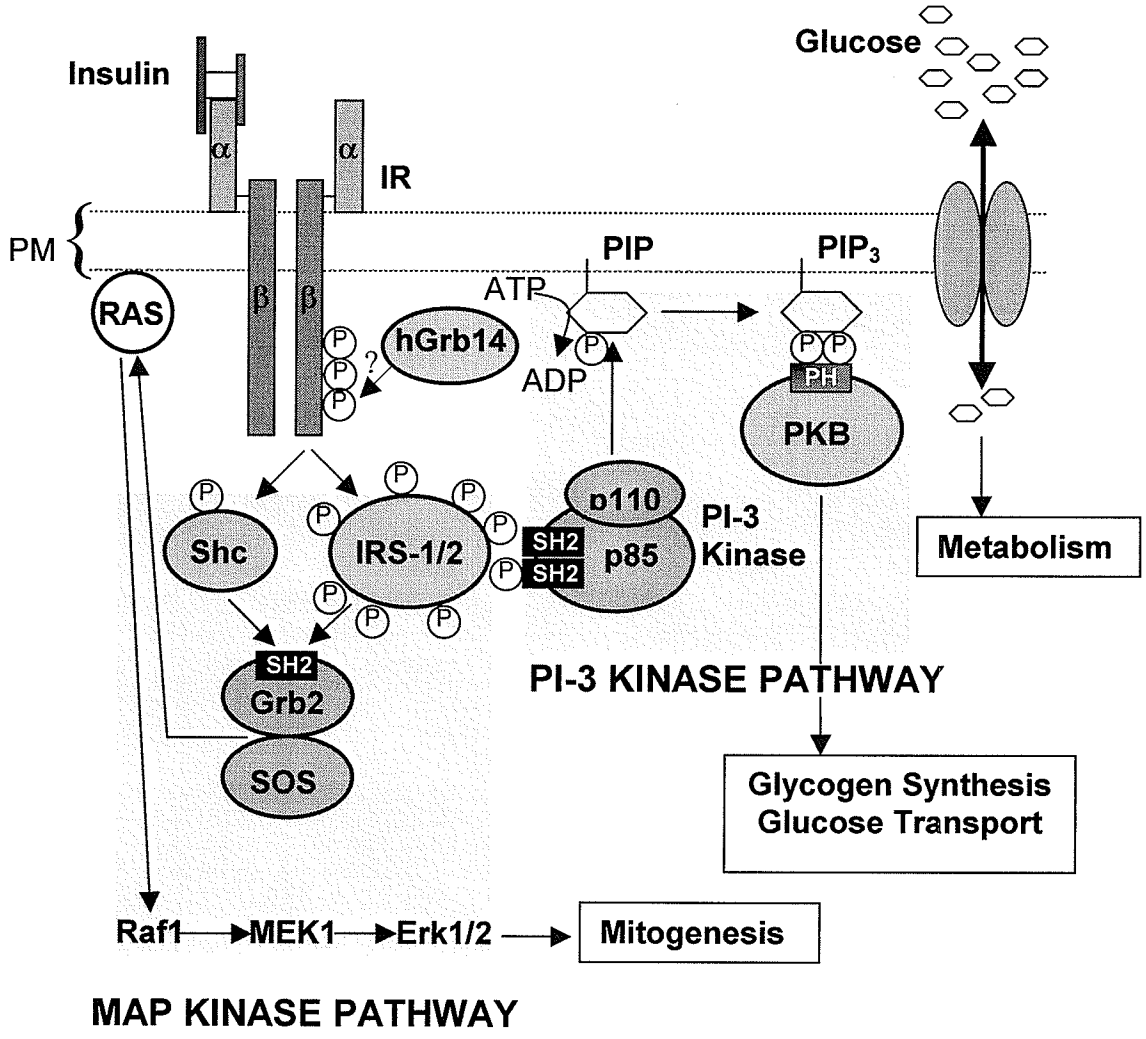

Figure 2. **Overview of the insulin signaling pathway**. Insulin binds to the α-subunit of the IR triggering auto-phosphorylation (P) of the intracellular tyrosine kinase domain of the adjacent covalently linked β-subunit. Downstream signaling proteins are recruited to the activated receptor and become phosphorylated by the activated kinase domain which leads to a cascade of signaling events, including the activation of the MAP Kinase and PI 3-Kinase pathways.

by the GTP exchanger protein, Sos, which in turn becomes activated in conjunction with Grb2 [11]. The continuing cascade of reactions includes SOS activation of the Ras protein at the plasma membrane. Ras, a potent activator of the MAP kinase pathway, can then induce a sequential activation of Raf, MEK, and Erk-1/2 proteins, which ultimately stimulate gene transcription. Although both the IRS and Shc molecules can function to stimulate the MAP kinase pathway, several reports indicate that Shc is indeed the main signaling molecule of this pathway [12].

Another signaling pathway activated by the insulin ligand is the phosphoinositide 3-kinase (PI3-K) pathway, which functions to carry out downstream metabolic signal transduction events [13]. Although the PI3-K pathway is separate from the MAP kinase pathway, both can be activated by the IRS. The phosphorylated IRS recruits the p85 subunit of the PI3-K protein through its SH2 domain. The activated p85 subunit in turn activates the p110 subunit of the PI3-K protein [14]. The activated PI3-K can then phosphorylate membrane bound phosphatidylinositol phospholipids (PIP) to yield PIP_3 [15] a secondary messenger that activates protein kinase B (PKB) through interactions with its PH domain. Activated PKB targets proteins involved in glucose-uptake and glycogen and protein synthesis [9] [16]. This explanation of the insulin signaling pathway represents a brief overview. Below, individual components of the insulin signaling cascade are discussed, with specific emphasis on the Grb family of proteins which are the focus of this research.

1.5. Proteins interacting with the IR

Type 2 diabetes is associated with signaling defects downstream of the IR. In our work we were interested in molecules that acted in first response to the activated receptor. IR substrate (IRS) proteins convey signals from the activated IRs to downstream effector molecules. Four mammalian IRS proteins have been identified and their roles have been analyzed using transgenic and/or knockout mice. IRS-1, encoded on chromosome 2q36-37, acts in response to insulin action in muscle and adipose tissue, and is primarily involved in somatic cell growth [17], whereas IRS-2 carries out its functions in the pancreas. liver, brain, and reproductive organs to regulate β-cell survival and growth, [18]. The precise roles of IRS-3 and IRS-4 are still under investigation and will not be further discussed in this study [19;20].

In addition to the IRS and Shc signaling proteins, several other proteins have been shown to bind to the activated IR. PSM/SH2-B is phosphorylated on tyrosine residues by the activated IR and carries out stimulation of mitogenesis [21;22]. Another binding partner of the IR is the APS (adaptor protein with a PH and SH2 domain), which is expressed in insulin-sensitive tissues. APS is a strong binding partner of the IR, and once bound, is phosphorylated on several tyrosine residues [23]. The APS and PSM proteins are both members of the tyrosine kinase adaptor protein family and share similar structural features including an N-terminal proline rich domain, a central PH domain, and a C-terminal SH2 domain [24]. Interestingly, there is another family of adaptor proteins that are structurally similar to APS and PSM, called the Grb7 family of adaptor proteins.

1.6. Grb7 family of adaptor proteins

Grb7 family adaptor molecules consist of Grb7, Grb10, and Grb14. Each member of the Grb7 family was originally identified using the CORT (Cloning of receptor targets) technique, [25] in which cDNA expression libraries were screened with the tyrosine phosphorylated C terminus of the epidermal growth factor receptor (EGFR) [26-28]. The Grb7 family members do not exhibit measurable enzymatic activity and are therefore believed to act as adaptor proteins in signaling pathways [29]. Members of this family contain conserved protein modules known to mediate protein:protein and protein:lipid interactions that include an amino-terminal proline rich motif (PS/AIPNPFPEL), an internal PH (Pleckstrin Homology) domain, a newly characterized BPS (Between Pleckstrin and Src Homology) domain, and a carboxyl-terminal SH2 (Src Homology 2) domain (Fig. 3). Although it is not well documented, an internal RA (Ras association) domain has also been described for this family of adapter proteins, however, it will not be discussed further in this work [30]. Grb7 proteins differ in their growth factor receptor and binding partner affinities, providing potential for specificity in their signaling. The binding specificity of Grb7 proteins is largely determined by the sequences surrounding the phosphotyrosines of the SH2 domain [31] and these proteins appear to function in a tissue-specific manner linking certain receptor tyrosine kinases to signaling proteins.

1.6.1. Growth factor receptor bound-7 (Grb7)

Grb7 was the first member of the Grb7 family of adaptor proteins to be described [26]. The human *GRB7* gene is located on chromosome 11 [32] and is highly expressed in pancreas, kidney, prostate, small intestine, and placenta [33]. In mammalian cells, Grb7 interacts

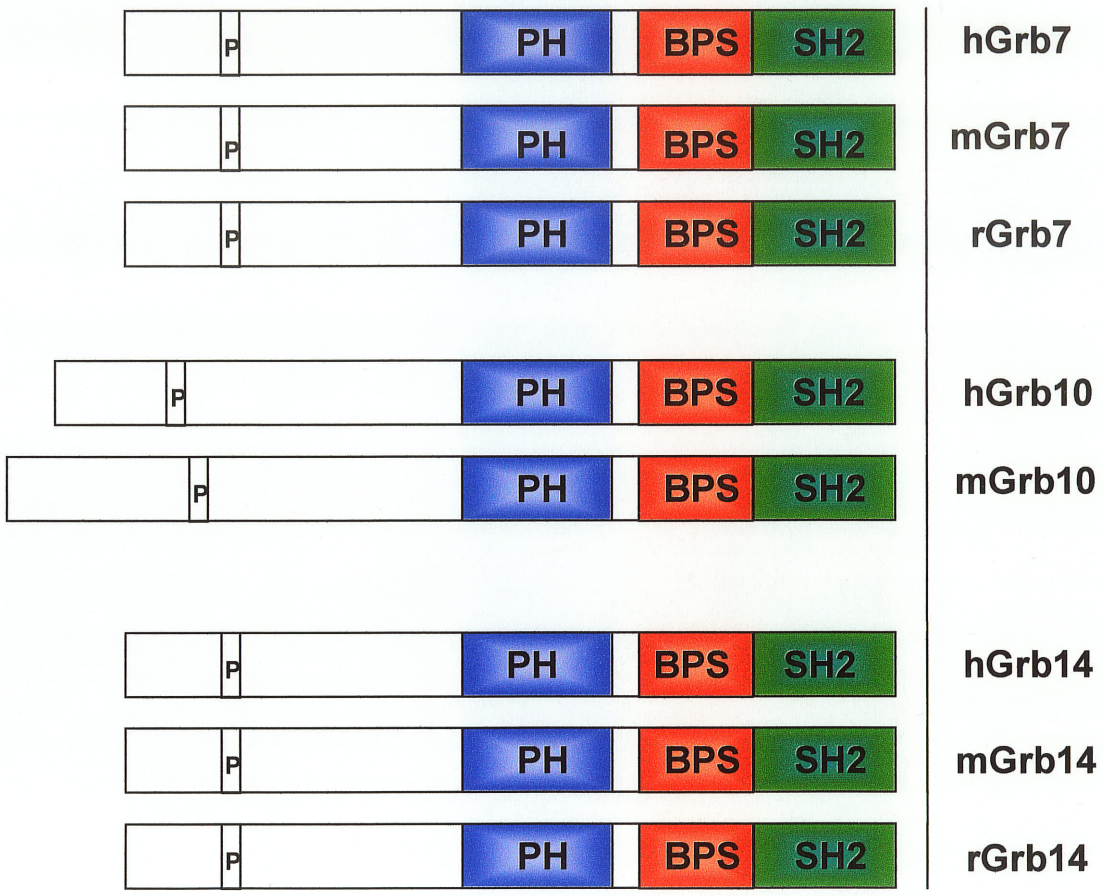

Figure 3. Diagram of the structure of the Grb7 protein family. All members of the Grb7 family of proteins contain the following conserved modules: an N-terminal conserved (P(S/A)IPNPFPEL) region shown as a hollow black box, the PH (Pleckstrin Homology) domain in blue, the BPS (Between PH and SH2) domain in red, and the SH2 (Src Homology 2) domain in green.

with the tyrosine receptors EGFR, HER2 [33], RET (Receptor Tyrosine Kinase) [34], erbB3/4 [35], platelet derived growth factor receptor (PDGFR) [28], and the IR. Although Grb7 binds the activated IR, it is not phosphorylated by the tyrosine kinase activity of the receptor [36]. Grb7 has also been reported to interact with other signaling proteins, including Shc [33] and SHPTP2, an SH2-containing tyrosine phosphatase [37]. Grb7 has been found to regulate cell migration and has also been implicated in tumour progression, but its specific mechanism of action is unknown [38;39].

1.6.2. Growth factor receptor bound-10 (Grb10)

Grb10 is the second member of the Grb7 family of proteins to be discovered. The human homologue of Grb10 was mapped to 7p11.2-7p12 [40] [41] and is highly expressed in skeletal muscle, pancreas, heart, and brain tissue. Like Grb7, Grb10 has been shown to interact with several tyrosine kinases including EGFR, RET [42], PDGFR [43], and the IR [44] [45], but unlike Grb7, Grb10 also interacts with the IGFR-1 (insulin-like growth factor receptor) [44;46]. Grb10 proteins are phosphorylated on serine residues by activated insulin, EGF, PDGF, and FGF (fibroblast growth factor) receptors [27]. Grb10 has been shown to undergo tetramerization in mammalian cells [47] and also interacts with MAP kinase pathway signaling molecules, Raf1 and MEK1 [48]. Other Grb10 binding partners were reported, such as an *in vitro* interaction with Nedd4 [49], Tec tyrosine kinase [50], and Bcr-Abl [51].

The function of Grb10 remains controversial. Overexpression of Grb10 has been reported to have a stimulatory role in insulin signaling [52], specifically in stimulation of DNA synthesis

[53]. However, other groups who have overexpressed Grb10 reported inhibition of IR signaling [44]. Consistent with all of these findings was that Grb10 inhibited phosphorylation of IRS and PI 3-kinase activity was reduced. When the BPS domain of Grb10 was overexpressed it was shown to inhibit insulin stimulated mitogenesis [43;54].

1.6.3. Growth factor receptor bound-14 (Grb14)

In this work we focused on studying the function of Grb14, the newest member of the Grb7 family of proteins. The human *GRB14* gene maps to chromosome 2q22-24 [55] and encodes a 540 amino acid protein with a molecular mass of 58 kDa. hGrb14 is highly expressed in liver, kidney, pancreas, and the ovaries; it is expressed to a lesser extent in the heart and skeletal muscle, and is present at low levels in the placenta, brain, heart, small intestine, and colon [28]. The sub-cellular localization of hGrb14 is currently unknown, however it is assumed to be cytoplasmic. Phosphoamino acid analysis of human Grb14 (hGrb14) indicates that it is phosphorylated on serine residues in response to growth factor stimulation [28]. Furthermore, Hemming *el al* have shown that hGrb14 interacts directly with the activated IR in a yeast two-hybrid system model and in CHO-IR cells overexpressing hGrb14. This result was also detected with the rat homologue of Grb14 (rGrb14) which was shown to bind the IR *in vivo* [56]. Grb14 also interacts with other receptor tyrosine kinases, including IGFR-1 [57], FGFR [58], and Tek/Tie2 receptors [59]. Recently, tankyrase, a mitogen-activated protein kinase substrate involved in Golgi vesicle trafficking was shown to interact with Grb14 using a two-hybrid screen [60].

In this study, we were interested in the mechanism by which the hGrb14 protein binds to the IR. Previously, it was established that the SH2 domain of human Grb14 plays an important role in IR binding [61]. The SH2 domain of rat Grb14 has also been shown to contribute significantly in IR binding. However, studies using rGrb14 suggested that the BPS domain alone mediated the Grb14-IR interaction [56] [62]. This is consistent with studies showing that both SH2 and BPS domains are involved in the Grb10-IR interaction [62]. Using the two-hybrid system and cell culture assays, we examined the role of the BPS and SH2 domains of hGrb14 in order to further elucidate the function of this protein in insulin signaling.

1.7. Objective

To characterize the role of the hGrb14 BPS and SH2 domains in insulin signaling.

1.8. Hypothesis

The BPS and SH2 domains function co-operatively in the interaction with the IR. These domains function in binding to the receptor to alter downstream signaling in the insulin signaling pathway.

1.9. Aims

A. To characterize the interaction between the hGrb14 BPS and SH2 domains and the IR.

B. To identify, by mutation experiments, key amino acid residues in the BPS domain that mediate its interaction with the IR.

C. To examine the roles of the hGrb14 BPS and SH2 domains in insulin signaling using BPS and SH2 mutation constructs.

2. MATERIALS AND METHODS

2.1. Reagents

Cell culture reagents were from Invitrogen (Burlington, ON) and restriction and modifying enzymes were from NEB (New England Biolabs) (Mississauga, ON) unless stated otherwise. Suppliers of specialty reagents are given in the appropriate methods section.

2.1.1. Antibodies

Table 1. Antibodies

Materials	Source	Location	Working Dilution
Actin [a]	Chemicon	Temecula, CA	1:5,000
Donkey anti-rabbit IgG	Amersham	Oakville, ON	1:10,000
FLAG [b]	Santa Cruz Biotechnologies	Santa Cruz, CA	1:2,500
Grb14 [b]	Santa Cruz Biotechnologies	Santa Cruz, CA	1:2,500
Goat anti-mouse	Jackson Laboratories	Avondale, PA	1:10,000
Insulin Receptor (IRβ) C-19 [b]	Santa Cruz Biotechnologies	Santa Cruz, CA	1:1,000
Insulin Receptor (IRβ) 29B4 [a]	Santa Cruz Biotechnologies	Santa Cruz, CA	-
Phosphotyrosine (pY99) [a]	Santa Cruz Biotechnologies	Santa Cruz, CA	1:5,000
GAL4AD [a]	Santa Cruz Biotechnologies	Santa Cruz, CA	1:2,500

[a] monoclonal
[b] polyclonal

2.1.2. Yeast strains

Yeast cells were grown and maintained using standard methods [63]. Yeast strains used in this study are listed below in Table 2.

Table 2. *S. cerevisiae* yeast strains

Strain	Genotype	Source
KGY37	*MATa, ade2, trp1-Δ901, leu2Δ-inv::pUC18, his3Δ-200, gal4Δ, gal80, ura3Δinv::GAL1-lacZ, lys2Δ-inv::GAL1-HIS3*	R.D. Gietz [64]
KGY94	*MATa, ade2, trp1-Δ901, leu2-3.112, his3Δ-200, gal80, gal4, ura3-52, leu2::pUC18, URA3::GAL1-lacZ, lys2::lexAop(x3)GAL1-HIS3*	R.D. Gietz [64]

2.1.3. Bacterial strains

The bacterial strain used in this study was *Escherichia coli* DH5α with genotype: F-, *recA*1, *endA*1, *gryA*96, *thi*, *supE*44, *relA*1, Δ(*arg lacZYA*) U169 (ϕ80d/*lacZ*ΔM15)λ-.

2.1.4. Oligonucleotides

Table 3. Oligonucleotides.

Oligonucleotide	Sequence
WPG79 (F)	5'-CCC AAG CTT ATG AGA AAG AAG CAG CCA GAT GGG C-3'
WPG80 (R)	5'-CCC AAG CTT TTA GGA AGG ATT GGA CCG AGG C-3'
WPG106 (R)	5'-G TGA ACT TGC GGG GTT TTT CAG TAT CTA CGA T-3'
WPG164 (F)	5'-ACC GCG ACC GTC TAG GCC TGT AT-3'
WPG170 (F) [a]	5'-TTT CTT GGT AC**A** GGA TAG TCA-3'
WPG171 (R)	5'-CTC TGA CTA TCC **T**GT ACC AAG AAA-3'
WPG172 (R)	5'-AGA GGT AGA AGC CCC AGA GGT GC-3'
WPG230 (F) [b]	5'-C GGG ATC CTG CAG CTG TAC CAG AAT TAT ATG-3'
WPG234 (R)	5'-CGG GAT CCG AAA CCA TGG CTG GGA CC-3'
WPG246 (F)	5'-CAG ATG TTT CTG AGT TCA AGC ACA-3'
WPG248 (R)	5'-ATT TTC TAT AAC TCT GCT TTT CTG G-3'
WPG251 (F)	5'-TTG TCA GCA GAC CTA TTT CCC AAA-3'
WPG252 (R)	5'-AG CAC TTC AAT CAC CAG TTC-3'
WPG279 (R)	5'-TAC CAA GAA AAC TCC ATC CAC AAG-3'
WPG294 (F)	5'-G CGA CAA TTG ATG CAG CTG TAC CAG AAT TAT ATG-3'
WPG295 (F)	5'-T TAT GTG TCA CTG GCA GGC AA-3'
WPG296 (F)	5'-A TCA CCT ATG **CA**A AGT ATA TCA GA-3'
WPG297 (R)	5'-TC TGA TAT ACT T**TG** CAT AGG TGA T-3'
WPG298 (F)	5'-C CAG AAA AGC **CA**A GT ATA GAA AA-3'
WPG299 (R)	5'-TT TTC TAT AAC T**TG** GCT TTT CTG G-3'
WPG311 (F)	5'-TGC AGT TCA CAG AGC ATA TCA CCT ATG-3'
WPG312 (F)	5'-ATG GAC TTC TCA GGC CAG AA**T G**GC -3'
WPG313 (F)	5'- GGA CTT GTG GAT GGA GTT TTC TT**T** GT-3'
WPG316 (R)	5'-GAG AGC AAT CCT AGC ACA ATA ATG-3'
WPG323	5'-G GAA TTC ATG ACC ACT TCC CTG CAA GAT GGG-3'
WPG324	5'-A ACC ATG CCA TGG GCC ACT TCT ACC TTG ATA TGG ATG-3'

[a] Substitutions are in bold letter(s).

[b] Non-complimentary sequences that generate restriction sites are underlined.

2.2. Transformation of *E. coli*

2.2.1. Preparation of electrocompetent cells

Electrocompetent cells were prepared by inoculating 250 mL of Low Salt LB medium (Appendix 6.3.1.2) with a 40 µL aliquot of previously prepared DH5α competent cells. The culture was grown at 37°C with aeration until the absorbance (OD_{600}) measured 0.5-1.0, usually 6-8 hours. After growth, the culture was cooled on ice and harvested by centrifugation at 3300x*g* for 15 min at 4°C. The cell pellet was washed once with 250 mL, and twice with a 125 mL volume of cold sterile ddH_2O. After each wash step, the cell pellet was collected by centrifugation (described above). The final cell pellet was resuspended in 5 mL of cold, filter-sterilized 10% glycerol. Cells were dispensed in 40 µL aliquots, frozen on dry ice, and stored at -80°C. The competency of the cells was determined by transforming 1 ng of pUC18 DNA (TA Cloning Kit, Invitrogen) into the cells by electroporation (Section 2.2.2). Following an overnight incubation, colonies were counted and the efficiency of the competent cells was calculated using the following equation:

$$(\text{colonies})(\text{vol. plated}[\mu L])\left(\frac{\text{ng of DNA}}{\text{vol. plated }[\mu L]} \times \frac{1\ \mu g}{1000\ ng}\right) = \text{colonies}/\mu g$$

Cells were considered highly competent when yielding 10^8–10^9 colonies/µg of DNA.

2.2.2. Electroporation

Plasmid DNA was introduced into *E. coli* cells by electroporation using an Electro Cell Manipulator 600 (BTX Inc., San Diego CA). A frozen 40 µL sample of electrocompetent cells was thawed on ice for 10 min and mixed with 1 µL of 1 ng/µL of plasmid DNA. The

mixture was then transferred into an ice-cold 1mm gap Electroporation cuvette and pulsed at 2.5kV, with 129 Ω. Cells were immediately resuspended in 960 μL of warm (37°C) SOC medium (Appendix 6.3.1.3) and incubated at 37°C for 60 min. Aliquots of 20, 100, and 200 μL from the transformation mixture were spread onto LB plates (Appendix 6.3.1.1) containing ampicillin (100 μg/mL) and incubated overnight at 37°C.

2.3. Preparation of plasmid DNA

Plasmid DNA was isolated using Mini, Midi, or Maxi Plasmid DNA Isolation Kits (Qiagen, Mississauga, Ontario). DNA was resuspended in sterile water and the concentration was determined by absorbance at 260 nm.

2.4. Polymerase chain reaction (PCR)

A standard PCR reaction consisted of template DNA, 200 μM dNTPs (equal mix of dATP, dCTP, dGTP, dTTP), 100 ng of each primer, 1x PCR Buffer containing 1.5 mM $MgCl_2$ (Invitrogen), and 5 U of Recombinant Taq Polymerase (Invitrogen) in a final volume of 100 μL. Reactions were overlaid with mineral oil and amplified using a PerkinElmer Cetus thermocycler with the following parameters: initial denaturation at 94°C for 3 min, 30 cycles of denaturation at 94°C for 1 min, annealing at T_m-5°C for 1 min, and elongation at 72°C for 1 min/1 Kb of nucleotides to be amplified. Reaction products were kept on ice or stored at -20°C until ready for analysis.

Mutations were introduced into the hGrb14 constructs using a PCR-based site directed mutagenesis method [65]. Refer to Fig. 4A, for a schematic representation of PCR-based site directed mutagenesis.

2.4.1. PCR-based mutation detection

Mutation in the hGrb14 BPS and SH2 domains R369Q and R387Q, as well as R466Q, respectively, (Section 3.1.8) were detected using a PCR-based strategy. To screen for the desired mutations, relevant regions from the plasmids were amplified by PCR using specific primers and products were digested with a restriction enzyme that only cut in the presence of the mutation. The digested PCR products were separated on 12% polyacrylamide gels, stained with EtBr, and visualized using a UV transilluminator. The R369Q mutation was detected after amplification with primers WPG311/WPG279 and digestion with the *Hpy*CH4V restriction endonuclease. The 317 bp amplification product was digested to a 291 bp fragment only if the R369Q mutation was present. Similarly, the R387Q mutation was detected using the forward mutant primer WPG312 and the reverse primer WPG279. Digestion of this 260 bp amplification product with *Msc*I produced a 237 bp fragment only if the R387Q mutation was present. For detection of the R466Q mutation, forward mutant (WPG313) and reverse (WPG316) primers were used to amplify a 251 bp product. Digestion of this product using *Bsr*GI produced a 227 bp fragment only if the R466Q mutation was present. See Fig. 4B for a schematic diagram outlining the PCR-based mutation detection method.

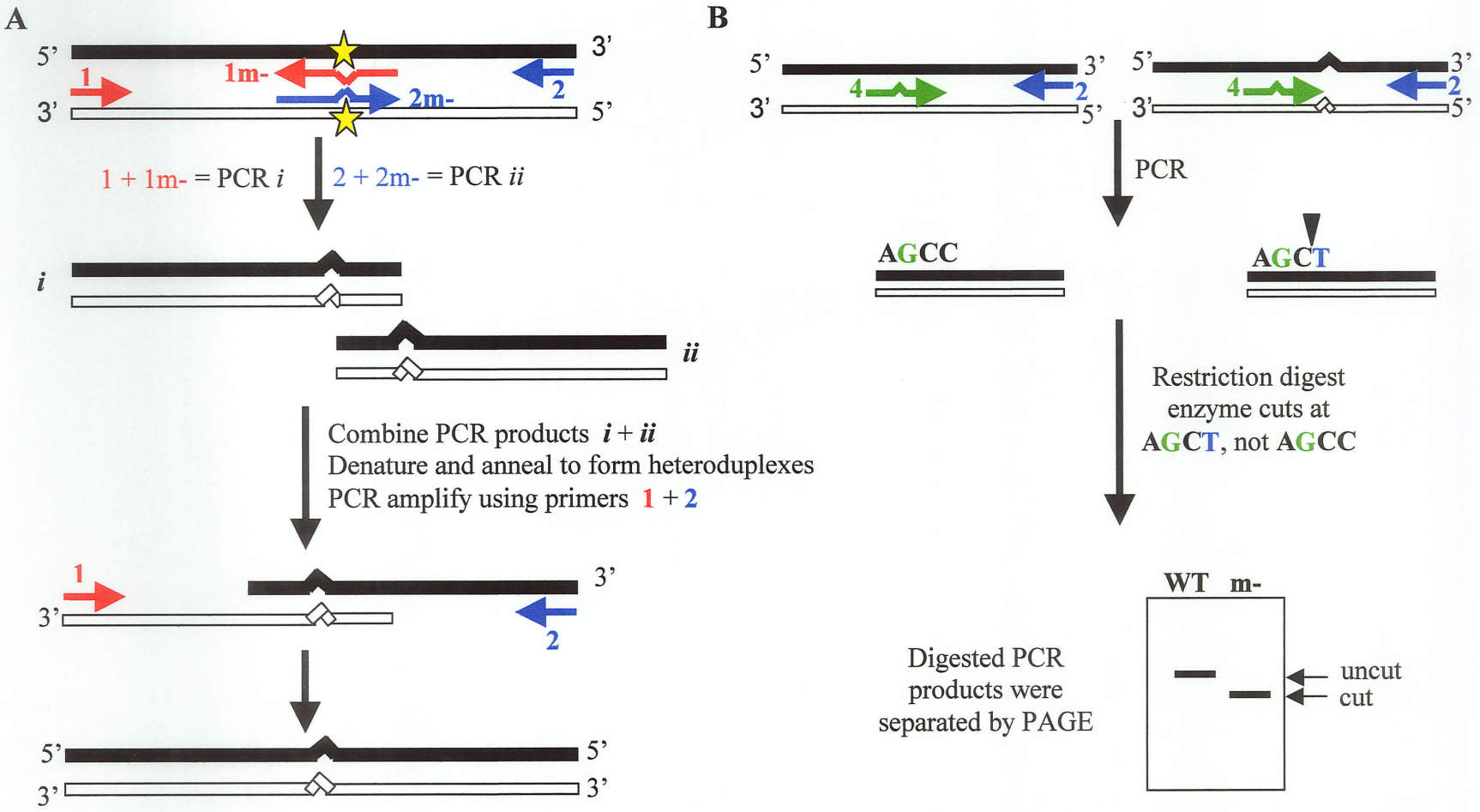

Figure 4. Diagram depicting the PCR-based site directed mutagenesis and PCR-based mutation detection methods. PCR site directed mutagenesis (A) was carried out to mutate the nucleotide indicated by the star using the forward primer (1) with the reverse mutant primer (1m-) to produce PCR product (*i*) and forward mutant primer (2m-) with the reverse primer (2) to produce PCR product (*ii*). PCR products (*i*) and (*ii*) were combined, denatured, and annealed to form heteroduplexes. The annealed templates were used for another PCR reaction using only the outer primers (1 + 2). PCR-based mutation detection (B) was carried out using forward mutant primer (4) with a reverse primer (2), and plasmid DNA as template. The PCR products were digested using a restriction endonuclease that cuts at the **AGCT** site created in the presence of the (**C→T**) mutation but not in the absence of this mutation (**AGCC**). The digested PCR products were separated by PAGE. The wild-type (WT) PCR product is not cut by the restriction endonuclease and migrates more slowly than the smaller digestion product generated in the presence of the (**C→T**) mutation.

2.5. DNA cloning techniques

2.5.1. Treatment of DNA fragments with restriction endonuclease, Klenow, and phosphatase

Restriction endonuclease reactions were carried out according to the manufacturer's recommendations. Nucleic acids were digested in a 20-100 μL volume containing 1x reaction buffer, restriction enzyme (5-20 U/ μg DNA), and 1-5 μg of plasmid DNA. Each reaction was incubated for 2 hours at the optimal temperature for the restriction enzyme.

The Klenow fragment of DNA Polymerase I lacks the 5' to 3' exonuclease activity of intact DNA polymerase I, but contains the 3' to 5' exonuclease activity which facilitates the removal of overhanging 3' ends and filling-in of overhanging 5' ends. The Klenow enzyme (1 U/μg DNA) was used in the presence of 33 μM of each dNTP in a 20 μL reaction volume that was incubated at room temperature for 15 min.

Re-circularization of vector DNA was prevented by treatment with Calf-intestinal alkaline phosphatase (CIP), an enzyme that removes 5' terminal phosphates from DNA. CIP reactions (0.5 U/μg DNA) were incubated at 37°C for 60 min.

2.5.2. Isolation of DNA from gels

DNA fragments separated by agarose gel electrophoresis were visualized by EtBr staining and bands were excised from the gel using a scalpel. Gel segments were transferred to a microfuge tube and DNA was purified using the GENECLEAN III Kit

(Q-BIOgene) according to the manufacturer's specifications. The DNA was eluted into sterile water and the concentration was quantitatively determined by absorbance at 260 nm and qualitatively determined after separation on agarose gels; the intensity of the fluorescence of the EtBr stained bands was compared to the DNA Mass Ladder (Invitrogen).

2.5.3. Ligations

Plasmids were linearized by digestion with restriction endonucleases and treatment with CIP (Section 2.5.1). For cohesive-end ligations, DNA fragments were ligated into linearized plasmids with compatible overhang ends. For blunt-end ligations, DNA fragments and/or plasmids with incompatible-ends were first treated with Klenow polymerase to create blunt-ends before the ligation reaction was performed (Section 2.5.1).

For all ligation reactions, approximately 200 ng of linearized plasmid DNA was mixed with insert DNA in a 3:1 molar ratio. Reactions contained 1.5 μL of 10x T4 DNA ligation buffer (500 mM Tris-HCl, 100 mM $MgCl_2$, 100 mM DTT, 10 mM ATP, 250 μg/mL BSA, pH 7.5) and 1 μL of T4 DNA ligase (400 U/μL) in a final volume of 15 μL. Reactions were incubated for 16-18 hours at 14°C.

2.5.4. Manual DNA sequencing

Manual DNA sequencing was performed using a T7 DNA Sequencing Kit (USB Corporation, Cleveland, OH). For each reaction, 32 μL (2-4 μg) of plasmid DNA was

treated according to the manufacturer's instructions. Labeling was accomplished using [αS^{35}]dATP (1000-1500 Ci/mmol) isotope (NEN Boston, MA). DNA sequencing products were separated by polyacrylamide gel electrophoresis (PAGE). Prior to loading, samples were incubated in a boiling water bath for 3 min. A 4.0 μL sample of each sequencing reaction was loaded onto gels pre-warmed to 55°C in TBE buffer (Appendix 6.4.8). The DNA products were separated at 60 W for 1.5-3 hours. After electrophoresis, the gels were transferred to Whatmann paper (3MM) and dried at 80°C for 1-2 hours. Dried gels were placed directly onto X-OMAT AR film (Kodak, Toronto, ON) and exposed overnight at room temperature. Film was then processed manually using GBX Developer/Fixer (Kodak) and following the manufacturer's specifications.

2.5.5. Automated Sequencing

Automated sequencing of DNA was carried out at The Center for Applied Genomics (TCAG) DNA Sequencing Facility, (Hospital for Sick Children, Toronto, ON) using an ABI 377 sequencer. Nucleotide sequence data and electropherograms were generated from the automated sequencing reactions. All constructs were sequenced to confirm that no errors were introduced during PCR amplification.

2.6. Bioinformatic tools and methods

Bioinformatic tools were used to identify protein sequences related to hGrb14 (GenBank accession number NP_004481). To determine if there were other protein sequences in public databases that were similar to the hGrb14 protein sequence the NCBI comparison tool, BLAST (Basic Local Alignment Search Tool) was used. A standard protein-protein

BLAST search with NP_004481 as the query sequence was performed against the nr (non-redundant) protein database and a standard nucleotide-nucleotide BLAST search was performed using the EST (Expressed Sequence Tag) database. The statistical significance of the sequence matches revealed by BLAST was assessed based on the calculated Expect values. The Expect value is a measure of the number of sequence matches expected by chance, according to the stochastic model of Karlin and Altschul (1990). We deemed sequence matches to be statistically significant with Expect values exceeded the default Expect value of 10 (E=10).

To predict the boundaries and identify conserved residues in the BPS domain, we used CLUSTALW [66] to align and compare multiple sequences. BPS domain sequences of Grb14, Grb10, and Grb7 from the human, mouse, and rat, which were matches from the hGrb14 BLAST query, were aligned and compared.

2.7. Yeast two-hybrid system

2.7.1. Yeast two-hybrid plasmids

An illustration of the yeast two-hybrid system is shown in Fig. 5. The yeast two-hybrid plasmids used in this study are listed in Table 4 and are depicted in Fig. 6.

Table 4. Yeast two-hybrid plasmids

Plasmid	Yeast two-hybrid domain
pGAD424	GAL4AD
pGBT9	GAL4BD
pBTM116	LexABD

Figure 5. **Diagram of the yeast-two hybrid system**. hGrb14 wild type and mutant, full-length and sub-domain cDNA fragments were sub-cloned into pGAD424, a vector encoding the GAL4 activation domain (AD) and a LEU selection marker. cDNA encoding the insulin receptor kinase (IRK) cytoplasmic domain was inserted into pGBT9, a vector containing the GAL4 DNA binding domain (BD) and TRP genes. Yeast cells were co-transformed with the pGAD424 and pGBT9 vectors expressing the GAL4AD::hGrb14 and GAL4BD::IRK fusion proteins, respectively. The transformants were plated onto media that selects for the activation of the *HIS3* reporter gene and activation of *lacZ* was monitored using filter lift (blue colonies) and the aqueous β-galactosidase (yellow colour) assay.

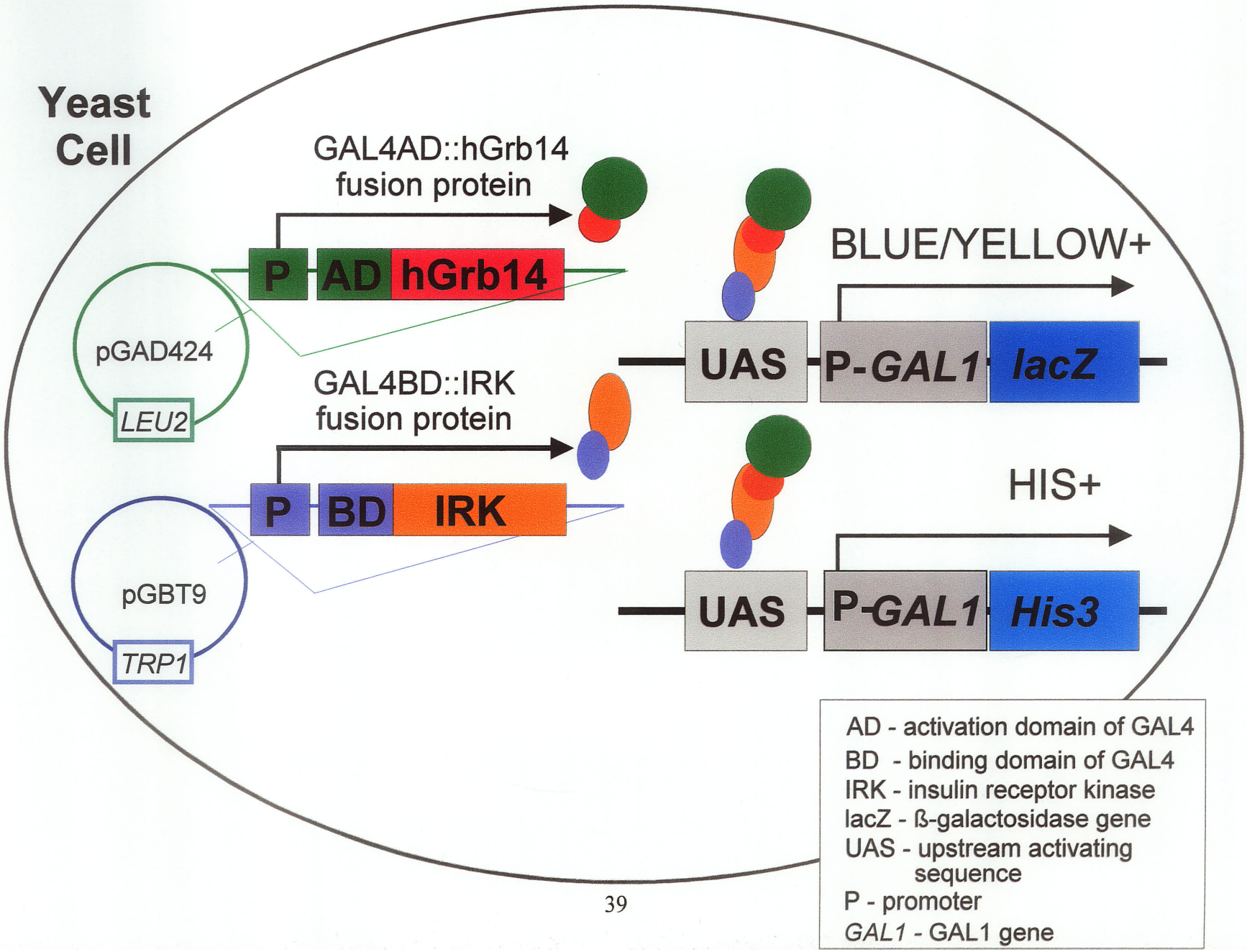
Yeast Cell
GAL4AD::hGrb14 fusion protein
P
AD
hGrb14
pGAD424
LEU2
GAL4BD::IRK fusion protein
P
BD
IRK
pGBT9
TRP1
BLUE/YELLOW+
UAS
P-GAL1
lacZ
HIS+
UAS
P-GAL1
His3
AD - activation domain of GAL4
BD - binding domain of GAL4
IRK - insulin receptor kinase
lacZ - ß-galactosidase gene
UAS - upstream activating sequence
P - promoter
GAL1 - GAL1 gene

A

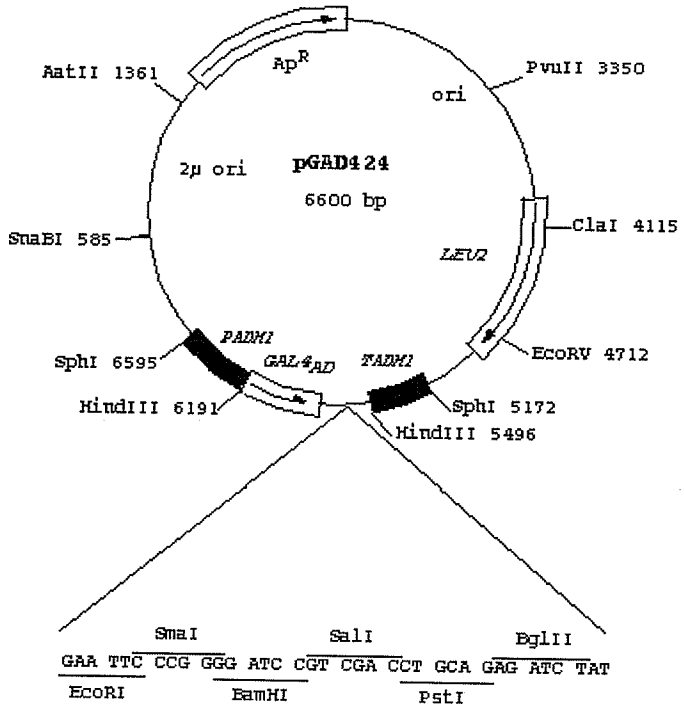

Figure 6. Diagram of the yeast two-hybrid plasmids. Plasmids pGAD424 (A), pGBT9 (B) (continued on next page), and pBMT116 (C) contain the *E. coli* DNA replication origin (ori), the β-lactamase gene responsible for ampicillin resistance (Ap^R), the yeast alcohol dehydrogenase promoter ($ADH1_p$) and terminator ($ADH1_t$), and a 2 micron circle origin of replication (2μ, ori). For selection purposes pGBT9 and pBTM116 carry the yeast *TRP1* and pGAD424 contains the *LEU2* gene. pGBT9 and pBTM116 also contain the GAL4 or the LEXA Binding Domains (BD), respectively, and pGAD424 contains the GAL4 Activation Domain (AD). Restriction sites for each MCS are depicted below each vector. Used with permission from R.D. Gietz [64].

B

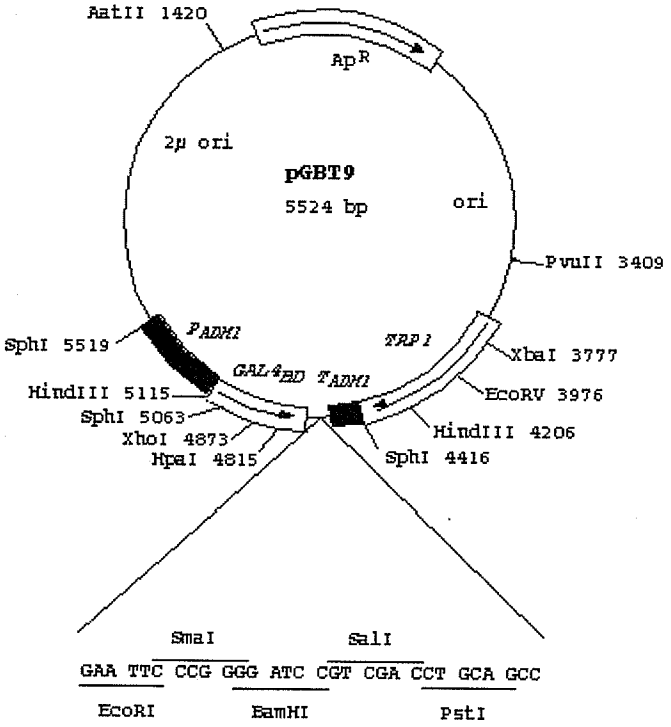
AatII 1420
Ap^R
2μ ori
pGBT9
5524 bp
ori
PvuII 3409
SphI 5519
P ADH1
TRP1
XbaI 3777
GAL4 BD
T ADH1
HindIII 5115
EcoRV 3976
SphI 5063
HindIII 4206
XhoI 4873
HpaI 4815
SphI 4416
SmaI
SalI
GAA TTC CCG GGG ATC CGT CGA CCT GCA GCC
EcoRI
BamHI
PstI

C

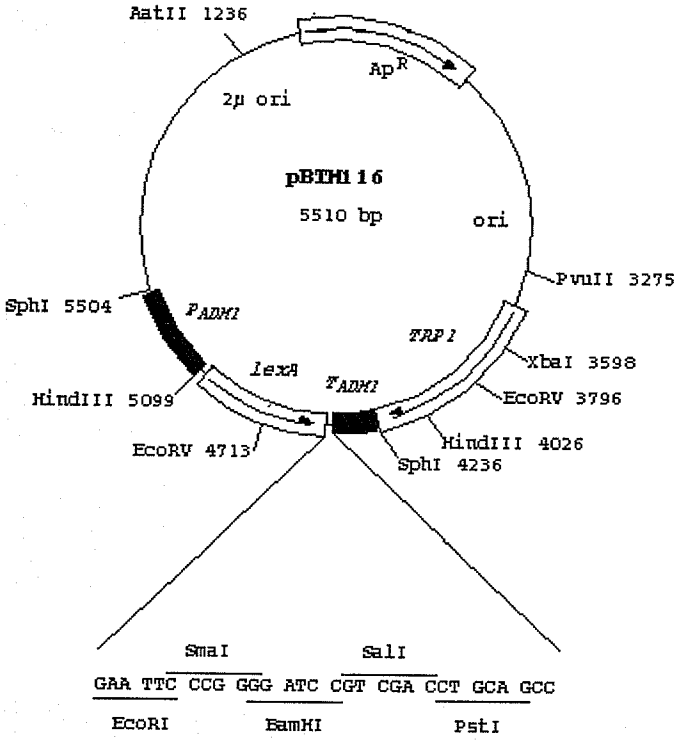
AatII 1236
Ap^R
2μ ori
pBTM116
5510 bp
ori
PvuII 3275
SphI 5504
P ADH1
TRP1
XbaI 3598
lexA
T ADH1
HindIII 5099
EcoRV 3796
EcoRV 4713
HindIII 4026
SphI 4236
SmaI
SalI
GAA TTC CCG GGG ATC CGT CGA CCT GCA GCC
EcoRI
BamHI
PstI

2.7.2. Transformation of S. cerevisiae

All plasmid constructs were transformed into yeast using the high-efficiency LiAc transformation protocol [67]. The pGAD424 constructs expressing full-length hGrb14 or its derivatives, fused with the GAL4AD, were co-transformed into yeast with the active or inactive pGBT9::IRK plasmid. After transformation, cells were pelleted, resuspended in 100 µL of sterile ddH_2O, plated on SC-TRP-LEU-HIS+1 mM 3-AT (Synthetic Complete Selection -TRP-LEU-HIS + 3 Amino-1,2,3-Triazole) and SC-TRP-LEU agar medium plates, and grown for 72 hours at 30°C.

2.7.3 β-Galactosidase filter lift assay

The β-galactosidase filter lift assay was performed using co-transformed yeast colonies that were grown on selective media as described in Section 2.7.2. Colonies grown to 1-2 mm in diameter were covered with filter paper (90 mm, Whatmann #3) and lifted off the plate. Colonies lifted on filters were frozen in liquid nitrogen for 10-15 s and then thawed. This freeze-thaw cycle was repeated two additional times. Filters were then placed separately on a similarly sized filter paper saturated with 1.25 mL of Z buffer/β-ME/X-gal (Appendix 6.4.13) and incubated in a sealed petri dish at 37°C. The breakdown of the β-galactosidase substrate resulted in the development of blue coloured colonies; colour development was assessed qualitatively at 15 min intervals; colour intensity was considered directly proportional to the degree of activation of the *lacZ* reporter gene [64].

2.7.4. Liquid β-galactosidase

Quantitative measurement of β-galactosidase activity in yeast was performed using a modification of the method reported by Miller [68]. SC-T-L broth (10 mL) was inoculated with 5-10 co-transformed yeast colonies (Section 2.7.2) and grown overnight at 30°C with aeration on a shaking platform (200 RPM). The overnight culture was sub-cultured into 10 mL fresh SC-T-L broth to an absorbance (OD_{600}) of 0.2, and further grown to mid-late log phase at 30°C (OD_{600} = 0.8). Yeast cell pellets from 9.5 mL of the sub-culture broth were resuspended in 100 µL Z-buffer (Appendix 6.4.12). Glass beads (50% volume) were added to the suspension and cells were lysed by vortexing vigorously for eight 20 s cycles with intermittent cooling on ice for 30 s. Glass beads were removed by centrifugation for 30 s and supernatants (50 µL) were transferred to fresh tubes containing 750 µL of warm (37°C) Z-buffer/β-ME containing 160 µL fresh 4 mg/mL ONPG (ortho-nitrophenyl β-$_D$-galactopyranoside) (Sigma-Aldrich Canada, Oakville, ON). Samples were mixed by vortex action and then incubated at 37°C until a yellow colour developed. Reactions were terminated by adding 400 µL of 1 M $NaCO_3$ and the reaction time was recorded. Cellular debris was removed by 1 min centrifugation at room temperature and absorbance (OD_{420}) measurements were carried out on the supernatants. The β-galactosidase activity, measured in Miller units, was determined using the following equation:

$$\text{Miller Unit} = \frac{(A_{420})(1000)}{(\text{Vol in mL})(\text{t in min})(A_{600})}$$

Theses values were reported as percentage values obtained by assigning the value obtained between full-length hGrb14 and the active IRK to be 100%.

2.7.5. hGrb14 protein expression in yeast

To assess the expression of the hGrb14 proteins in yeast, cells were transformed with a pGAD424::hGrb14 vector using the high-efficiency LiAc transformation protocol; the transformation mixtures were plated onto SC-L plates, as only the pGAD424 (*LEU2*) vector was present in the transformation.

The transformation colonies from SC-L plates were used to inoculate 5 mL of SC-L media and grown overnight at 30°C with aeration. The overnight culture was then sub-cultured into 50 mL of SC-L and grown to mid-log phase (OD_{600} 0.4-0.6). Cells were pelleted in centrifuge tubes half filled with ice at 1000x*g* for 5 min at 4°C. Pellets were washed with 50 mL ice-cold ddH_2O and recovered by centrifugation, as above. Lysates were prepared following the Yeast Protocol #PT3024-1 from CLONTECH. Briefly, pellets resuspended in 100 µL of ice-cold TCA (Trichloroacetic acid) buffer (Appendix 6.4.10) were transferred to a tube containing 100 µL of glass beads plus 100 µL of 20% TCA per 7.5 OD_{600} units of cells. Cells were lysed by eight cycles of vigorous vortexing for 30 s followed by cooling on ice for 30 s. Supernatants were transferred to new tubes and combined with supernatants obtained by washing the beads with 500 µL of a 1:1 mixture of 20% TCA:TCA buffer. Proteins were pelleted by centrifugation at 14,000 rpm for 10 min at 4°C and resuspended in 10 µL of TCA Laemmli loading buffer/OD_{600} units of cells (Appendix 6.4.11). Separation of proteins was carried out on 10% SDS-PAGE gels with transfer and detection performed as described in Section 2.8.

2.8. Mammalian cell culture methods

2.8.1. Mammalian cell lines

Cell lines used in this study are listed in Table 5.

Table 5 . Mammalian cell lines

Cell line	Tissue of Origin	Overexpressed Proteins	Source
CHO-IR	Chinese Hamster Ovary	Human IR	R. Roth
CHO-42	Chinese Hamster Ovary	Human IR/ Human Grb14:$_F$ (high expression)	Hemming *et al.*, 2001

2.8.2. Cell transfection

CHO-K1 cells overexpressing the IR (CHO-IR) were stably transfected with the pRcCMV::hGrb14$_F$ plasmid (Fig. 7), as described by Hemming (2001). Control cells, named Mock cells, received only the delivery vector, pPUR (Clontech, Palo Alto, CA). Transfected cells were selected in Ham's F12 medium (Appendix 6.3.3.1) containing 10% FBS, 100 U penicillin-streptomycin, 200 μg/mL geneticin, and 10 μg/mL puromycin and were maintained in the same media, except the puromycin concentration was reduced to 4 μg/mL.

Stable cell lines expressing mutant hGrb14 protein were created by separately transfecting CHO-IR cells with either pRcCMV::hGrb14$_F$ R466Q, pRcCMV:hGrb14$_F$ R387Q, or pRcCMV:hGrb14$_F$ R387Q R466Q mutant vectors (Fig. 28, shown later). Transfection was carried out using the DOSPER transfection reagent (Roche, Laval, QUE) according to the manufacturer's specifications with a 4:1 DOSPER:DNA ratio. Transfection DNA consisted of 3 μg of the pRcCMV::hGrb14$_F$ based vector and 1 μg of

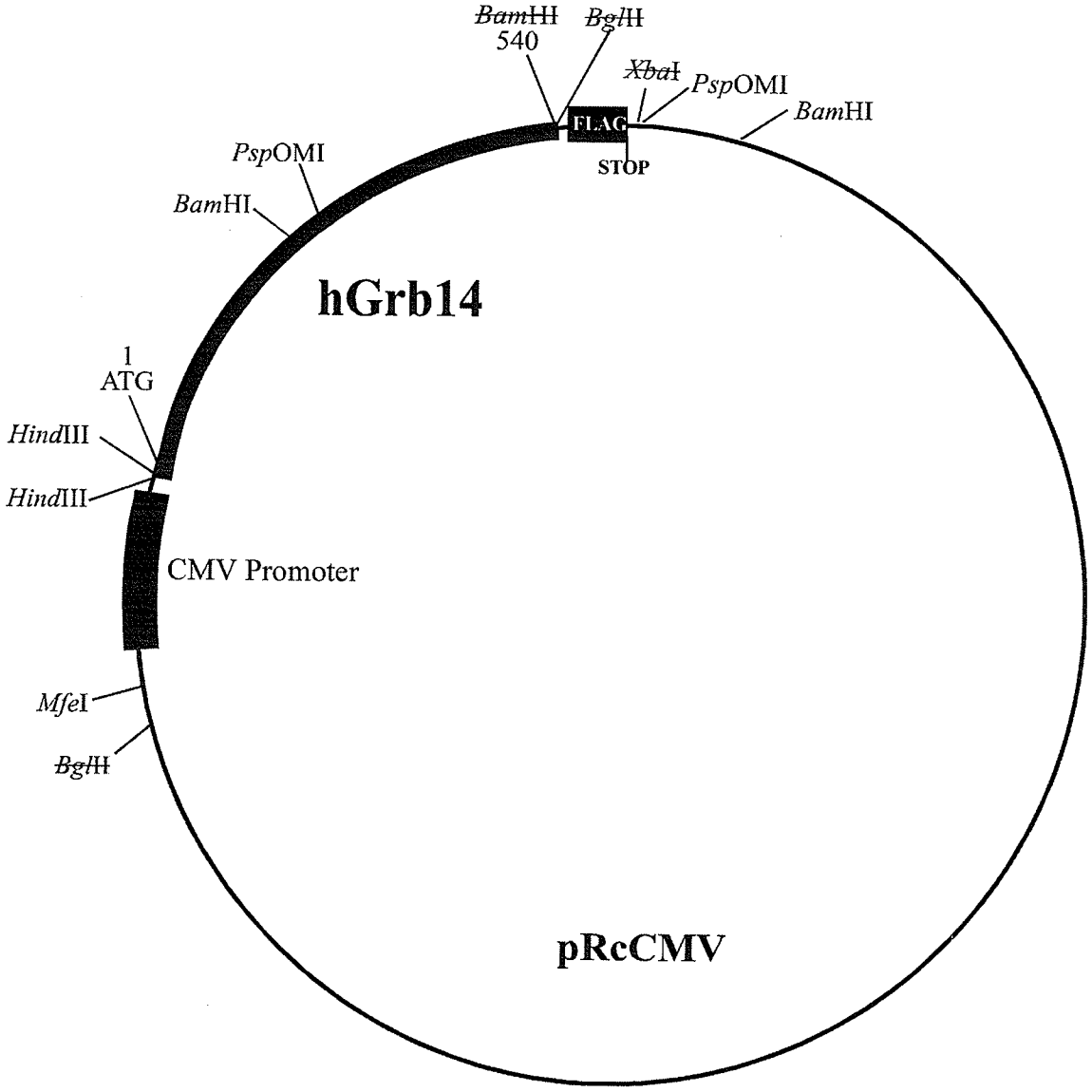

Figure 7. Diagram of the pRcCMV::hGrb14$_F$ vector. The full-length hGrb14 cDNA was cloned into the pRcCMV vector and a C-terminal FLAG epitope, was added that is terminated with a stop codon. Restriction sites used in cloning strategies are indicated; the strike-out text indicates restriction sites destroyed during cloning. Cloning carried out by the research group of R. Daly[28].

the pPUR vector. Stably transfected cells were grown in selection medium for several passages and then maintained in maintenance medium. The CHO-42 IR::hGrb14$_F$ cell lines (Hemming *et al*, 2001) were used as control. Cells which were maintained in maintenance medium were plated at 5 x 10^5 cells/ 60mm dish and grown for 48 h at 37°C or until they reached 80% confluency. Cells were collected and expression of FLAG-tagged hGrb14 protein from the cell lysates was assessed by immunoblotting.

2.8.3. Insulin stimulation

Cells grown to 80% confluency were transferred to serum-free media for 18-24 h and then stimulated with insulin for 2 min using 2 mL Ham's F12 serum-free medium supplemented with 10 nM Humulin R (human insulin: 27-28 U/mg protein) (Eli-Lilly Canada, Toronto, ON).

2.8.4. Cell lysis

Cells stimulated with insulin were washed twice with ice-cold PBS (Appendix 6.4.3) to remove any contaminating extracellular material and lysed by incubating in 500 µL of cell lysis buffer (Appendix 6.4.1) for 20 min on ice. Insoluble material was pelleted by centrifugation for 10 min at 4 °C and supernatants were transferred to a fresh tube.

2.9. Bradford protein assay

Protein concentrations were determined using a modification of the method reported by Bradford (1976). Samples were prepared by combining 2 µL of cell lysate with 798 µL of MilliQ H_2O and 200 µL of Bradford reagent (BioRad Life Science Group, Hercules,

CA). Samples were mixed by gentle vortexing action and incubated for 2 min at room temperature to allow colour to develop. Absorbance (A_{595}) was measured for each sample and the protein concentrations were determined from a standard protein curve of Gamma Globulin protein (5-15 μg/μL) (BioRad).

2.10. Immunoblotting

Cell lysate proteins were separated on 7.5% SDS-PAGE and transferred to nitrocellulose filters using a BioRad Transblot apparatus and following the method reported by Towbin (1979). Immunoblots were blocked for 1h in TBS-T buffer (Appendix 6.4.9) containing 5% skim milk powder, except for anti-pTyr blots, which were blocked in TBS-T containing 2% BSA. Primary and secondary antibodies were diluted in the same solutions and washes were in TBS-T. Filters were incubated either with diluted primary polyclonal antibodies (see Table 1 for Antibody dilutions) for 1h or with diluted monoclonal antibodies for 1.5 h, washed three times for 10 min, incubated with the corresponding secondary antibody for 45 min, and washed again four times for 10 min per wash. Antibody binding was detected by enhanced chemiluminescence following the manufacturers specifications (Amersham). The volume of the band intensities were quantitatively assessed in Counts (CNT)*mm^2 units using Fluor S-Max MultiImager and Quantity One software.

2.11. Immunoprecipitation

Cell lysate proteins (2.0 mg) were prepared as in section 2.6.4 and then pre-cleared with a 20% solution of Sepharose protein G beads (50 μl) (Amersham) by gentle rotation of the

samples at 4°C for 60 min. The beads were pelleted by centrifugation and the supernatants were transferred to a new tube and incubated for 16 h with primary antibodies and 60 µL protein G beads supplemented with the 2% azide, a bacteriostatic agent. The beads were pelleted by centrifugation and placed on ice. A second capture was performed for 60 min at 4°C. The capture beads were pooled and washed twice with 500 µL of cold immunoprecipitation lysis buffer (Appendix 6.4.2) and once with 500 µL of cold PBS. The beads were then resuspended in 22µl of 4x SDS loading buffer (Appendix 6.4.4), diluted two-fold with lysis buffer and boiled for 2 min. The boiled solution was then separated from the beads by centrifugation and transferred to a fresh tube. These beads were then resuspended in 18µl of 4x SDS loading buffer diluted two-fold with lysis buffer and the solution was again separated from the beads and pooled with the loading buffer from the previous step. Proteins were separated by SDS-PAGE, transferred to nitrocellulose, and immunoblotted.

2.12. Transgenic experiments

2.12.1. Animals

The strain of breeder mice used in the transgenic experiments was Bl/6 from Jackson Labs (Bar Harbor, Maine), the transgenic mice were Bl/6 x CBA from the CGDN Core Transgenic Facility (University of British Columbia), and the progeny mice are derivatives of these strains. Once the founders were identified, they were shipped to the University of Manitoba Animal Care Facility where they were then ear tagged for identification, housed, and bred.

2.12.2. Transgenic construct preparation

The hGrb14 fragment used for microinjection to create hGrb14 transgenic mice was isolated by digesting the pRcCMV::hGrb14$_F$ plasmid with *MfeI/Bam*HI and purifying the resulting 2.8 Kb fragment (Fig. 8A) using a Gel Extraction Kit (Qiagen).

2.12.3. Microinjection of mouse embryos

To create hGrb14 transgenic mice, mouse embryos were microinjected with the purified hGrb14 fragment at the CGDN Transgenics Core Facility in Vancouver, BC, under the direction of Dr. Frank Jirik. The F1 (C57Bl/6 x CBA) females were superovulated at 3-4 weeks of age with injections of Pregnant Mare Serum (PMS) and Human Chorionic Gonadatropin (HCG) hormones, with a 46 h interval between injections. After the HCG injection, the F1 females were mated to F1 studs (1 female/male). The females were then collected at 0.5 d post coitus for embryo harvesting at the 1-cell stage.

The collected embryos were incubated in an environment of 90% N_2, 5% O_2, 5% CO_2 for pronuclear microinjection. F2 embryos (306) were injected with 1-5 ng of purified hGrb14$_F$ DNA construct and surviving embryos (257) were incubated overnight. The 2-cell stage embryos were then implanted into a 0.5 d pseudopregnant female. Gestation period was approximately 18 days. A mouse-tail biopsy was taken from the pups at 3-4 weeks of age and this sample was shipped to our laboratory for screening.

2.12.4. Preparation of mouse-tail DNA

DNA was extracted from 1-2 mm of the tail biopsies by digestion in 300 µL of modified

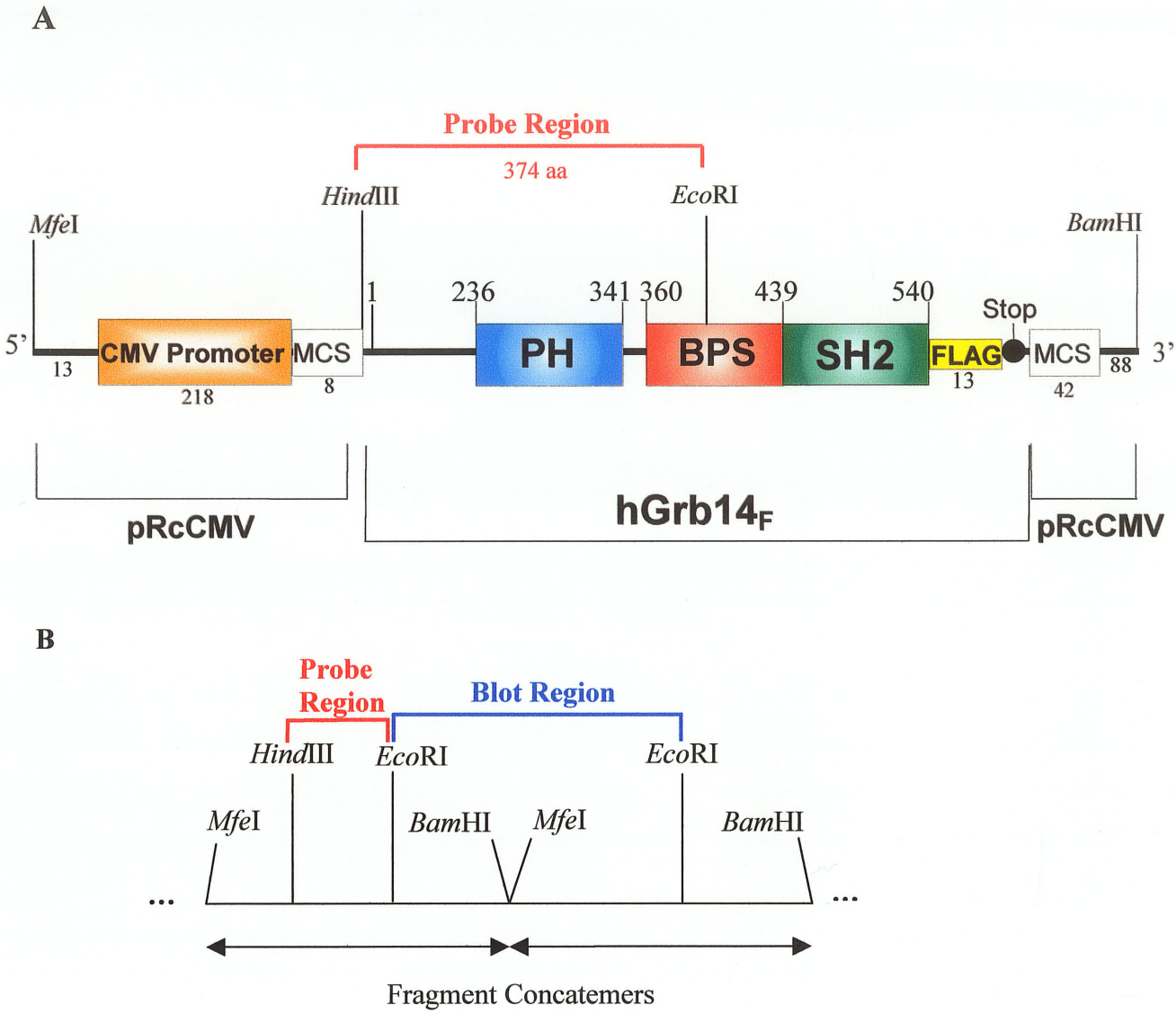

Figure 8. Diagram of hGrb14 *Mfe*I/*Bam*HI DNA fragment used for microinjection to create transgenic mice. (A) The *Mfe*I/*Bam*HI hGrb14$_F$ fragment was excised from pRcCMV::hGrb14$_F$. This fragment contains an N-terminal CMV promoter and a C-terminal FLAG tag flanked with a stop codon. The amino acid lengths are indicated adjacent to their corresponding regions (diagram not drawn to scale). (B) *Mfe*I/*Bam*HI fragment concatemers showing the *Hind*III/*Eco*RI probe region for Southern blot analysis in red and the *Eco*RI digest region in blue.

STE buffer (Appendix 6.4.5) plus 18 μL of 20 mg/mL Proteinase K at 55°C for 1.5 h. Samples were mixed by vortex action and boiled for 10 min to denature residual protein. The resulting DNA was used for PCR amplification.

2.12.5. Founder screening

2.12.5.1. PCR reactions

DNA prepared from the mouse-tail samples was screened for the hGrb14 transgene by PCR. Control DNA from the tail of a non-transgenic mouse was prepared as described in Section 2.10.4. PCR primers WPG164/WPG160 that amplify a 400 bp region of mouse *Hyal2* were used to as a control to verify the quality and integrity of the DNA. Two sets of human Grb14 specific PCR primers, WPG246/WPG248 and WPG251/WPG252, were used in separate PCR reactions to identify DNA samples that harboured the hGrb14 transgene. Successful PCR amplifications yielded 494 bp and 241 bp PCR products, respectively. PCR reactions were carried out in duplicate for all primer sets using 2 μL of template DNA and following the PCR protocol (Section 2.10.5.1).

2.12.5.2. Southern blot analysis

Non-transgenic control and putative transgenic mouse-tail DNA was further purified by phenol/chloroform extraction followed by ethanol precipitation. Pellets were washed with 70% ethanol and resuspended in 20 μL ddH_2O. Fifteen μg of DNA from each sample was digested with *Eco*RI, an enzyme that cuts internally in the *MfeI/Bam*HI hGrb14 fragment at base pair 1659 (Fig. 8).

Estimated equivalents of (1), (2), (5), and (10) copies of the *hGrb14* gene were loaded in separate wells on a 0.8% TAE agarose gel along with *Eco*RI–digested control and transgenic mouse-tail DNA samples. The concatemerized *Mfe*I/*Bam*HI hGrb14 fragment was cut with *Eco*RI resulting in a 2.8 Kb fragment (Fig. 8B). This fragment can only ligate with the vector in the correct orientation. The approximate amount of DNA required to represent a single copy gene, in micrograms of DNA, for the *Mfe*I/*Bam*HI-digested pRcCMV::hGrb14$_F$ was calculate to be:

$$1 \text{ copy} = \frac{(7196 \text{ bp of } \textit{Mfe}\text{I}/\textit{Bam}\text{HI digested pRcCMV::hGrb14}_F) \times 15\mu g}{3 \times 10^9 \text{ bp in haploid mouse genome}} = 36 \text{ pg}$$

The size of the DNA (7196 bp) includes the 2799 bp *Mfe*I/*Bam*HI digested hGrb14 insert plus 4397 bp from the pRcCMV vector, as the *Mfe*I/*Bam*HI fragment was not isolated in the generation of samples used for the copy number standards. However, only the hGrb14 *Hind*III/*Eco*RI (541-1659) region would be hybridized by the *Hind*III/*Eco*RI probe DNA (Fig. 8B). The gel was run at 100V for 3 h in 1x TAE buffer and transferred to nitrocellulose following the standard Southern blotting protocol outlined by Sambrook *et al.* [69]. DNA was fixed to the filter by cross-linking using the Spectrolinker XL-1000 UV Crosslinker at the Optimal Crosslink setting. Filters were then incubated in pre-hybridization solution (Appendix 6.6.4) for 2h at 65°C, probed (see below for preparation of probe) overnight in hybridization solution, washed, and exposed to X-OMAT AR film (Kodak) for 20 min, 1.5, 4.5, 16, and 68 hours. A 1119 bp probe was prepared by digesting pRcCMV::hGrb14$_F$ with *Hind*III/*Eco*RI, separation by agarose gel electrophoresis and purification with a GENECLEAN Kit. This fragment was then re-purified following the same procedure. The purified DNA fragment (75 ng) was labeled

overnight with [α-^{32}P]dATP and isolated using a Nick Column (Amersham Pharmacia, Piscatavay, NJ) [70]. The resulting probe had a specific activity of 1.25 x 10^8cpm/μg.

2.12.5.3. Protein expression analysis

hGrb14 transgenic founder mice were bred, the progeny were sacrificed, and the following tissues were immediately collected and frozen on dry ice: liver, muscle, kidney, brain, heart, pancreas, fat, lung, spleen, large intestine, small intestine, blood, and gonads. Each tissue was homogenized separately in tissue lysis buffer (Appendix 6.4.6) on ice for 15 s using a Kinematics PGA Polytron and sonicated twice at 40 W for 15 s on ice with a Braun-sonic 1510 Sonicator. Cell lysates (80 μg) were immunoblotted using the FLAG antibody.

3. RESULTS AND DISCUSSION

In order to characterize the role of hGrb14 BPS and SH2 domains in insulin signaling, we employed the yeast two-hybrid system to test the binding of BPS and SH2 sub-domains with the IR. The results of the yeast two-hybrid hGrb14-IR interaction analysis served as a guide for mammalian cell culture experiments to analyze the interaction between the IR and hGrb14 BPS and SH2 domains and the effects of this interaction on insulin signaling.

3.1. Analysis of the interaction of hGrb14-IR in the yeast two-hybrid system

3.1.1. Analysis of the interaction of full-length hGrb14 with the IR

To use the yeast two-hybrid system for the analysis of the hGrb14 domains, it was first necessary to confirm that the system could detect the interaction between full-length hGrb14 and the active IRK, as had been demonstrated previously [56;61].

Full-length hGrb14 cDNA was cloned into the GAL4 Activation Domain (AD) yeast two-hybrid vector, pGAD424 (Fig. 6A), by blunt-end ligation of the hGrb14 *Hind*III/*Bcl*I fragment (aa 1-540) into the *Xma*I-digested pGAD424 vector, to generate the pGAD424::hGrb14 vector (Fig. 9). The cytoplasmic domain (aa 953-1343) of the IR (Fig. 1) was cloned into the GAL4 Binding Domain (BD) yeast two-hybrid vector, pGBT9 (Fig. 6B), to generate the pGBT9::IRK vector. The pGAD424::hGrb14 and pGBT9::IRK vectors were co-transformed into the KGY37 yeast strain (Section 2.7.2) and selected on SC-T-L-H plates. If there was an interaction between the GAL4AD::hGrb14 fusion protein expressed from the pGAD424::hGrb14 plasmid and the GAL4BD::IR fusion protein expressed from the pGBT9::IRK plasmid, then the *HIS3*

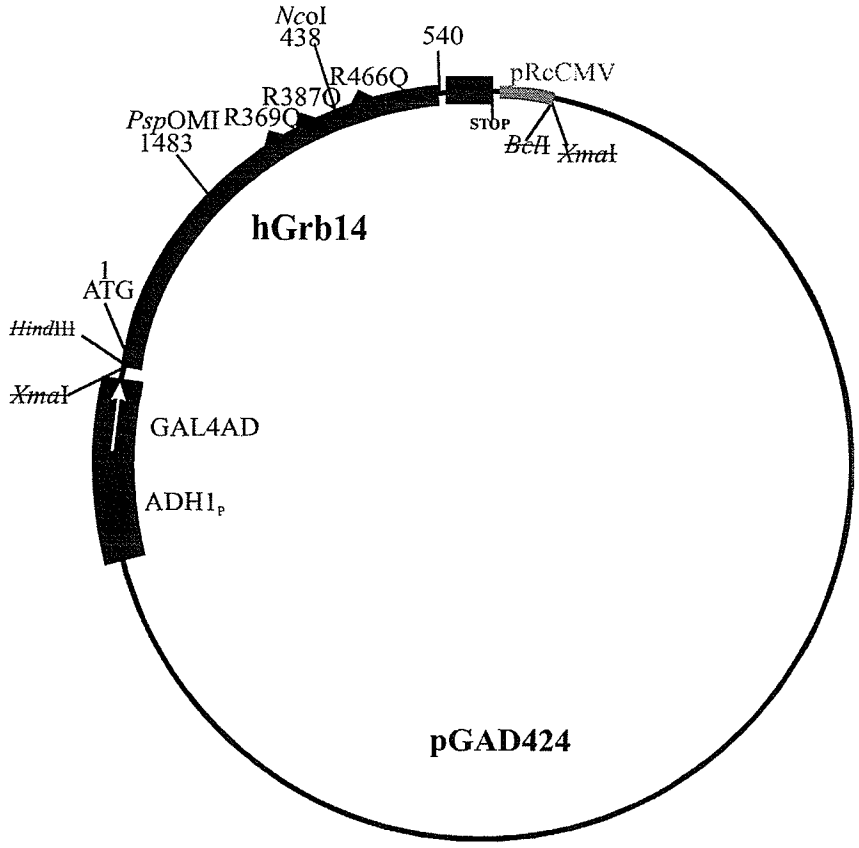

Figure 9. **Diagram of the pGAD424::hGrb14$_F$ vector.** The *Hind*III/*Bcl*I fragment (aa 1-540) from pRcCMV::hGrb14$_F$ was blunt-end ligated into the XmaI-digested pGAD424 vector that contained the GAL4 Activation Domain (AD). The hGrb14 cDNA contained a C-terminal FLAG epitope that ended with a stop codon. A segment of the pRcCMV vector was included in the *Hind*III/*Bcl*I fragment sub-cloning. The R369Q BPS substitution was introduced into the pGAD424::hGrb14$_F$ vector by PCR amplification. Forward primer WPG295, with reverse mutant primer WPG279 and reverse primer WPG106 with forward mutant primer WPG296 were used in separate PCR reactions to generate PCR products of 531 bp and 682 bp, respectively, from pGAD424::hGrb14$_F$. These products were then used as templates in a PCR reaction containing only the outer primers, WPG295 and WPG106, to create a fused 913 bp product. This product was cloned into pCR2.1, the *Psp*OMI/*Nco*I fragment excised, and used to replace the wild-type fragment in the *Psp*OMI/*Nco*I-digested pGAD424::hGrb14$_F$ vector. The R387Q BPS substitution was generated as described for the pGAD424::hGrb14$_F$ R369Q construct, except the reverse mutant primer was WPG299 and the forward mutant primer was WPG298. The *Psp*OMI/*Nco*I R369Q or R387Q mutant fragments were also inserted in the *Psp*OMI/*Nco*I-digested pGAD424::hGrb14$_F$ R466Q vector to create the pGAD424::hGrb14$_F$ R369Q R466Q or R387Q R466Q constructs, respectively. The positions of the R369Q, R387Q, and R466Q substitutions are indicated by solid triangles; the strike-out text indicates restriction sites destroyed during cloning.

gene will be transcribed, thus allowing growth of these colonies on SC-T-L-H plates (Fig. 4). The interaction between full-length hGrb14 and the IR was tested by filter-based and aqueous β-galactosidase yeast two-hybrid assays. A very strong interaction between hGrb14 and the IR was shown using the filter-lift assay where colonies developed an intense blue colour after only 15 min at 37°C (Fig. 10). The hGrb14-IR interaction was also found to be very strong using the aqueous β-galactosidase assay; the colour change for this colorimetric assay occurred at 1 min. The β-galactosidase activity from the aqueous assay of the hGrb14-IR interaction was set to 100%, the standard to which all other interaction values were compared (Fig. 11).

To verify that neither the product of the GAL4AD vector, pGAD424, nor of the GAL4BD vector, pGBT9, could independently activate the expression of the His or β-gal genes in the yeast two-hybrid system, the empty pGAD424 vector was co-transformed with pGBT9::IRK and plated on SC-T-L-H media. No growth was observed after 3 days of incubation at 37°C, indicating that the pGAD424 vector was not self-activating in the presence of the GAL4BD::IRK fusion protein (data not shown). The empty pGBT9 vector was also tested for self-activation by co-transformation with pGAD424::hGrb14$_F$, and again showed no self-activation (data not shown).

3.1.2 Confirmation that hGrb14 interacts with the IR in a kinase dependent manner

To confirm previous analyses that showed hGrb14 interacts with the IR in a kinase dependent manner [56;61], we tested for an interaction between GAL4AD::hGrb14 fusion protein and the kinase active and inactive forms of the IR. The cytoplasmic

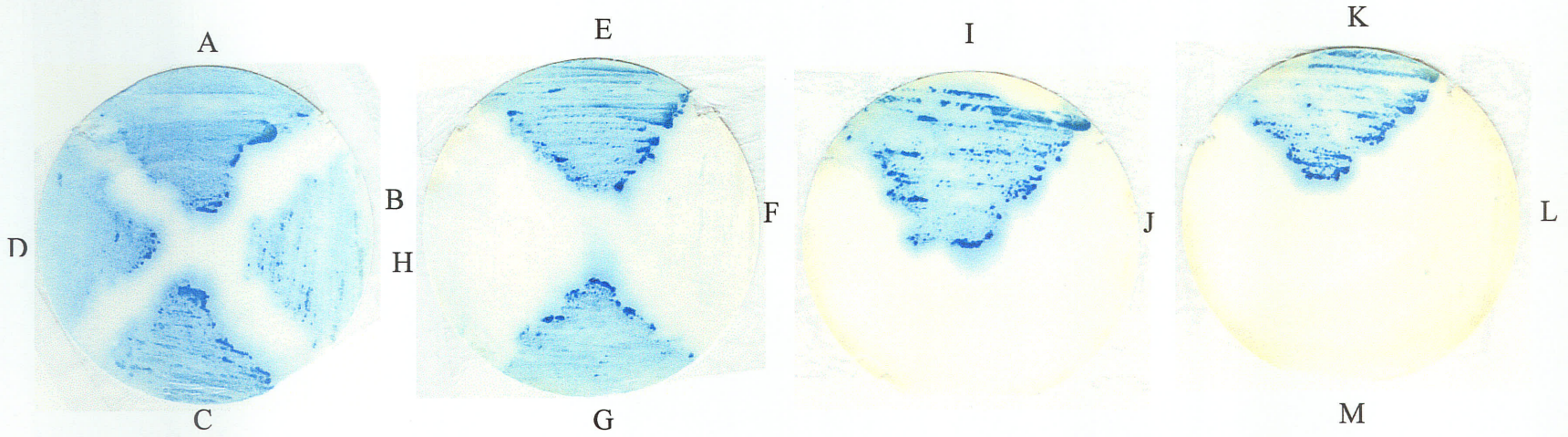

Fusion proteins expressed on SC-T-L-H+3AT media			Time of incubation at 37°C					
			15 min	30 min	45 min	1 h	2 h	o/n
A	hGrb14	IRK active	+	+	+	++	++	+++
B	hGrb14 R466Q	IRK active					+	++
C	hGrb14 R369Q	IRK active		+	+	++	++	+++
D	hGrb14 R369Q R466Q	IRK active		+	+	+	+	++
E	BPS+SH2	IRK active		+	+	+	+	+++
F	BPS+SH2 R466Q	IRK active						
G	BPS+SH2 R369Q	IRK active		+	++	++	++	+++
H	BPS+SH2 R369Q R466Q	IRK active						
I	BPS+SH2 R387Q	IRK active		+	+	+	++	+++
J	BPS+SH2 R387Q R466Q	IRK active						
K	SH2	IRK active		+	++	++	++	+++
L	SH2 R466Q	IRK active						
M	hGrb14	IRK inactive						

Figure 10. Analysis of hGrb14–IR interactions using β-galactosidase filter lift assays. Yeast cells were transformed with plasmids expressing full-length or sub-domain, wild-type or mutant GAL4AD::hGrb14 along with GAL4BD IRK-active (A-L) or IRK-inactive (M) fusion proteins. β-galactosidase filter lift assay blue colour development indicated by (+) was observed at timed intervals.

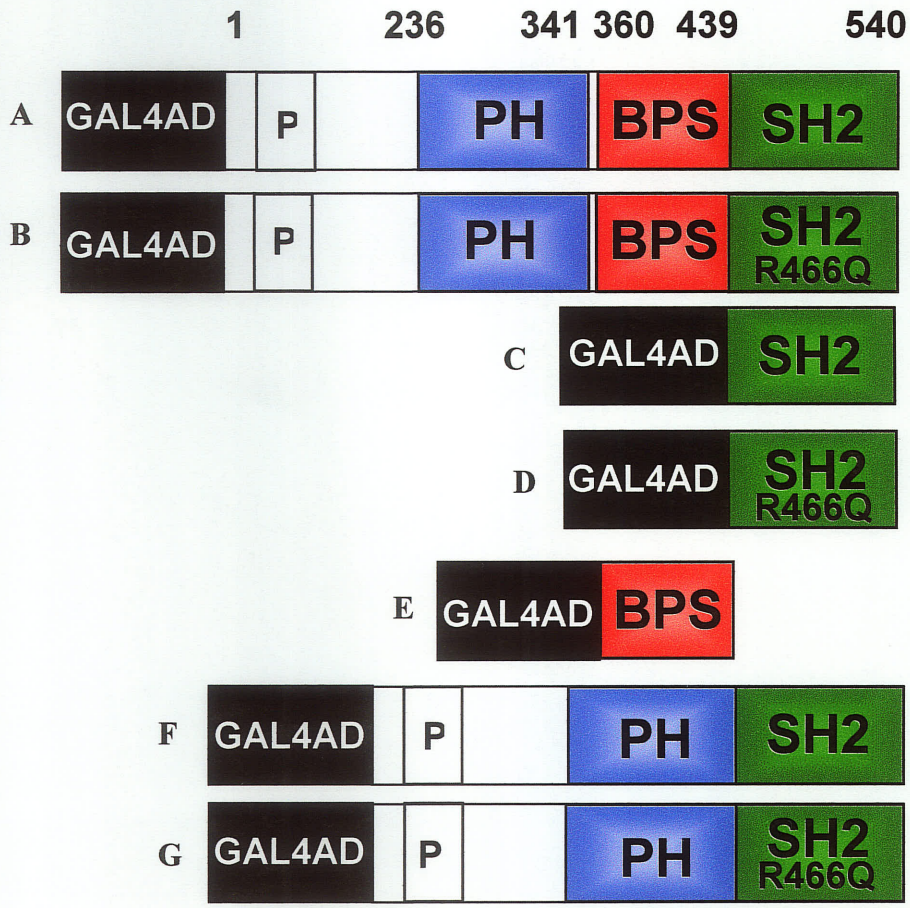

IRK Active		IRK Inactive	
Miller Units	Avg.%	Miller Units	Avg. %
12.5 38.4 26.5	100.0	0.0 0.0 0.0	0.0
3.1 8.3 6.1	26.3 ± 2.1	0.0 0.0 0.0	0.0
1.3 1.2 1.6	7.2 ± 2.2	0.0 0.0 0.0	0.0
0.0 0.0 0.1	0.2 ± 0.2	0.0 0.0 0.0	0.0
0.0 0.0 0.0	0.0 ± 0.0	0.0 0.0 0.0	0.0
1.8 3.4 3.5	12 ± 2.3	0.0 0.0 0.0	0.0
0.2 0.0 0.1	0.6 ± 0.6	0.0 0.0 0.0	0.0

Figure 11. Interaction of hGrb14 full-length and sub-domain GAL4AD fusion proteins with the IRK in yeast. β-galactosidase assays were performed on KGY37 yeast co-transformed with either GAL4BD::IRK active or GAL4BD::IRK inactive and the GAL4AD plasmid with all or part of the hGrb14 cDNA. The specific GAL4AD::hGrb14 fusions that were analyzed are: (A) full length wild-type, (B) full length R466Q, (C) SH2 domain, (D) SH2 domain R466Q, (E) BPS domain, (F) BPS dropout, (G) BPS dropout R466Q. The hGrb14 full-length protein structure with the numbering of the predicted amino acid bounding the domain is shown above the diagram. β-galactosidase assay interaction values from three separate trials represented in Miller Units are shown in three colour codes, trial one (blue), two (red), three (green). The mean ± SD values from the three trials were calculated and shown as a percentage of the full-length hGrb14 value (set to 100%).

domain of the IRK was inactivated by substituting the tyrosines (Y) at positions 1046, 1050, and 1051 with phenylalanine (F) residues [71]. The GAL4BD::IRK-inactive fusion protein showed no interaction with full-length hGrb14 (Fig. 11), indicating that the IR must be autophosphorylated for hGrb14 to bind.

3.1.3 Analysis of the role of the SH2 domain in the hGrb14-IR interaction

Several lines of evidence suggest the SH2 domain of hGrb14 plays an important role in binding to the IR. First, the initial hGrb14 fragment that was identified to bind the IR in a yeast two-hybrid screen was primarily comprised of the SH2 domain [61]. Second, when the R466Q of the SH2 domain was introduced into full-length hGrb14, it significantly reduced the ability of hGrb14 to interact with the IR. The expression levels of the wild-type and mutant hGrb14 proteins were similar in yeast (Fig. 26A, shown later). Third, Kasus-Jacobi *et al* (1998) showed that the SH2 domain of the rGrb14 could mediate the interaction with the IR. Finally, because SH2 domains recognize pTyr, they are explicitly involved in tyrosine kinase signaling pathways and proteins containing SH2 domains bind selectively to autophosphorylation sites on tyrosine kinase receptors [72]. Previously, we demonstrated that the C-terminal region (aa 373-540) of human Grb14, which encodes the SH2 domain, showed a strong interaction with the IR [61]; however, this construct unknowingly contained a portion of the BPS domain. We referred to this construct as GAL4AD::bps+SH2 and it was designed before the identification of the BPS domain. Therefore, to avoid any interference from residual BPS regions, we created a GAL4AD fusion construct that contained solely the SH2 domain (Fig. 12) and tested its

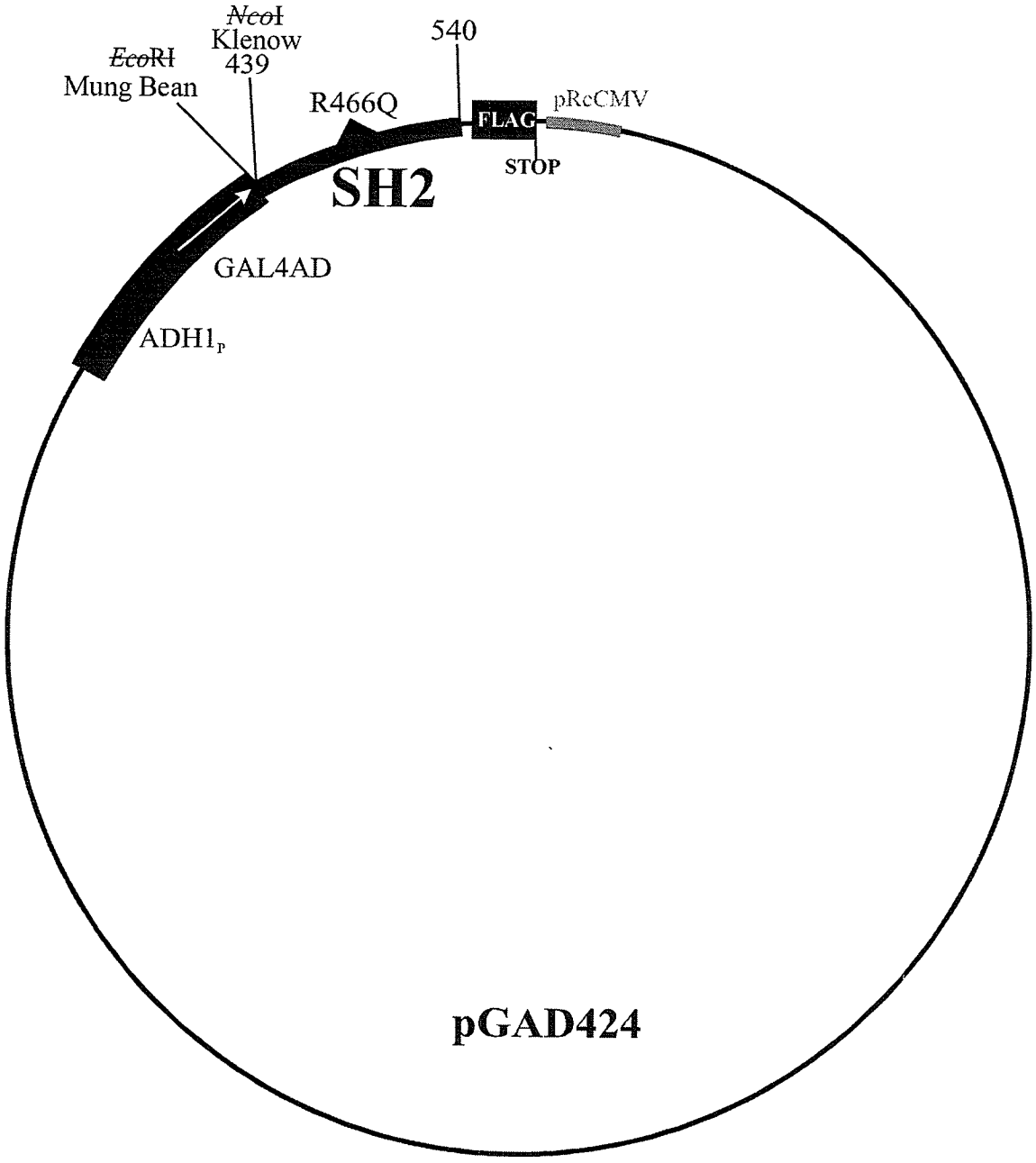

Figure 12. **Diagram of the pGAD424::SH2 vector.** To create the GAL4AD::SH2 domain (aa 439-540) construct, the pGAD424::hGrb14$_F$ vector was digested with *Nco*I and the ends were filled with Klenow. This linearized plasmid was then digested with *Eco*RI, treated with Mung Bean exonuclease, and re-circularized. The pGAD424::hGrb14 R466Q was treated similarly to create the pGAD424::SH2 R466Q construct. The position of the R466Q substitution is indicated by a solid triangle; the strike-out text indicates restriction sites destroyed during cloning.

ability to bind to the IR in the yeast two-hybrid system. Yeast two-hybrid experiments showed that the SH2 domain of hGrb14 alone interacted with the IR, albeit at a significantly reduced level (7.2%), compared to that of full-length hGrb14 (Fig. 11). In terms of protein expression, levels of the SH2 sub-domain protein were much higher that that of the full-length hGrb14 (Fig. 27A, shown later).

In order to confirm the importance of the SH2 domain in the interaction with the IR, the contribution of this domain to the binding ability of hGrb14 to the IR was eliminated using mutagenesis experiments. Previously, it has been shown that substitution of the arginine 466 of the conserved FLVR(D/E)S motif of the SH2 domain with a glutamine (Q) residue in the full-length hGrb14 protein reduced the interaction with the IR to 26.3% [61]. Interaction of the pGAD424::hGrb14 R466Q construct with the active IRK was repeated in this experiment to allow for comparison with other two-hybrid interaction values; it was found to have a similar interaction value (26.3%)(Fig. 11). In contrast, the Kasus-Jacobi group reported a much stronger interaction for the rat Grb14 R466Q and the IR (93% of the level of wild-type rGrb14 and the IR) [56]. In the previous yeast two-hybrid assay carried out by Hemming *et al* (2001), the R466Q mutation was also introduced into the GAL4AD::bps+SH2 construct, which contains a portion of the BPS domain. In this experiment, the interaction of this fusion protein with the IR was reduced by fourteen fold, but the interaction was not abolished as the partial BPS region encoded in this construct could still actively interact with the IR [61]. Therefore, in this work the R466Q mutation was introduced into a newly constructed GAL4AD::SH2 fusion protein that did not include any portion of the BPS domain (Fig. 12). When the R466Q mutation

in the SH2 domain was introduced, this modification abolished the interaction with the IR (Fig. 11), a finding consistent with that for the rGrb14 SH2 R466Q mutant interaction with the IR [56]. The expression levels of the mutant SH2 sub-domain proteins were greatly reduced compared to the wild-type SH2 domain levels and SH2 mutant protein levels more closely resembled those for the wild-type full-length hGrb14 proteins (Fig. 27A, shown later). The results from the SH2 domain R466Q mutation experiment suggest that arginine 466 plays a critical role in the interaction between the SH2 domain of hGrb14 and the IR. The significance of this finding lies in the principle that single amino acid substitutions provide insights into the native function of the protein; if the single amino acid substitution abolishes a certain function of the protein or the domain of a protein, this is an indication of the role of this protein or its protein domain [65].

3.1.4. Identification of a second hGrb14 domain involved in IR binding

Since the SH2 domain alone accounted for only a fraction of the ability of hGrb14 to bind to the IR there was likely another region of hGrb14 involved in this interaction. This idea was consistent with findings by Kasus-Jacobi *et al* (1998) who identified the BPS domain as a second binding domain of rGrb14 [56]. Previously, it was shown that both the SH2 and BPS domains of hGrb10 interact with the IR [43] and the rGrb14 BPS domain alone interacted strongly with the IR [56]. To test the ability of regions of hGrb14 other than the SH2 domain to interact with the IR, we created constructs encoding hGrb14 sub-domains. In order to clone the individual hGrb14 sub-domains, it was necessary to define their respective boundaries using a multiple alignment of the sequences of the Grb7

family of proteins (Fig. 13) (Section 2.6). The hGrb14 sequence (aa 1-540) was aligned against the human (h), rat (r), and mouse (m), Grb7/10/14 protein sequences. The alignment of the hGrb14 protein sequence with mouse and rat Grb14 showed 86% and 85% amino acid identity, respectively. hGrb14 bears 51-52% and 45-46% amino acid identity, respectively, with the Grb10 and Grb7 protein members. Based on the identity of family members, a dendrogram for the Grb7 family of proteins was constructed (Fig. 14). With the multiple alignment strategy, The PH, BPS, and SH2 domain boundaries were identified in a similar fashion as was described previously for the PH and SH2 domain alignment of hGrb14, mGrb7, and mGrb10 by Daly *et al* (1996).

3.1.5. Bioinformatic analysis of the BPS domain

When seeking to elucidate the function of an uncharacterized protein, the first step is to determine if the protein has sequence identity to other sequences in a protein database. If protein sequences are very similar, and that matched protein has an assigned function, one can infer a similar function for the unknown protein. To determine if the BPS domain of the hGrb14 protein was similar to any other known sequences, we performed a protein-protein BLAST search (Section 2.7). The BLAST search of the non-redundant (nr) protein database and EST database using the hGrb14 BPS domain sequence (aa 360-438) resulted in matches to the Grb7, Grb10, and Grb14 protein sequences from human, mouse, and rat. This indicated that other than in the Grb7 protein family, the BPS sequence is not conserved in any other known proteins (Fig. 15).

```
mGrb10  ------------------------------------------------MNNDINSSVESL 12
hGrb10  MQAAGPLFRSKDKVEQTPRSQQDPAGPGLPAQSDRLANHQEDDVDLEALVNDMNASLESL 60
rGrb14  ------------------------------------------------MTTSLQDG 8
mGrb14  ------------------------------------------------MTTSLQDG 8
hGrb14  ------------------------------------------------MTTSLQDG 8
mGrb7   ------------------------------------------------MELDLSPT 8
rGrb7   ------------------------------------------------MELDLSPS 8
hGrb7   ------------------------------------------------MELDLSPP 8
                     :  .:.

mGrb10  NSACNMQSDTDTAPLLEDGQHASNQGAASSSRG--QPQASPRQKMQRSQPVHIL--RRLQ 68
hGrb10  YSACSMQS--DTVPLLQNGQHARSQPRASGPPRSIQPQVSPRQRVQRSQPVHILAVRRLQ 118
rGrb14  QSAAGRAGAQDSPLAVQVCRVAQGKGDAQDPAQ--VPGLHA--LSPASDATRRGAMDRRK 64
mGrb14  QSAAGRAGAQDSPLAVQVCRVAQGKGDAQDPAQ--VPGLHA--LSPASDATLRGAIDRRK 64
hGrb14  QSAASRAAARDSPLAAQVCGAAQGRGDAHDLAP--APWLHARALLPLPDGTRGCAADRRK 66
mGrb7   HLSS---SPEDVCPTPATPPETPPPPDNPPPGD-----------VKRSQPLPIPSS-RKL 53
rGrb7   HLSS---SPEDVCPTPGTPPETPPPPDNPPPGD-----------VKRSQPLPIPSS-RKL 53
hGrb7   HLSS---SPEDLCPAPGTPPGTPRPPDTPLPEE-----------VKRSQPLLIPTTGRKL 54
          :.    .  *  :          .:         *

mGrb10  EEDQQLRTASLPAIPNPFPELTGAAPGSPPSVAPSSLPPPPSQPPAKHCGRCEKWIPGEN 128
hGrb10  EEDQQFRTSSLPAIPNPFPELCG--PGSPPVLTPGSLPP--SQAAAK------------- 161
rGrb14  AKD--LEVQETPSIPNPFPELCCS--PLTSVLSAGLFPR--SNSRKK------------- 105
mGrb14  MKD--LDVLEKPPIPNPFPELCCS--PLTSVLSAGLFPR--ANSRKK------------- 105
hGrb14  KKD--LDVPEMPSIPNPFPELCCS--PITSVLSADLFPK--ANSRKK------------- 107
mGrb7   REEE-FQATSLPSIPNPFPELCSP-PSQKPILGGSSGARGLLPRDSSR------------ 99
rGrb7   REEE-FQATSLPSIPNPFPELCSP-PSQKPILGGSSGARGLLPRDSSR------------ 99
hGrb7   REEE-RRATSLPSIPNPFPELCSP-PSQSPILGGPSSARGLLPRDASR------------ 100
          ::    . . *.********       . :     .       .

mGrb10  TRGNGKRKIWRWQFPPGFQLSKLTRPGLWTKTTARFSKKQPKNQCPTDTVNPVARMPTSQ 188
hGrb10  ------------------------------------------------------------
rGrb14  ------------------------------------------------------------
mGrb14  ------------------------------------------------------------
hGrb14  ------------------------------------------------------------
mGrb7   ------------------------------------------------------------
rGrb7   ------------------------------------------------------------
hGrb7   ------------------------------------------------------------
```

Figure 13. Multiple sequence alignment of Grb7/10/14 protein sequences. An alignment of human (h), rat (r), and mouse (m) Grb7/10/14 sequences was generated using CLUSTALW. The GenBank Accession numbers for the aligned sequences are: hGrb14 (NP_004481), mGrb14 (NM_016719), rGrb14 (NP_113811), hGrb10 (XM_033762), mGrb10 (NP_034475), hGrb7 (XP_012695), mGrb7 (NP_034476), rGrb7 (NP_445855). The N-terminal conserved (P(S/A)IPNPFPEL) region is boxed, the PH domain is shown in blue, the BPS domain in red, and the SH2 domain in green text. The consensus sequence is indicated below the aligned sequence using symbols for (*) conserved residues, (:) conserved substitutions, (.) semi-conserved substitutions.

Figure 13. Multiple sequence alignment of Grb7/10/14 protein sequences (continued).

```
mGrb10   AQSAALEEGHAWRN-GSTRMNILSS-QSPLHPSTLNAVIHRTQHWFHGRISREESHRIIK 535
hGrb10   AQSAALEEGHAWRK-RSTRMNILGS-QSPLHPSTLSTVIHRTQHWFHGRISREESHRIIK 502
rGrb14   ALSVAVEEGLAWRKKGCLRLGNHGSPTAPSQSSAVNMALHRSQPWFHHRISRDEAQQLIT 452
mGrb14   ALSVAVEEGLAWRKKGCLRLGNHGSPSAPSQSSAVNMALHRSQPWFHHRISRDEAQRLII 452
hGrb14   ALSVAVEEGLAWRKKGCLRLGTHGSPTASSQSSATNMAIHRSQPWFHHKISRDEAQRLII 454
mGrb7    ALSAAMEEAQAWRKKTNHRL----SLPTTCSGSSLSAAIHRTQPWFHGRISREESQRLIG 449
rGrb7    ALSAATEEAQAWRKKTNHRL----SLPTPCSGLSLSAAIHRTQPWFHGRISREESQRLIG 449
hGrb7    ALSVALEEAQAWRKKTNHRL----SLPMPASGTSLSAAIHRTQLWFHGRISREESQRLIG 446
         * *.* **. ***:    *:    *   .    : . .:**:* *** :***:*::::*

mGrb10   QQGLVDGLFLLRDSQSNPKAFVLTLCHHQKIKNFQILPCEDDGQTFFTLDDGNTKFSDLI 595
hGrb10   QQGLVDGLFLLRDSQSNPKAFVLTLCHHQKIKNFQILPCEDDGQTFFSLDDGNTKFSDLI 562
rGrb14   RQGPVDGVFLVRDSQSNPRTFVLSMSHGQKIKHFQIIPVEDDGEVFHTLDDGHTKFTDLI 512
mGrb14   RQGPVDGVFLVRDSQSNPRTFVLSMSHGQKIKHYQIIPVEDDGELFHTLDDGHTKFTDLI 512
hGrb14   QQGLVDGVFLVRDSQSNPKTFVLSMSHGQKIKHFQIIPVEDDGEMFHTLDDGHTRFTDLI 514
mGrb7    QQGLVDGVFLVRESQRNPQGFVLSLCHLQKVKHYLILPSEDEGCLYFSMDEGQTRFTDLL 509
rGrb7    QQGLVDGVFLVRESQRNPQGFVLSLCHLQKVKHYLILPSEDEGCLYFSMDDGQTRFTDLL 509
hGrb7    QQGLVDGLFLVRESQRNPQGFVLSLCHLQKVKHYLILPSEEEGRLYFSMDDGQTRFTDLL 506
         :** ***:**:*:** **: ***::.* **:*:: *:* *::*  :.::*:*:*:*:**:

mGrb10   QLVDFYQLNKGVLPCKLKHHCIRVAL 621
hGrb10   QLVDFYQLNKGVLPCKLKHHCIRVAL 588
rGrb14   QLVEFYQLNKGVLPCKLKHYCARMAV 538
mGrb14   QLVEFYQLNRGVLPCKLKHYCARMAV 538
hGrb14   QLVEFYQLNKGVLPCKLKHYCARIAL 540
mGrb7    QLVEFHQLNRGILPCLLRHCCARVAL 535
rGrb7    QLVEFHQLNRGILPCLLRHCCARVAL 535
hGrb7    QLVEFHQLNRGILPCLLRHCCTRVAL 532
         ***:*:***:*:*** *:* * *:*:
```

Figure 13. Multiple sequence alignment of Grb7/10/14 protein sequences (continued). The conserved arginine at position 466 is highlighted in bold.

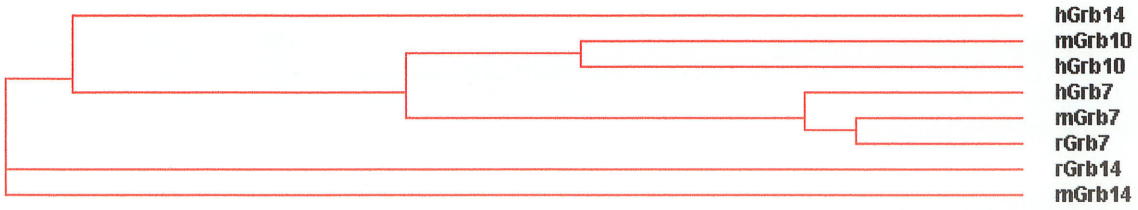

Figure 14. Dendrogram of the Grb7/10/14 protein sequences. Diagram of a sequence alignment tree generated using CLUSTALW for the Grb7 family protein sequences from human, mouse, and rat Grb7/10/14. Smaller tree branch lengths represent greater sequence conservation.

BLAST alignment Results:

	Score (bits)	E Value
>gi|17439452|ref|XP_010770.2| (XM_010770) growth factor receptor-bound protein 14 [Homo sapiens]	140	3e-33
>gi|4758478|ref|NP_004481.1| (NM_004490) growth factor receptor-bound protein 14 [Homo sapiens]	138	9e-33
>gi|13928858|ref|NP_113811.1| (NM_031623) growth factor receptor bound protein 14 [Rattus norvegicus]	126	5e-29
>gi|7710032|ref|NP_057928.1| (NM_016719) growth factor receptor bound protein 14 [Mus musculus]	108	1e-23
>gi|6754066|ref|NP_034476.1| (NM_010346) growth factor receptor bound protein 7 [Mus musculus]	70	5e-12
>gi|16758132|ref|NP_445855.1| (NM_053403) growth factor receptor binding protein GRB7 [Rattus norvegicus]	69	1e-11
>gi|4885355|ref|NP_005301.1| (NM_005310) growth factor receptor-bound protein 7 [Homo sapiens]	67	3e-11
>gi|2136153|pir||I39175 SH2-domain protein Grb-IR - human	67	3e-11
>gi|6166186|sp|Q13322|GRBA_HUMAN GROWTH FACTOR RECEPTOR-BOUND PROTEIN 10 (GRB10 ADAPTOR PROTEIN)	67	3e-11
>gi|13631633|ref|XP_012695.2| (XM_012695) growth factor receptor-bound protein 7 [Homo sapiens]	67	3e-11
>gi|1518101|gb|AAC50671.1| (U66065) Grb10- and Grb-IR-related splice variant 1 [Homo sapiens]	67	3e-11
>gi|4885353|ref|NP_005302.1| (NM_005311) growth factor receptor-bound protein 10 [Homo sapiens]	67	3e-11
>gi|16162157|ref|XP_033762.2| (XM_033762) growth factor receptor-bound protein 10 [Homo sapiens]	67	4e-11
>gi|1503998|dbj|BAA13198.1| (D86962) similar to mouse growth factor receptor-binding protein	67	4e-11
>gi|16359305|gb|AAH16111.1|AAH16111 (BC016111) Similar to growth factor receptor bound protein 10 [Mus	65	1e-10
>gi|2465447|gb|AAB72103.1| (AF022072) adapter protein [Mus musculus]	65	1e-10
>gi|6754064|ref|NP_034475.1| (NM_010345) growth factor receptor bound protein 10; maternally	64	4e-10
>gi|3256233|dbj|BAA29060.1| (AB008790) Grb7V protein [Homo sapiens]	62	1e-09

Figure 15. BPS domain BLAST query output. This query was performed using the standard protein-protein BLAST program with the default Expect value (E=10). The hGrb14 BPS sequence (aa 360-438) (Accession number: NP_004481) was compared to the nr (non-redundant) protein database and the output is shown.

Since the BPS domain sequence was only common between members of the Grb7 family of proteins, we wanted to determine the extent to which the BPS sequence was conserved between protein family members. Generally, protein domain sequences that are highly conserved between individual members of the same protein family encode functionally important domains. Using a multiple alignment, we tested the degree to which sequence identity was conserved between the BPS domain sequences from human, rat, and mouse Grb7/10/14 BPS protein sequences (Fig. 16). This alignment showed that the hGrb14 BPS domain had an amino acid identity of 87-89% with mouse and rat Grb14 and a 41-53% sequence identity with human, mouse, and rat Grb7 and Grb10 BPS protein sequences. Since the BPS domain is highly conserved among members of the Grb7 family of proteins, it could be inferred that this domain plays an important functional role.

3.1.6. Analysis of the role of the BPS domain in hGrb14-IR interaction

To test for an interaction between the BPS region of hGrb14 and the IR, the BPS domain alone (aa 360-438) was cloned into the GAL4AD plasmid (Fig. 17) and interaction of the GAL4AD::BPS fusion protein with the active IRK was tested using the yeast two-hybrid system. The BPS domain boundaries used in preparing this clone were selected based on the alignment of the Grb7 protein family members. No interaction between the GAL4AD::BPS fusion protein and the IR was detected. All two-hybrid experiments we carried out using the KGY37 yeast strain, which contained the yeast GAL4 operator to regulate *lacZ* expression (Fig. 6A). Since no interaction was detected between the BPS domain alone and the active IRK using the KGY37 strain, we also tested the same

A

```
hGrb14   360  CSSQSISPMRSISENSLVAMDFSGQKSRVIENPTEALSVA  399
mGrb14   358  CNSQSMSPMRSVSENSLVAMDFSGEKSRVIDNPTEALSVA  397
rGrb14   358  CSSQSVSPMRSVSENSLVAMDFSGQKTRVIDNPTEALSVA  397
hGrb10   416  LLSPFSTPVRSVSENSLVAMDFSGQTGRVIENPAEAQSAA  455
mGrb10   443  LPPPFNAPMRSVSENSLVAMDFSGQIGRVIDNPAEAQSAA  482
hGrb7    356  PSCLGSPPLRSASDNTLVAMDFSGHAGRVIENPREALSVA  395
mGrb7    359  LSYLGSPPLRSVSDNTLVAMDFSGHAGRVIDNPREALSAA  398
rGrb7    358  LSYLGSPPLRSVSDNTLVAMDFSGHAGRVIENPQEALSAA  397
                    .*:** *:*:********.  ***:** ** *.*

hGrb14   400  VEEGLAWRKKGCLRLGTHGSPTASSQSSATNMAIHRSQP  438
mGrb14   398  VEEGLAWRKKGCLRLGNHGSPSAPSQSSAVNMALHRSQP  436
rGrb14   398  VEEGLAWRKKGCLRLGNHGSPTAPSQSSAVNMALHRSQP  436
hGrb10   456  LEEGHAWRK-RSTRMNILGS-QSPLHPSTLSTVIHRTQH  494
mGrb10   483  LEEGHAWRN-GSTRMNILSS-QSPLHPSTLNAVIHRTQH  521
hGrb7    396  LEEAQAWRKKTNHRL----SLPMPASGTSLSAAIHRTQL  434
mGrb7    399  MEEAQAWRKKTNHRL----SLPTTCSGSSLSAAIHRTQP  437
rGrb7    398  TEEAQAWRKKTNHRL----SLPTPCSGLSLSAAIHRTQP  436
               **. ***:    *:    *   .    : . .:**:*
```

B

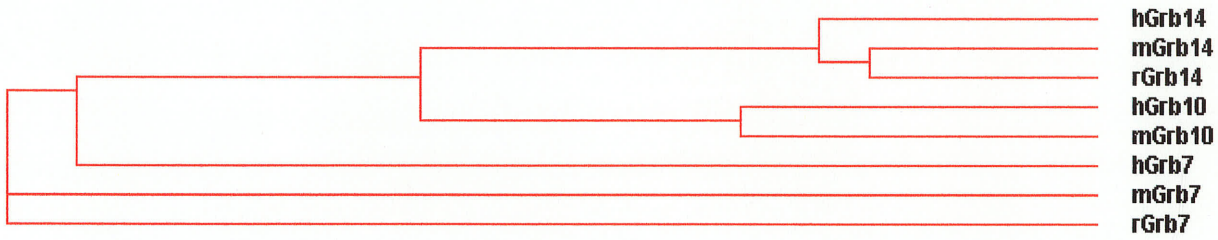

Figure 16. Multiple sequence alignment of the Grb7/10/14 BPS domain. (A) An alignment of human (h), rat (r), and mouse (m) Grb7/10/14 BPS domain sequences was generated with CLUSTALW. The GenBank Accession numbers for the aligned sequences are: hGrb14 (NP_004481), mGrb14 (NM_016719), rGrb14 (NP_113811), hGrb10 (XM_033762), mGrb10 (NP_034475), hGrb7 (XP_012695), mGrb7 (NP_034476), rGrb7 (NP_445855). The consensus sequence is indicated below the aligned sequences using symbols for: (*) conserved residues (:) conserved substitutions, (.) semi-conserved substitutions. Conserved arginine (R) residues are highlighted in red, conserved lysine (K) residues are highlighted in blue. The arginine residues (**R**) that were candidates for substitution mutation **R**369Q and **R**387Q are shown in bold. (B) Dendrogram generated using CLUSTALW for the BSP domain of the Grb7 family protein sequences from human, mouse, and rat Grb7/10/14.

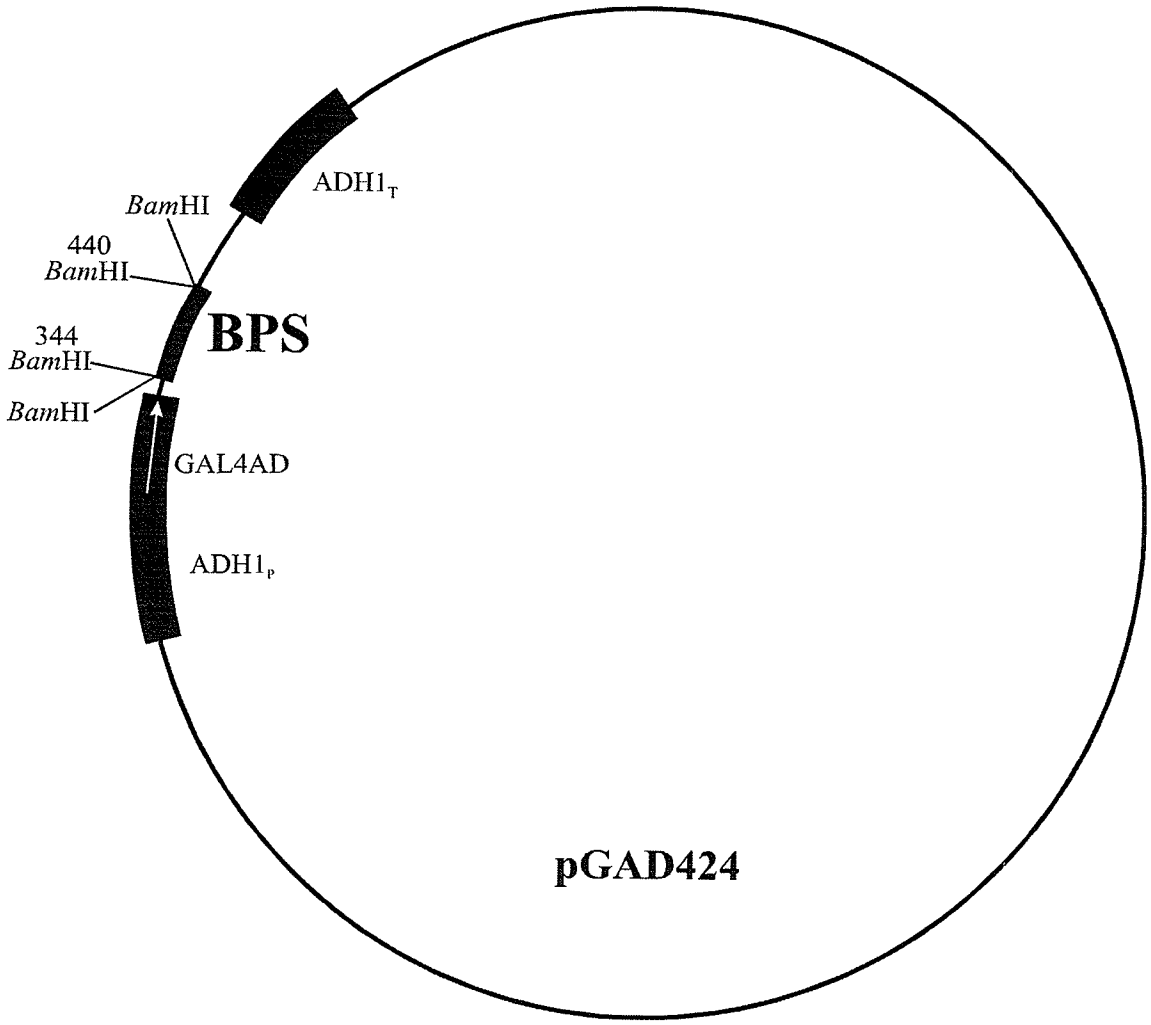

Figure 17. Diagram of the pGAD424::BPS vector. The BPS domain construct was created by amplifying the BPS domain region (aa 360-438) using the WPG230/WPG234 primers that contained 5' *Bam*HI restriction sites. This PCR fragment was inserted into pCR2.1, and then excised at the flanking *Bam*HI sites. The resulting fragment was ligated into the *Bam*HI-digested pGAD424 vector.

interaction using the KGY94 yeast strain. This yeast strain contained bacterial *lexA*, a strong promoter that is recognized by the lexA Binding Domain (BD) encoded within the pBTM116 vector (Fig. 6C), allowing a higher expression level of reporter genes. After transforming the GAL4AD::BPS construct along with the pBTM116:IRK active plasmid (a gift from Dr. RD. Gietz) into the KGY94 yeast strain no interaction between these proteins was found. These results suggested that we had not yet identified the minimal BPS domain had not yet been identified or that the isolated BPS domain was not properly folded. Subsequent studies that showed that the expression of the isolated BPS domain was very weak compared to the full-length hGrb14 protein expression supported the idea that this fusion protein was unstable and potentially poorly folded (Fig. 27B, shown later).

In another approach to test for the BPS-IR interaction, we reversed the bait and target proteins in the two-hybrid system by inserting the BPS domain region into the GAL4 Binding Domain vector, pGBT9 (Fig. 18). Consistent with our other findings, we observed no interaction between the GAL4AD::IRK and GAL4BD::BPS fusion proteins. Our results showed no interaction between the hGrb14 BPS domain alone and the IR which is contradictory to several findings including those from Kasus-Jacobi *et al* (1998) showing that the rGrb14 BPS domain alone (aa 358-436) interacted strongly (73%) with the IR [56], those from He *et al* (1998), which reported that the BPS domain alone (aa 358-434) of the hGrb10 protein did indeed interact with the IR (44%)[43], and those from Kasus-Jacobi *et al* (2000) showing an 18% interaction between the BPS domain of Grb7 (aa 345-438) and the IR [36].

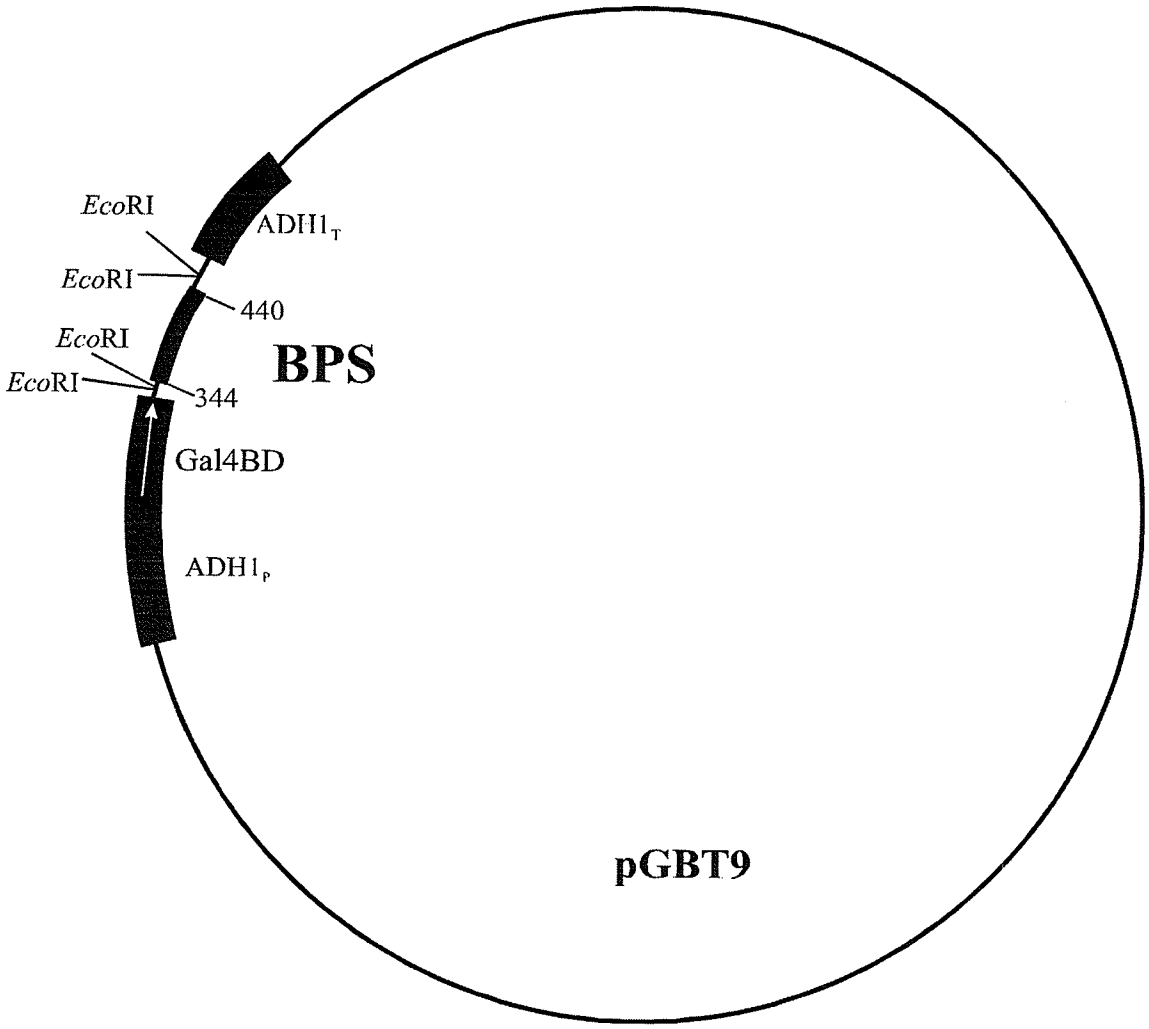

Figure 18. Diagram of the pGBT9::BPS vector. The pGBT9::BPS domain construct was created using the pCR2.1::BPS clone from the pGAD424::BPS cloning strategy (Fig. 17). The insert was excised at flanking *Eco*RI restriction sites and inserted into the *Eco*RI-digested pGBT9 vector. The pGBT9 vector contained the GAL4 Binding Domain (BD).

Since the BPS domain alone showed no interaction with the IR in the two-hybrid system, we created pGAD424 constructs containing either the complete or partial PH domain region adjacent to the BPS domain (Fig. 19, 20) to test whether the region upstream of and including the BPS domain interacted with the IR. Once carried out, these experiments showed that neither the PH+BPS nor the ½ PH+BPS GAL4AD fusion proteins showed any interaction with the kinase active IR in the yeast two-hybrid system (data not shown).

Since our results showing that neither the BPS domain alone nor the isolated PH+BPS region produced any interaction with the IR, we wanted to test the effect of deleting the BPS domain from the full-length hGrb14 on hGrb14-IR binding. The BPS domain was therefore removed from the full-length hGrb14 cDNA and the resulting BPS dropout fragment was inserted into the pGAD424 vector (Fig. 21). When tested in the two-hybrid system, the interaction between the hGrb14 BPS dropout fusion protein and the IR in was found to be much weaker (12%) than that of the full-length hGrb14 protein (100%); however, it was only marginally stronger than that with the SH2 domain alone (7.2%)(Fig. 11). Expression levels of BPS dropout fusion protein were similar to those measured for full-length hGrb14 (Fig. 27A, shown later). This result suggested that by removing the BPS domain from full-length hGrb14 it compromised the ability of hGrb14 to bind with the IR, indicating that the BPS domain plays a significant role in binding or cannot fold as an isolated peptide. However, as we were unable to detect an interaction between the isolated BPS domain and the IR, it seems that the hGrb14 BPS domain requires the SH2 domain to effect binding. When the SH2 domain was completely

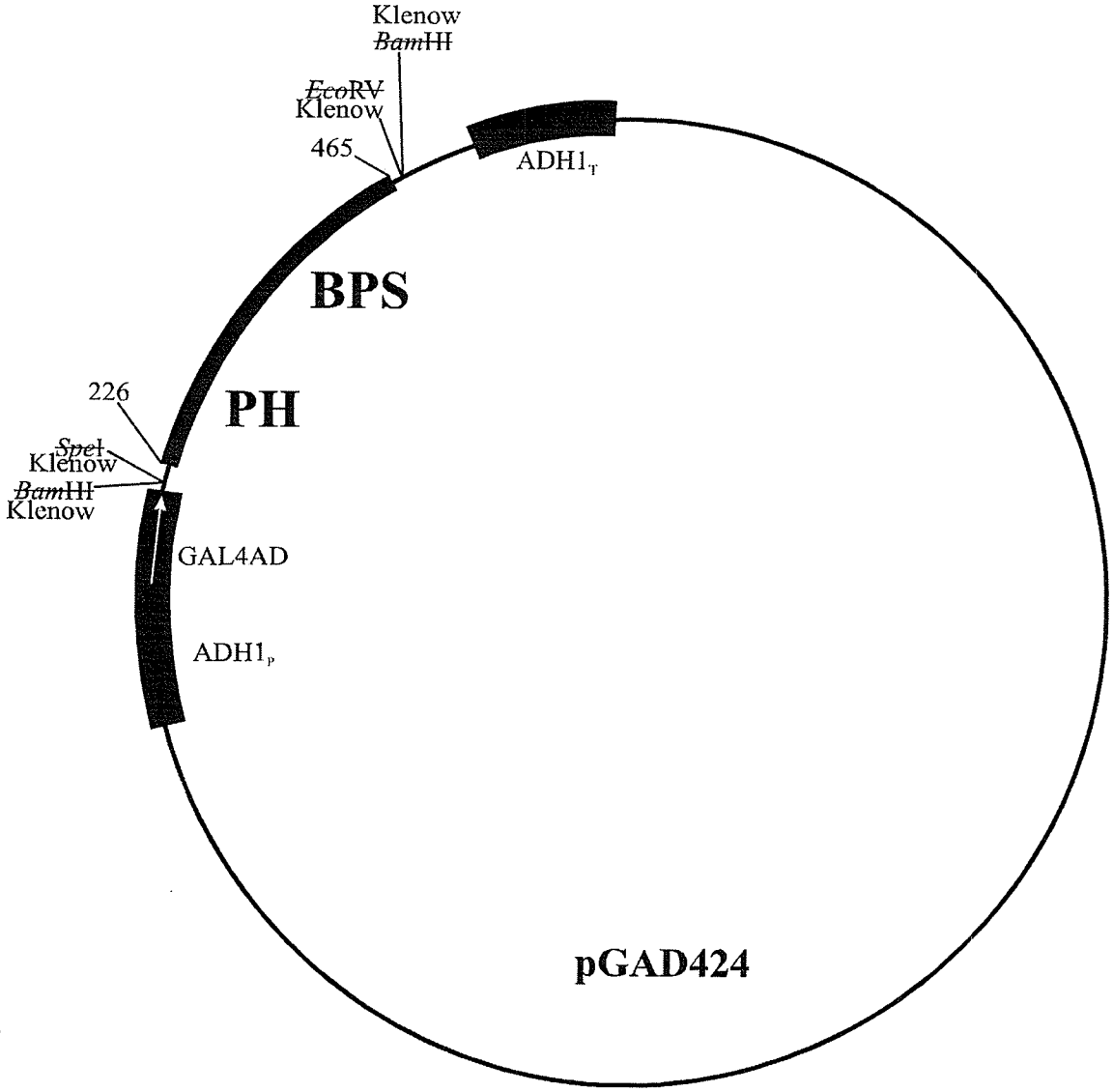

Figure 19. Diagram of the pGAD424::PH+BPS vector. The PH+BPS region (aa 226-465) was PCR amplified from the pRcCMV::hGrb14$_F$ vector using the WPG246/WPG279 primers and inserted into the pCR2.1 vector. The PH+BPS region insert was excised from pCR2.1 using *SpeI*/*Eco*RV restriction sites and then blunt-end ligated into the *Bam*HI-digested pGAD424 vector.

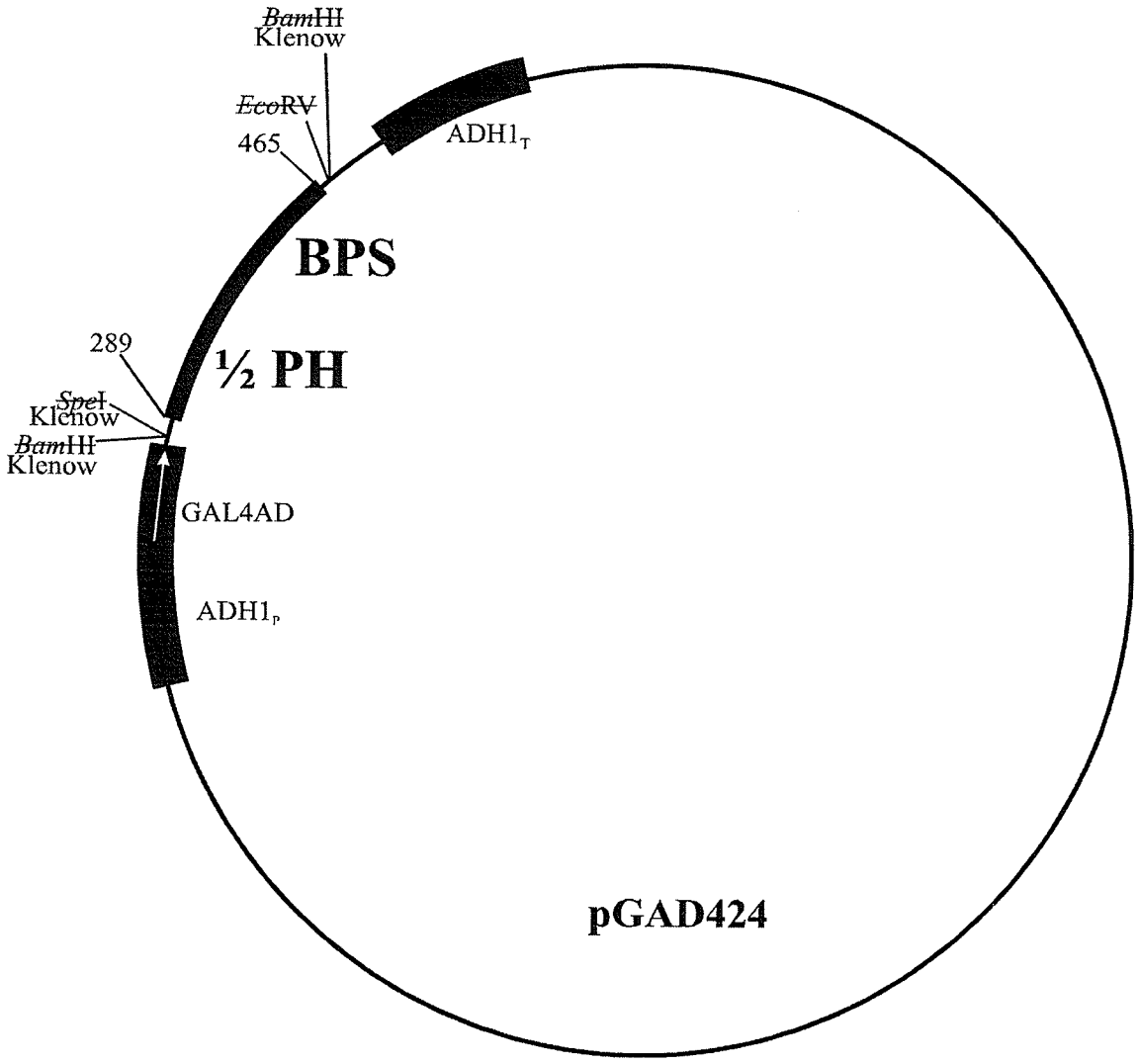

Figure 20. Diagram of the pGAD424::½ PH+BPS vector. The ½ PH+BPS region (289-465 aa) was PCR amplified from pRcCMV::hGrb14$_F$ using the WPG295/WPG279 primers and excised into the pCR2.1 vector. The ½ PH+BPS region insert was then excised from pCR2.1 with *Spe*I/*Eco*RV and blunt-end ligated into the *Bam*HI-digested pGAD424 vector.

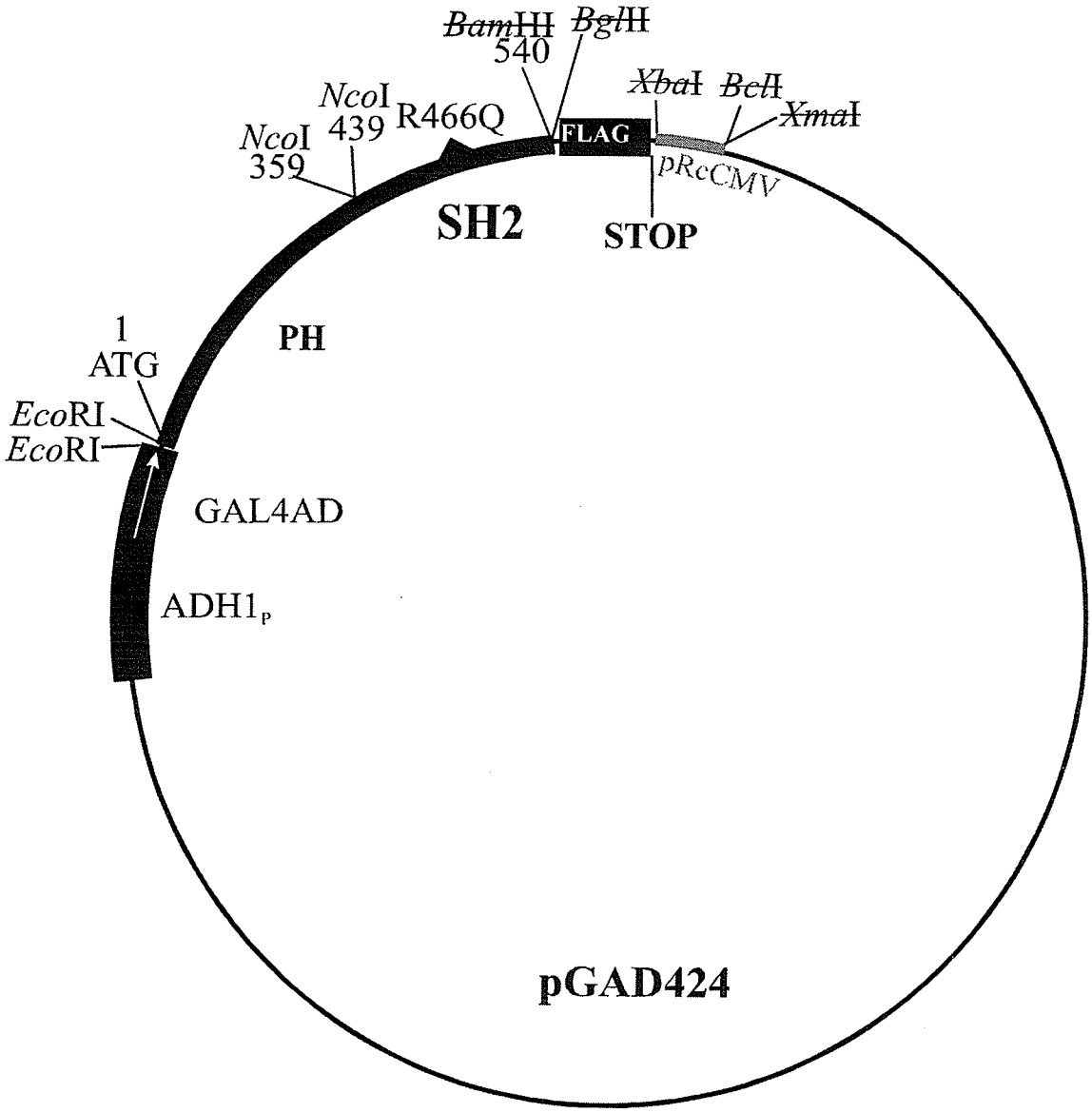

Figure 21. Diagram of the pGAD424::BPS dropout vector. A construct encoding the hGrb14 cDNA sequence lacking the BPS domain was created by PCR amplifying the PH domain region (aa 236-359) using forward primer WPG314 containing an *Eco*RI overhang site and reverse primer WPG324 containing an *Nco*I overhang site. This 1076 bp PCR-product was digested with *Eco*RI/*Nco*I and inserted into the *Eco*RI/*Nco*I-digested pGAD424::hGrb14$_F$ vector, which upon digestion contains only the SH2 domain (439-540 aa) of hGrb14. The PCR amplified *Eco*RI/*Nco*I-digested PH region (aa 236-359) was also inserted into the *Eco*RI/*Nco*I-digested pGAD424::hGrb14$_F$ R466Q vector to generate the pGAD424::BPS dropout R466Q construct. The position of the R466Q substitution is indicated by a solid triangle.

inactivated by introducing the R466Q substitution into the hGrb14 BPS dropout construct, there was little or no (0.6%) interaction with the IR. The expression levels of the BPS dropout fusion protein containing the R466Q mutation were reduced compared to levels of the non-mutated BPS dropout (Fig 27A, shown later). This result suggested that when the BPS domain was deleted and the SH2 domain was functionally inactivated by mutagenesis, the binding ability of the hGrb14 molecule was abolished. This was a novel approach for the examination of the hGrb14-IR interaction and has not been tested with other Grb7 family members.

3.1.7. Analysis of the interaction of the BPS+SH2 domain fusion protein with the IR

Having been unable to demonstrate an interaction between the BPS domain and the IR, we continued to study this interaction by creating a construct encoding both the BPS and SH2 domains (Fig. 22). The pGAD424::BPS+SH2 construct was transformed along with the pGBT9::IRK active plasmid into yeast and two-hybrid studies showed that the BPS+SH2 fusion protein only accounted for approximately half (47.6%) the interaction between hGrb14 and the IR (Fig. 23). However, this interaction was significantly stronger than that for the SH2 domain alone (7.2%)(Fig. 11). Expression levels of the BPS+SH2 fusion proteins were similar to those measured for full-length hGrb14 (Fig. 27A, shown later). Our results for the hGrb14 BPS+SH2-IR interactions were considerably lower than previously reported between the IR and the BPS+SH2 domain constructs for rGrb14 (134%) [56] and hGrb10 (129%) [43].

Figure 22. **Diagram of the pGAD424::BPS+SH2 vector.** The BPS region (aa 344-438) was PCR amplified from pRcCMV::hGrb14$_F$ using forward primer WPG294, which contains a 5' *Mfe*I site, and reverse primer WPG234. The 304 bp PCR product was digested with *Mfe*I/*Nco*I and ligated into the *Eco*RI/*Nco*I-digested pGAD424::hGrb14$_F$ vector, which contains the SH2 domain (aa 439-540). The *Eco*RI and *Mfe*I restriction sites are compatible with each other. The BPS domain R369Q substitution was introduced into the pGAD424::BPS+SH2 by PCR amplification. Forward oligonucleotide WPG294 containing a 5' *Mfe*I site and reverse mutant oligonucleotide WPG279 as well as reverse oligonucleotide WPG106 with forward mutant primer WPG296 were used to amplify the 307 and 682 bp PCR products, respectively, from pGAD424::hGrb14$_F$. These products were used as templates in a PCR reaction containing only the outer primers WPG294 and WPG106 to create a fused 722 bp product. This PCR product was inserted into pCR2.1 and the 290 bp *Mfe*I/*Nco*I fragment was excised, and used in place of the wild-type BPS domain from the *Eco*RI/*Nco*I-digested pGAD424::hGrb14$_F$ vector to create the pGAD424::BPS+SH2 R369Q construct. The R387Q BPS mutation was generated as described for the pGAD424::BPS+SH2 R369Q plasmid except that the PCR amplification was carried out using the reverse mutant WPG299 primer and the forward mutant WPG298 primer. The positions of the R369Q and R387Q substitutions are indicated by solid triangles. The pGAD424::BPS+SH2 R466Q construct was created by inserting the *Mfe*I/*Nco*I-digested PCR product from the BPS+SH2 cloning strategy into the *Eco*RI/*Nco*I-digested pGAD424::hGrb14$_F$ R466Q vector. BPS+SH2 constructs which contain R369Q or R387Q plus the R466Q SH2 domain substitution were created as described above except that the *Mfe*I/*Nco*I fragment cleaved from the pCR2.1 was used to replace the BPS domain fragment in the pGAD424::hGrb14$_F$ R466Q SH2 mutant vector.

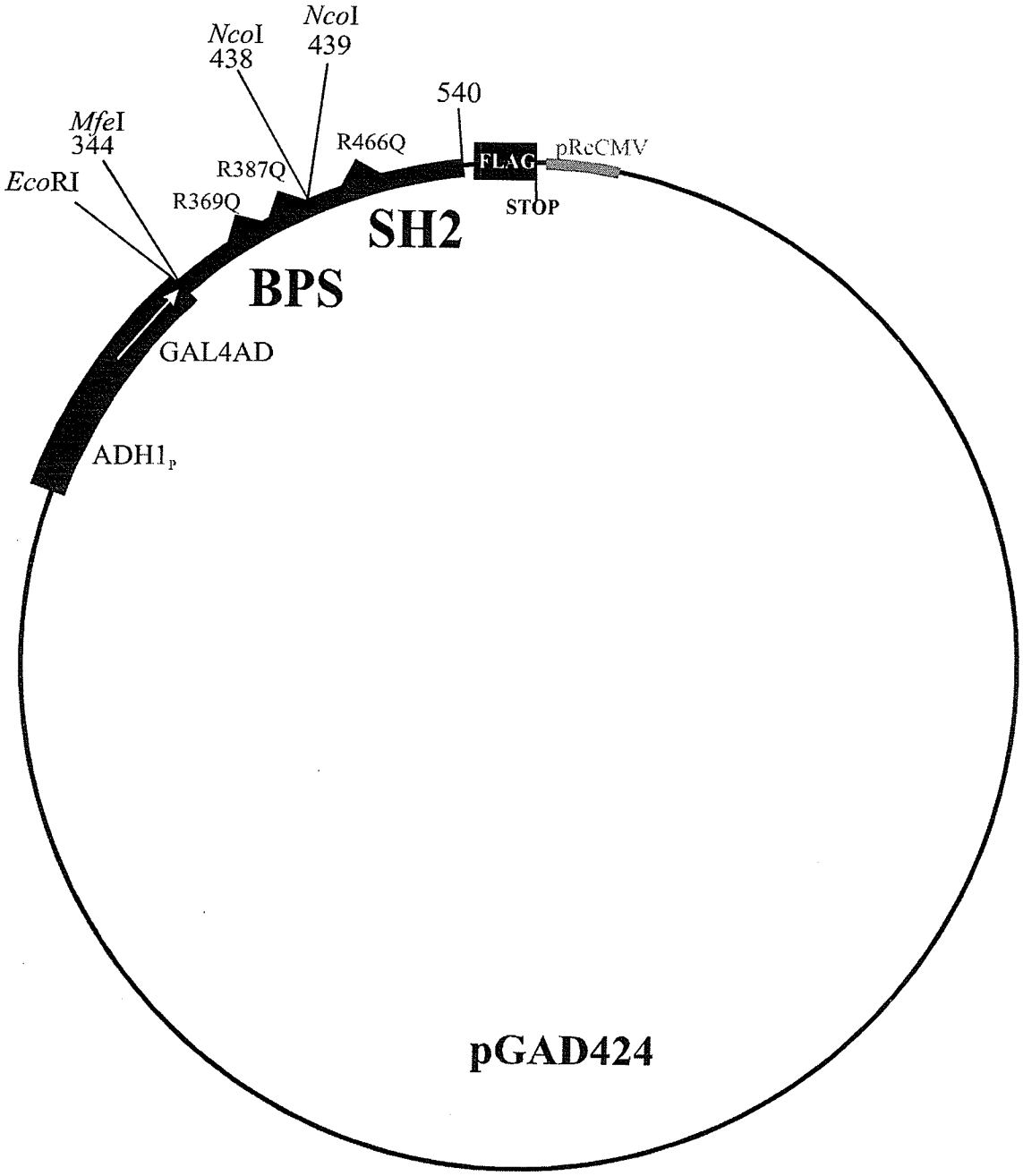
NcoI
438
NcoI
439
540
MfeI
344
R466Q
FLAG
pRcCMV
EcoRI
R387Q
R369Q
STOP
SH2
BPS
GAL4AD
ADH1P
pGAD424

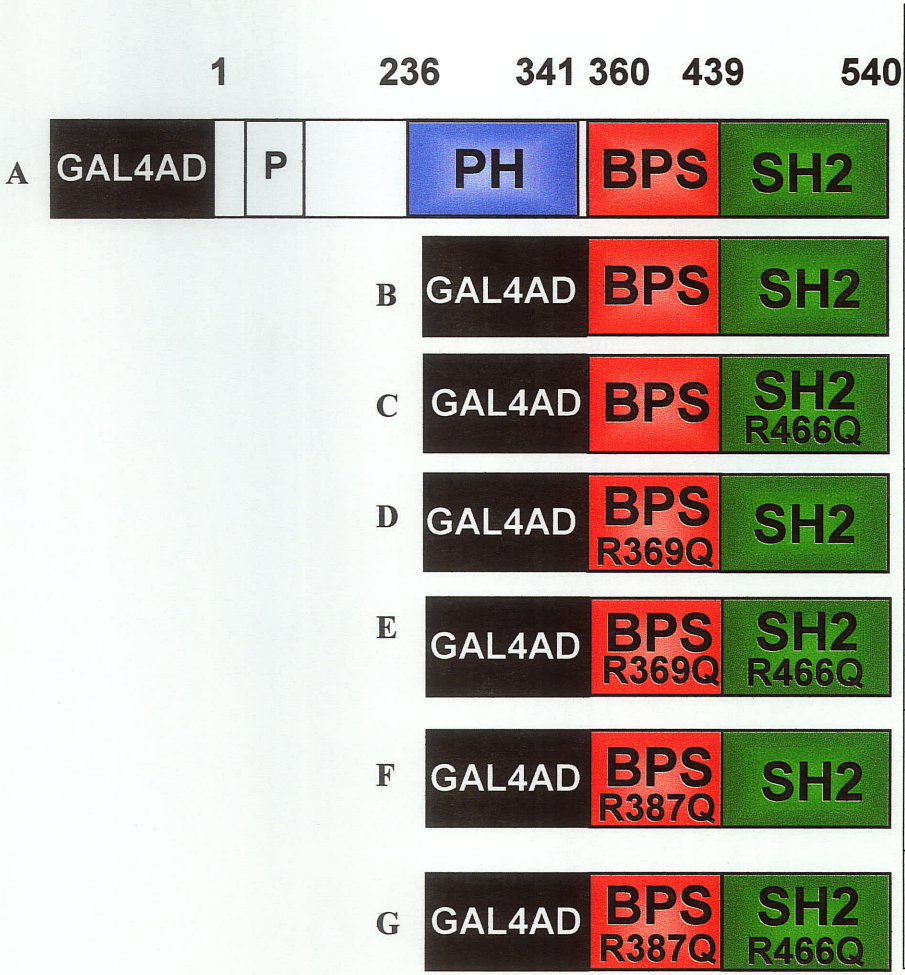

	IRK Active		IRK Inactive	
	Miller Units	Avg. %	Miller Units	Avg. %
A	12.5 38.4 26.5	100.0	0.0 0.0 0.0	0.0
B	6.2 22.8 12.3	47.6 ± 6.2	0.0 0.0 0.0	0.0
C	0.2 0.2 0.2	0.8 ± 0.5	0.0 0.0 0.0	0.0
D	3.8 12.8 10.4	33.3 ± 3.3	0.0 0.0 0.0	0.0
E	0.1 0.3 0.2	1.1 ± 0.7	0.0 0.0 0.0	0.0
F	2.5 7.3 7.8	23.6 ± 3.5	0.0 0.0 0.0	0.0
G	0.1 0.0 0.1	0.8 ± 0.8	0.0 0.0 0.0	0.0

Figure 23. **Interaction of the BPS+SH2 hGrb14 region with the IRK in yeast.** β-galactosidase assays were performed on KGY37 yeast cultures co-transformed with either GAL4BD::IRK active or GAL4BD::IRK inactive as well as GAL4AD::BPS+SH2 hGrb14$_F$ plasmids. The GAL4AD fusion constructs created were: (A) full-length hGrb14 (same construct as in Fig. 11) (B) BPS+SH2, (C) BPS+SH2 R466Q, (D) BPS+SH2 R369Q, (E) BPS+SH2 R369Q R466Q, (F) BPS+SH2 R387Q, (G) BPS+SH2 R387Q R466Q. β-galactosidase assay interaction values from three separate experiments reported in Miller Units are shown in three colour codes, experiment one (blue), two (red), three (green). The mean ± SD values from the three trials were calculated and shown as a percentage based on the full-length hGrb14 value (set to 100%).

To separate the relative contributions of the individual BPS and SH2 domains we tested the BPS+SH2 construct encoding the R466Q SH2 mutation, which essentially deactivated the SH2 domain. Our results revealed almost no interactions (0.8%) between the mutated BPS and SH2 R466Q construct and the IR (Fig. 23), indicating that although the hGrb14 BPS domain was involved in the binding of the protein to the IR, it required a functional SH2 domain to bind effectively. These findings, however, differed considerably from other studies measuring IR interactions with the BPS+SH2 R466Q construct from rGrb14 (62%) [56] and hGrb10 (101%) [43]. As discussed above, the discrepancy between our results and published work for rGrb14 and hGrb10 may be explained by a cooperative relationship between hGrb14 BPS and SH2 domain binding to the IR that is not present in rGrb14 or hGrb10. Taken together, the results for the BPS+SH2 domain fusion protein in the yeast two-hybrid system suggest that the hGrb14 BPS and SH2 domains function cooperatively in binding to the IR.

3.1.8. Identifying a key interacting residue in the BPS domain

In this work we have provided evidence establishing the importance of the hGrb14 BPS domain in its interaction with the IR. First, when we introduced the R466Q SH2 domain mutation into the full-length hGrb14, the resulting fusion protein still showed a 26.3% interaction with the IR, indicating that another hGrb14 domain was involved in binding, namely the BPS domain. Second, the BPS dropout protein showed decreased ability to bind the IR compared to full-length hGrb14. Finally, we showed that the BPS+SH2 fusion protein had a stronger binding ability that the SH2 domain alone. We therefore concluded that the BPS domain played an important role in the interaction of hGrb14

with the IR and we wanted to identify key amino acid residues within the BPS domain that mediated this interaction.

As a starting point for mutagenesis experiments to identify a critical residue in the BPS domain, we focused on the R466 residue of the SH2 domain, which belongs to a conserved FLV**R**(D/E)S motif. Since the hGrb14-IR interaction is IRK dependent, the actual binding interaction likely involves a negatively charged phosphorylated tyrosine residue from the IRK and a positively charged residue, such as an arginine from the hGrb14 protein. As previously shown, the R466 residue of the SH2 domain, when mutated, disrupts the interaction of hGrb14 with the IR [61]. Since a positively charged arginine residue of the hGrb14 SH2 domain played a key role in the interaction with the IR, we identified conserved arginine residues in the BPS domain using a multiple alignment of the BPS sequence (Fig. 16) which might play a key functional role for the BPS domain. Positively charged, conserved arginine (R) and lysine (K) residues were identified in the following positions: R369, R387, R407, K408, K409, R413, and R435. Two major conserved motifs in the BPS alignment were found, the first motif was P(M/V/L)RS(V/I)S(D/E)D(T/S)LVAMDFSG (aa 367-352), in which the R369 arginine residue was conserved and the second motif was RVI(D/E)NP, in which the R387 arginine residue was conserved. To assess the importance of these conserved residues, we created BPS mutant R369Q and R387Q constructs in the pGAD424::hGrb14 (Fig. 9) and pGAD424::BPS+SH2 vectors (Fig. 22) in which charged amino acids were substituted for two uncharged glutamine residues. Constructs were also created that contained the R369Q or R387Q BPS mutations along with the SH2 R466Q mutation to

determine if we could completely abolish the binding ability of hGrb14 by incorporating these two mutations.

For each mutant construct utilized for further experimentation, we first confirmed the presence of the BPS domain R369Q or R387Q substitutions and/or the R466Q SH2 domain substitution, using a PCR-based mutation detection strategy. PCR products encompassing the region of the target mutation site were digested with restriction enzymes having cut sites near the mutation and resulting DNA fragments were separated by PAGE. PCR products that were successfully cut using the appropriate restriction enzyme contained the desired mutation and could be distinguished from the larger wild-type products in which the same cut sites were absent resulting in larger uncut DNA that migrated more slowly during gel separations. This detection method showed that the desired R369Q, R387Q, and R466Q mutations were successfully generated in both the pGAD424 vectors containing full length or sub-domain hGrb14 inserts (Fig. 24).

3.1.9. Analysis of BPS-mutant hGrb14 fusion protein interaction with the IR

Having successfully created the BPS domain arginine to glutamine mutations in the full-length hGrb14 protein, we tested the effectiveness with which the mutated proteins could interact with the IR using the yeast two-hybrid system. Beginning with the full-length hGrb14 pGAD424::hGrb14 R369Q, we detected a strong (92%) interaction with the IR compared to the wild-type hGrb14 (Fig. 25). Mutation of the other conserved arginine residue in the BPS domain (R387Q) resulted in a much more attenuated interaction (26.4%) with the IR. When the R369Q BPS mutation was combined with the R466Q

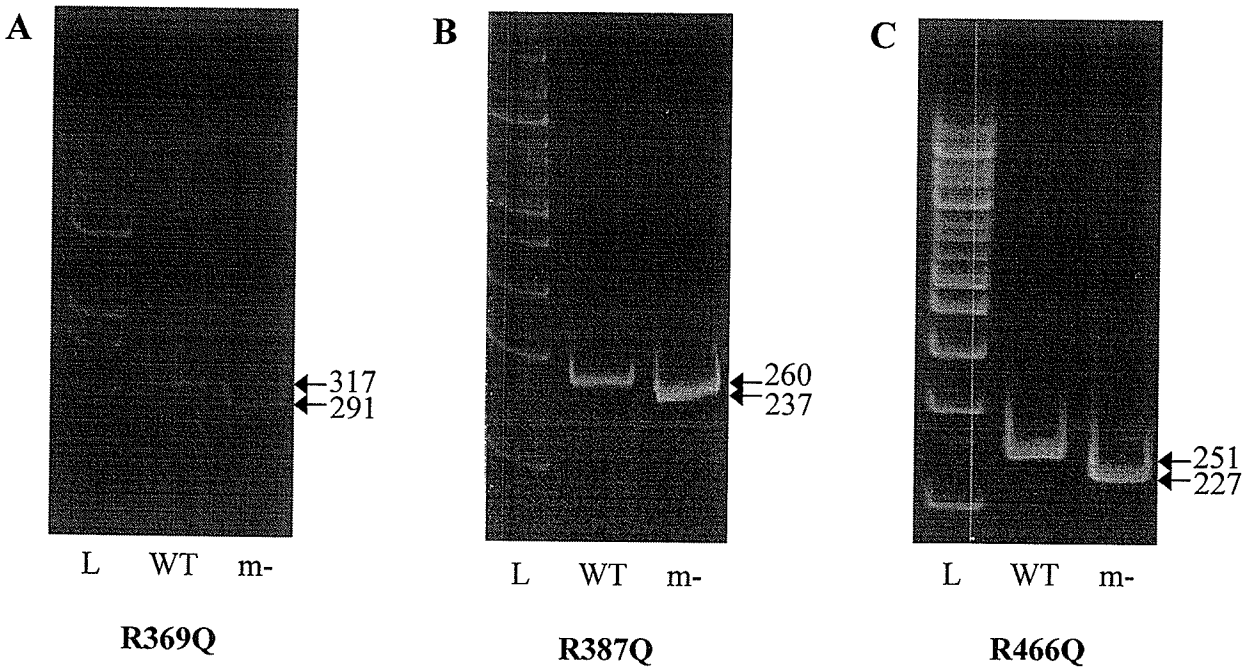

Figure 24. Detection of hGrb14 substitution mutants by PCR-based methods. PCR products encompassing the target mutation site were digested with restriction enzymes. (A) The region from the pGAD424 vector containing the hGrb14 insert containing the R369Q mutation was PCR amplified using WPG311/WPG279 primers and digested with *Hpy*CH4V. (B) The region encompassing the R387Q mutation was PCR amplified using WPG312/WPG279 primers and digested with *Msc*I. (C) The region encompassing the R466Q mutation region was PCR amplified using the WPG313/WPG316 primer set and digested with *Bsr*GI. Lanes are labeled as follows: 100 bp DNA ladder (L), wild-type PCR amplification products (WT), and mutant (m-) PCR amplification products treated with restriction enzymes.

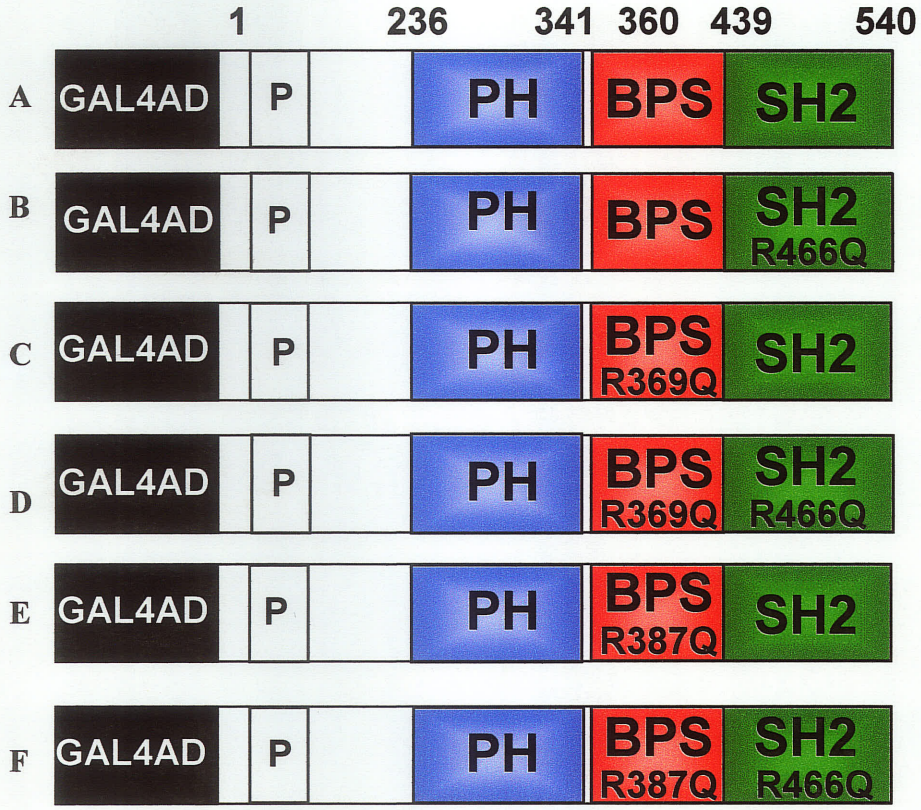

IRK Active		IRK Inactive	
Miller Units	Avg. %	Miller Units	Avg. %
12.5 38.4 26.5	100.0	0.0 0.0 0.0	0.0
3.1 8.3 6.1	26.3 ± 2.1	0.0 0.0 0.0	0.0
12.6 37.7 22.5	92.1 ± 13.1	0.0 0.0 0.0	0.0
2.2 ND ND	13.5 ± 3.8	0.0 0.0 0.0	0.0
2.8 5.9 11.0	26.4 ± 11.0	0.0 0.0 0.0	0.0
0.1 ND ND	1.5 ± 1.5	0.0 0.0 0.0	0.0

Figure 25. **Interaction of mutant GAL4AD::hGrb14 fusion proteins with the IRK in yeast.** β-galactosidase assays were performed on KGY37 yeast cultures co-transformed with either GAL4BD::IRK active or GAL4BD::IRK inactive as well as GAL4AD::hGrb14 mutant plasmids. The GAL4AD::hGrb14 fusion constructs were: (A) wild-type hGrb14, the same construct tested in Fig. 11, (B) hGrb14 R466Q, (C) hGrb14 R369Q, (D) hGrb14 R369Q R466Q, (E) hGrb14 R387Q, and (F) hGrb14 R387Q R466Q. β-galactosidase assay interaction values from three separate experiments reported in Miller Units are shown in three colour codes, experiment one (blue), two (red), three (green). The mean ± SD values from the three trials were calculated and shown as a percentage based on the full-length hGrb14 value (100%). ND indicates interactions not tested in this experiment set; the hGrb14 R369Q R466Q and hGrb14 R387Q R466Q constructs were tested in triplicate in a separate experiment using the wild-type hGrb14 as the reference interaction value (100%).

SH2 mutation, hGrb14 interaction with the IR was further reduced to 13.5% of the value for the wild-type hGrb14 protein (100%). In the presence of the R387Q BPS mutation, the SH2 mutation almost eliminated all interaction (1.5%) between hGrb14 and the IR. These results demonstrate that the R387Q residue of the BPS domain plays a much greater role in the hGrb14-IR interaction than does R369Q.

We also studied the effects of substituting the conserved arginine residues of the BPS domain in the isolated BPS+SH2 domain constructs. The BPS+SH2 R369Q mutant showed a decreased interaction (33.3%) with the IR compared to the wild-type BPS+SH2-IR construct (47.6%). In a similar fashion, the R387Q mutation in the BPS+SH2 construct decreased the ability of this fusion protein to interact with the IR protein by half (23.6%) compared to the wild-type BPS+SH2 construct (47.6%). Introducing the SH2 R466Q mutation along with the BPS R387Q mutation in the BPS+SH2 fusion protein essentially eliminated (0.8%) the interaction with the IR, suggesting that destroying the binding function of both the BPS and SH2 domains renders the hGrb14 molecule incapable of binding to the IR.

3.1.10. Analysis of the hGrb14 protein expression levels in yeast

In order for us to confidently compare protein-protein interactions between full-length and sub-domain or wild-type and mutant hGrb14 constructs, we measured the levels of hGrb14 protein expression in yeast to verify that expression levels were similar between the hGrb14 fusion proteins that were compared for their interaction with the IR (Section 2.7.5). These protein expression levels have been referred to throughout, but the overall

outcome is discussed here. Expression levels of wild-type and mutant full-length hGrb14 and BPS+SH2 sub-domain proteins were found to be similar in yeast (Fig. 26). The wild-type SH2 domain protein expression levels were 100-fold greater than those for the SH2 protein containing the R466Q mutation, and were comparatively much higher than full-length hGrb14 levels. Expression levels of the BPS dropout protein were similar to those for the full-length hGrb14 fusion proteins; however, protein expression levels of the BPS dropout containing the R466Q SH2 mutation were reduced compared to the non-mutated BPS dropout proteins (Fig. 27A). Protein expression of the isolated BPS domain was very weak, which may explain why no interaction was observed between this protein and the IR. The relative consistency of expression levels for the different hGrb14 fusion proteins in our yeast model indicated that we could confidently apply the two-hybrid interaction results for designing interactions assays in mammalian cells.

3.2. hGrb14-IR interaction in mammalian cells and effect on downstream insulin signaling

Using the yeast two-hybrid model, we demonstrated that both the BPS and SH2 domains were involved in mediating interactions between hGrb14 and the IR. In addition, we carried out mutagenesis experiments to identify the individual amino acids within the BPS and SH2 domains critical for interaction. Our next step was to move to a more physiologically relevant model and determine if these results could be reproduced in mammalian cells. The cell model we chose for these experiments was the Chinese hamster ovary cell line overexpressing the IR (CHO-IR).

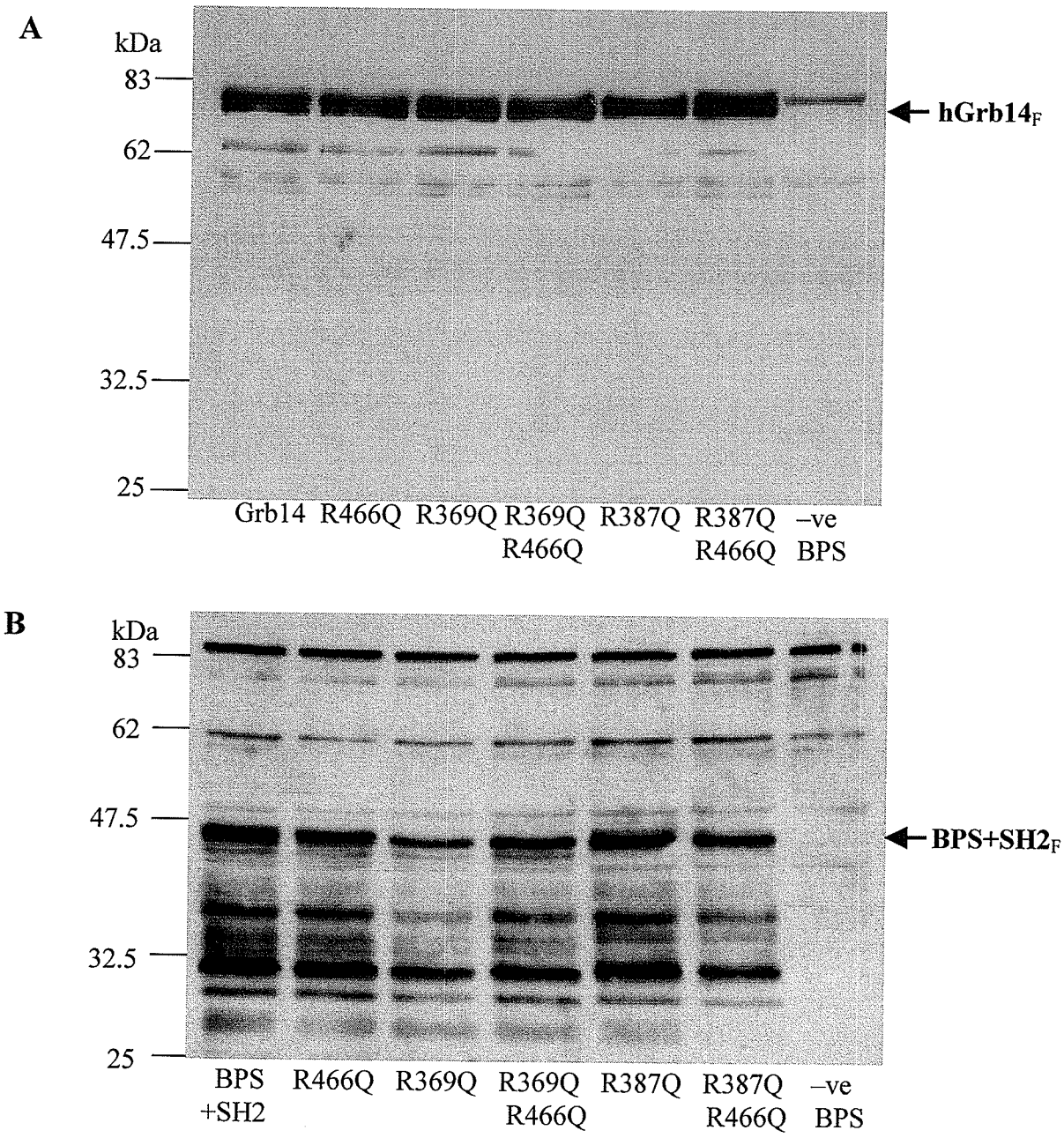

Figure 26. Western blot analysis of GAL4AD::hGrb14$_F$ and GAL4AD::BPS+SH2$_F$ fusion proteins. Fusion proteins isolated from yeast expressing wild-type or mutant (R466Q, R369Q, R387Q) (A) GAL4AD::hGrb14$_F$ and (B) GAL4AD::BPS+SH2$_F$ fusion proteins were resolved by SDS-PAGE and immunoblotted with anti-FLAG antibodies. hGrb14 and BPS+SH2 protein bands are indicated alongside the gels. The BPS domain construct protein served as a negative control, as it did not contain a FLAG epitope. Exposure times for these films were 15 min (panel A) and 5 min (panel B).

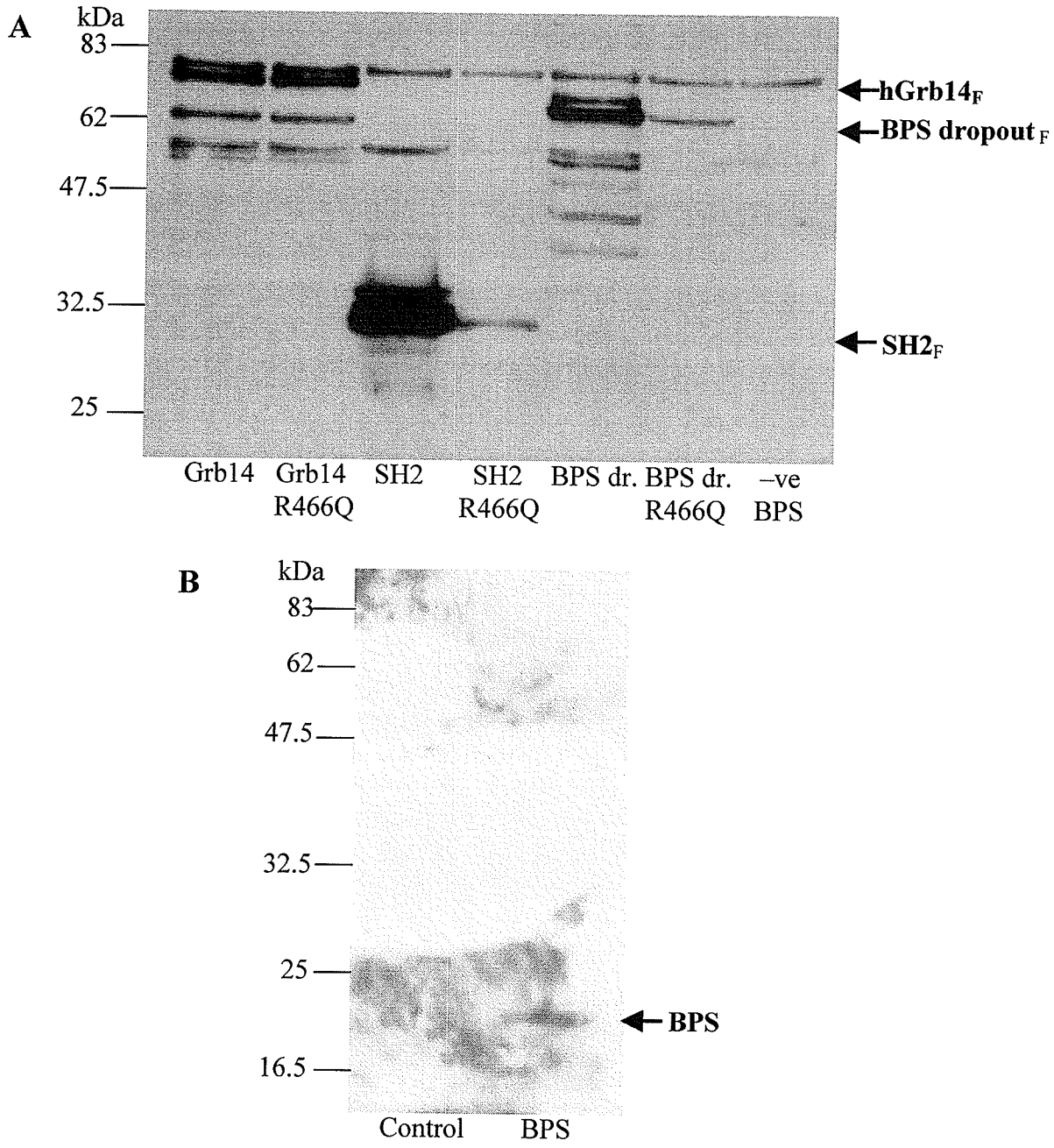

Figure 27. Western blot analysis of GAL4AD::SH2, BPS dropout, and BPS fusion proteins. Extracts from yeast expressing wild-type or mutant (A) GAL4AD::SH2 or BPS dropout (BPS dr.) compared to wild-type full length hGrb14 and (B) GAL4AD::BPS fusion proteins were resolved by SDS-PAGE and immunoblotted. The anti-FLAG antibody was used to detect FLAG-tagged hGrb14 proteins in panel A, with the BPS domain construct serving as a negative control because it was not tagged with a FLAG epitope. The anti-Grb14 antibody was used to detect the BPS domain fusion protein in panel B with non-transformed yeast extracts serving a negative control. Band identities are indicated alongside the blots. Films were exposed for 15 min.

3.2.1. Transfection of hGrb14 into CHO-IR cells

In order to introduce the full-length hGrb14 containing the R387Q BPS domain and R466Q SH2 domain mutations in our cell culture model, it was necessary to insert hGrb14 cDNA encoding the BPS and/or SH2 domain mutations into the pRcCMV mammalian expression vector (Fig. 28). This vector system was used because it was thought to provide strong expression of our hGrb14 protein in the CHO-IR cell line. The presence of the mutations we introduced was verified by PCR-based methods (Section 2.4.1).

After separately transfecting CHO-IR cells with BPS (R387Q) and/or SH2 (R466Q) mutant pRcCMV::hGrb14 plasmids, we assessed the levels of hGrb14 protein expression by immunoblotting the cell lysates with the anti-FLAG antibody. Given that we observed different protein expression levels between clones, we chose individual clones from each of the constructs, hGrb14 R387Q, hGrb14 R387Q, and hGrb14 R387Q R466Q, that displayed protein expression levels that were similar to the CHO-IR cell line previously stably transfected with wild-type pRcCMV::hGrb14 (Table 5, Section 2.6.2) [61]. Having selected clones for each construct, we tested that hGrb14 protein expression levels remained constant over subsequent cell passages and this established that, we had successfully created CHO-IR cell lines stably transfected with the full-length hGrb14 containing BPS and SH2 mutations (Fig. 29).

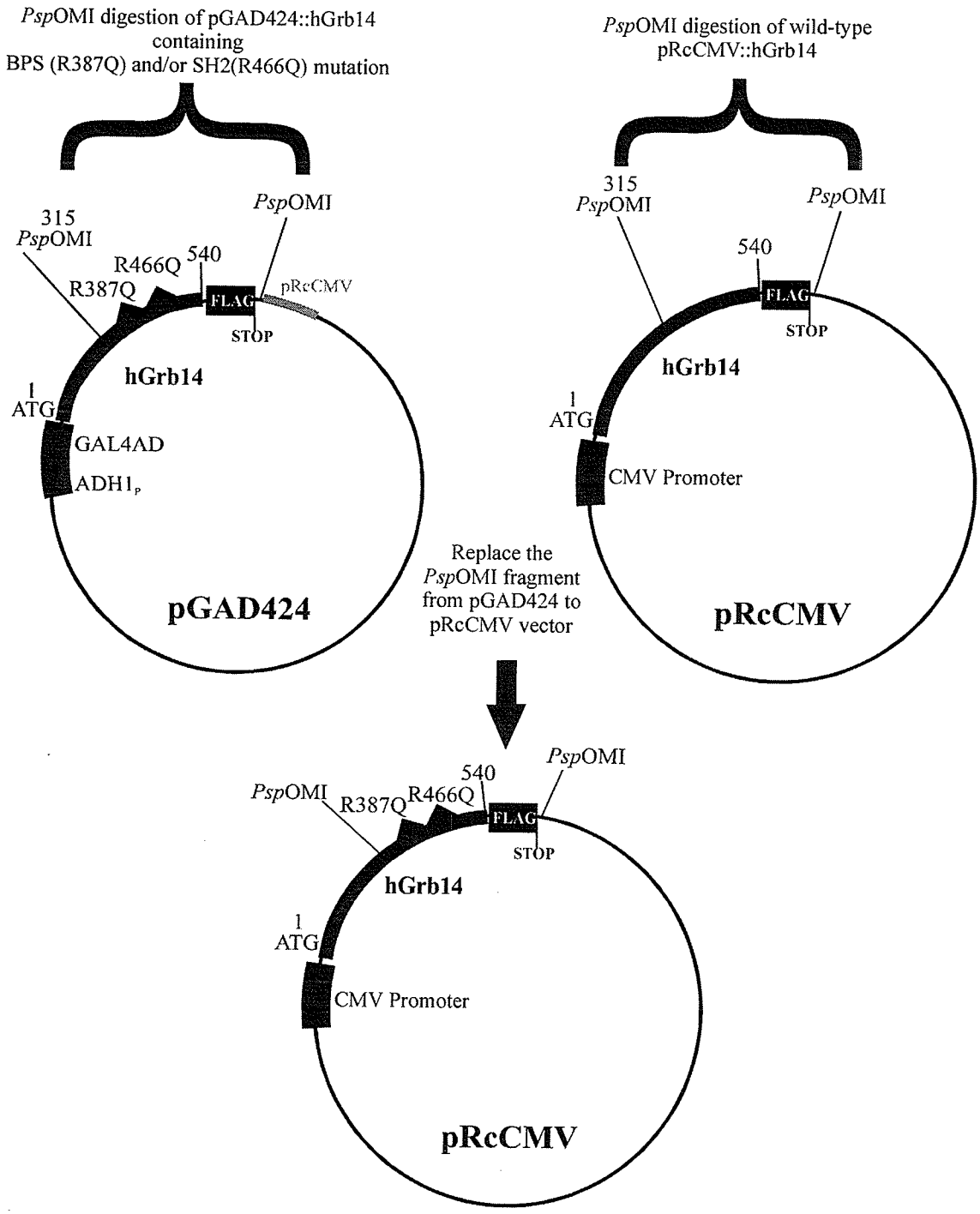

Figure 28. Diagram of the pRcCMV::hGrb14$_F$ R369Q R466Q or R387Q R466Q vector. The *Psp*OMI fragment (aa 315-540) was excised from pGAD424:: hGrb14$_F$ containing the R369Q or R387Q BPS and/or R466Q SH2 domain mutation and used to replace the wild-type *Psp*OMI fragment from pRcCMV::hGrb14$_F$. The positions of the R387Q and R466Q substitutions are indicated by solid triangles.

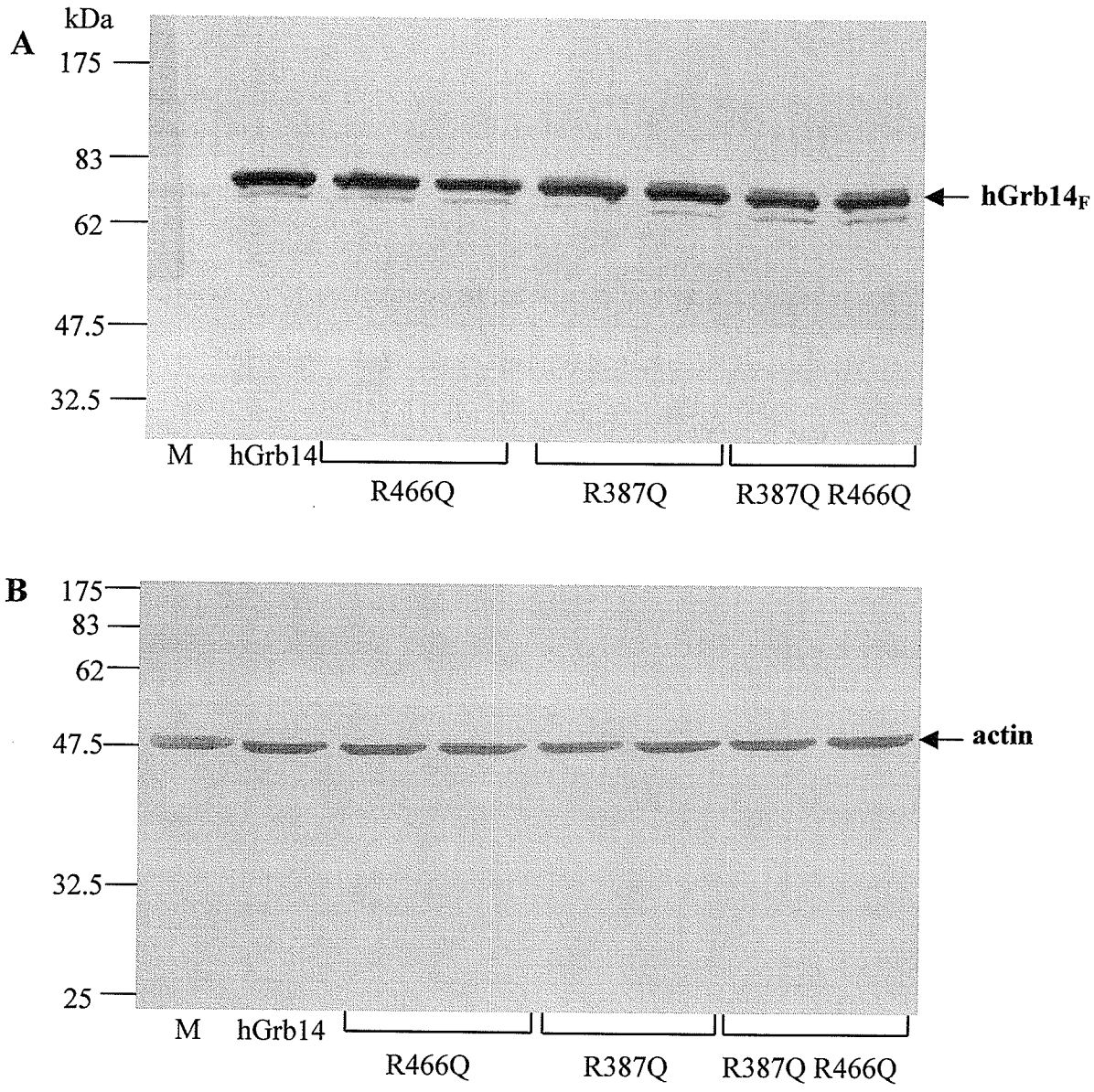

Figure 29. Immunoblot analysis of proteins from CHO-IR cell lines stably overexpressing wild-type and mutant hGrb14 (A) Expression of hGrb14 in mock transfected CHO-IR cells (M) and four CHO-IR cell lines stably transfected with wild-type $hGrb14_F$, hGrb14 R466Q, R387Q, or R387Q R466Q cDNA was assessed by immunoblotting with anti-FLAG antibodies. Cell lysates (35 μg protein) were separated (mutant samples were loaded in duplicate) by SDS-PAGE. The film was exposed for 1 min. The hGrb14 mutant samples were loaded in duplicate. (B) Uniform loading was assessed by blotting the filter from panel (A) with an anti-actin antibody. The film was exposed for 5 sec.

Table 6. Quantitative protein expression levels. (A) A crude estimation of the level of hGrb14 protein expression from the immunoblot in Fig. 29A was obtained using a Fluor S-Max MultiImager, in Counts (CNT)*mm^2 using a 10 s exposure. The mean for the immunoblot CNT*mm^2 values were calculated and shown as percentage values based on the full-length value (100%). The percent of all CNT*mm^2/mean values were then calculated. The standard deviations were derived for the hGrb14 mutant samples, which were loaded in duplicate on the gel in Fig. 29. (B) The actin band intensities from the immunoblot in Fig. 29B were measured in the same fashion.

A

Anti-FLAG Immunoblot Values

Sample	CNT*mm^2	Percent of CNT*mm^2/mean	SD
Mock	61.5	0%	-
hGrb14	39777.1	107.5%	-
R466Q	23852.3	64.5%	0.07
R466Q	27534.8	74.4%	
R387Q	35009.0	94.6%	0.00
R387Q	34805.4	94.1%	
R387Q, R466Q	37609.5	101.6%	0.03
R387Q, R466Q	39213.6	106.0%	
mean	37002.6	100.0%	-

B

Anti-actin Immunoblot Values

Sample	CNT*mm^2	Percent of CNT*mm^2/mean	SD
Mock	56194.8	93.1%	-
hGrb14	56504.3	93.6%	-
R466Q	57956.1	96.0%	0.04
R466Q	61032.9	101.1%	
R387Q	57642.5	95.5%	0.05
R387Q	62277.0	103.2%	
R387Q, R466Q	67000.9	111.0%	0.10
R387Q, R466Q	75941.7	125.8%	
Mean	60361.8	100.0%	-

3.2.2. Interaction of hGrb14 wild-type and mutant forms with the IR

The interaction between hGrb14 and the IR in CHO-IR cells stably overexpressing wild-type or mutant (R466Q, R387Q, R387Q R466Q) Grb14 protein was assessed by immunoprecipitation using an anti-IR antibody and immunoblotting with an anti-FLAG antibody. The immunoprecipitation-immunoblot experiments measured the ability of the Grb14 protein to interact with the IR protein in response to insulin-stimulation. Mock-transfected cells, which did not express hGrb14 protein, served as negative controls. The clearing fraction sample from the mock-transfected cells served as a background control for these immunoprecipitation experiments, and showed no background in the immunoblot.

CHO-IR cells overexpressing wild-type hGrb14 showed the highest level of hGrb14-IR association. When the R466Q SH2 mutation was introduced, we observed variable results showing 2-, 5-, and 100 fold reductions in hGrb14-IR interactions in the three analysis carried out (Fig. 30 represents the assay with the 5-fold reduction). Although variable, the SH2 mutation results in this system were consistent with our yeast two-hybrid results, which showed that, the GAL4AD:: hGrb14 R466Q fusion protein induced a four fold decrease (26.3%) in the interaction with the IR (Fig. 11). These findings in our mammalian cell model further confirmed the importance of a functionally active SH2 domain in binding of the hGrb14 protein to the IR.

The R387Q mutation in hGrb14 produced a very weak or non-existent interaction with the IR protein compared to the wild-type hGrb14 interaction with the IR. In comparing the effect of the R387Q BPS mutation between the mammalian and yeast models, we

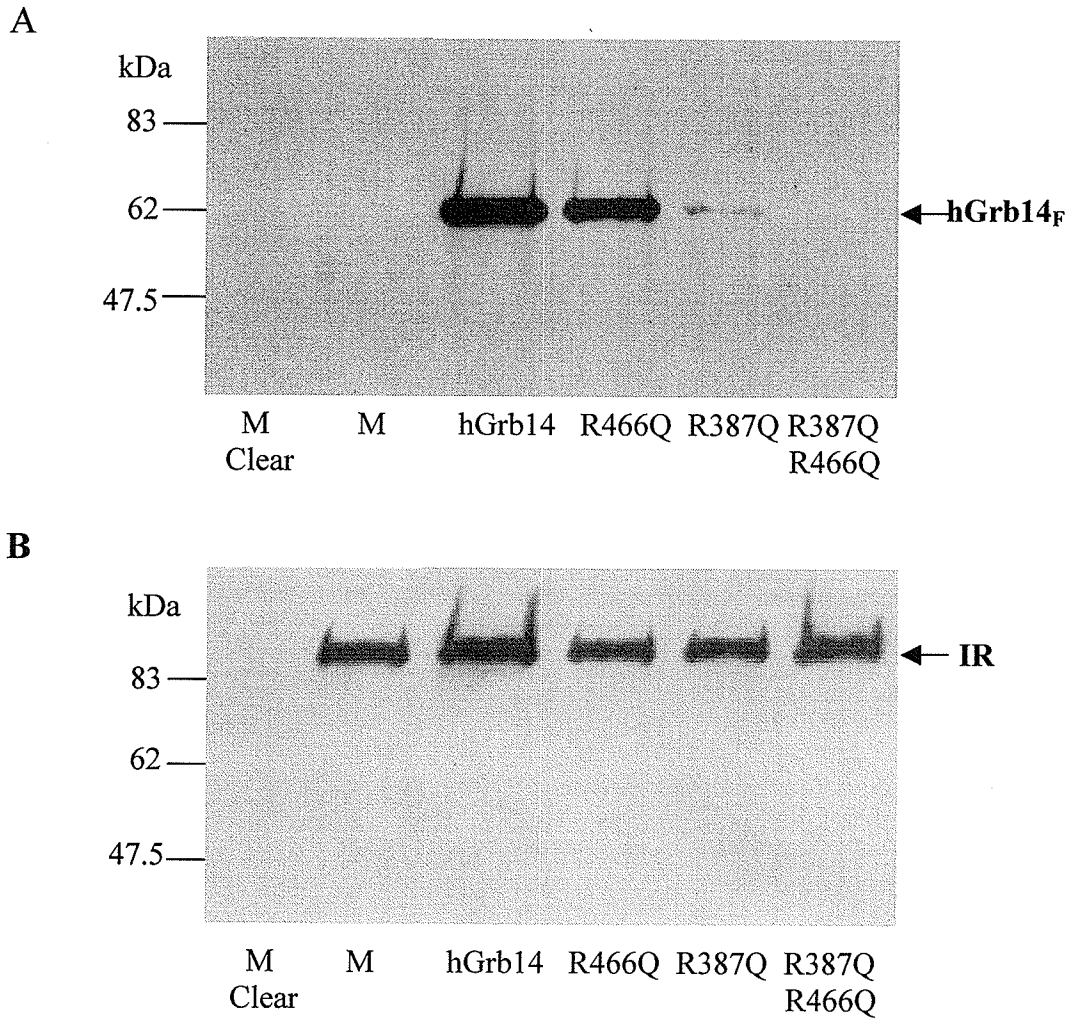

Figure 30. $hGrb14_F$-IR immunocomplexes from CHO-IR cells overexpressing hGrb14. $hGrb14_F$-IR immunocomplexes were eluted from CHO-IR cells overexpressing wild-type or mutant (R387Q, R387Q R466Q) hGrb14 and accompanying mock-transfected (M) cells using anti-IR antibodies followed by protein G beads and separated by SDS-PAGE. The mock transfected sample collected at the clearing stage of the experiment (M Clear) was loaded as a background control. (A) To assess the amount of hGrb14-IR immunocomplexes in each sample, the membrane was immunoblotted with anti-FLAG antibodies, as the hGrb14 protein is tagged with a FLAG epitope. (B) To assess the efficiency and consistency of capture of hGrb14-IR immunocomplexes the membrane from panel A was probed with anti-IR antibodies. The blots were exposed for 15 min.

observed a four-fold reduction of the hGrb14-IR interaction in the yeast model consistent with the reduction in the mammalian cell model findings, although the reduction was more drastic in this model. These finding indicate that even with a functionally active SH2 domain, the R387Q BPS domain mutation greatly hindered the ability of hGrb14 to interact with the IR. These results put further emphasis on the importance of the hGrb14 BPS domain in hGrb14-IR interactions.

CHO-IR cells stably expressing hGrb14 with both the BPS R387Q and SH2 R466Q mutations consistently showed no interaction with the IR. This finding was common with those from yeast two-hybrid experiments, which showed the GAL4AD::hGrb14 R387Q R466Q fusion protein had only 1.5 ± 1.5% interaction with the IR protein. We therefore concluded that when both the BPS and SH2 domains were mutated, the ability of hGrb14 to bind to the IR was destroyed. The results from these experiments established that a minimal binding region of the hGrb14 protein includes both the BPS and SH2 domains.

The efficiency and consistency of hGrb14-IR immunocomplex capture (Fig. 31) was tested by immunoblotting those membranes originally probed with FLAG antibodies with anti-IR antibodies. This procedure allowed us to quantify the degree to which the IR was bound and then eluted during the immunoprecipitation procedure, representing the overall efficiency of capture. By comparing the results between immunoprecipitation of different hGrb14 constructs, we were able to normalize the results obtained by probing with the FLAG antibodies.

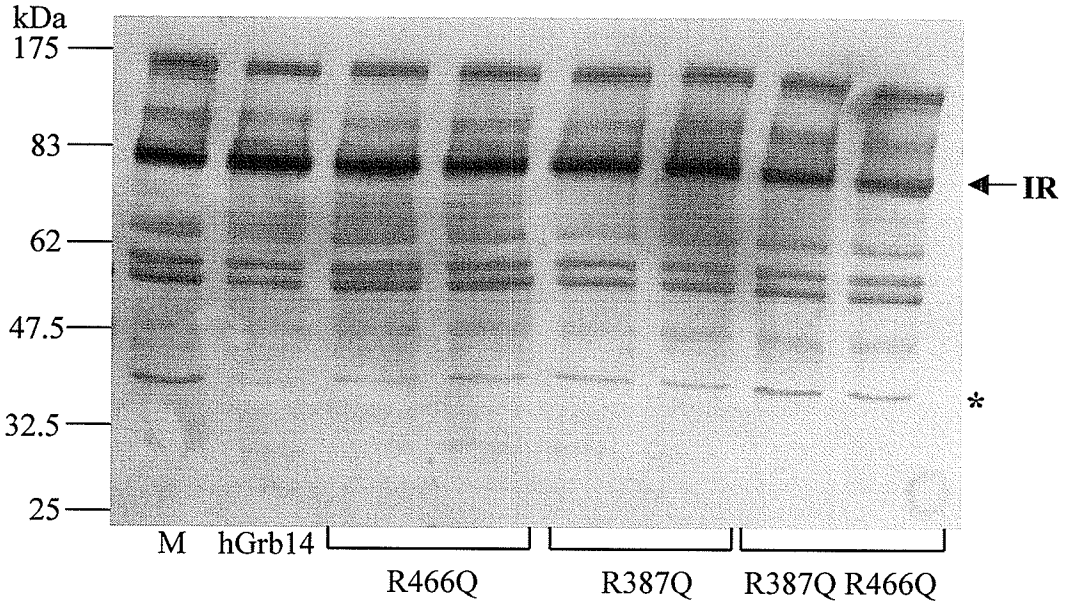

Figure 31. Tyrosine phosphorylation of proteins from CHO-IR cells overexpressing hGrb14. Proteins from CHO-IR cells overexpressing wild-type (hGrb14) or mutant R466Q, R387Q, R387Q R466Q hGrb14 (mutant samples were loaded in duplicate) and accompanying mock-transfected cell clones (M) were immunoblotted with anti-pTyr antibodies. The blot was exposed to film for 1 min. An arrow denotes the tyrosine-phosphorylated β-subunit of the IR and an asterisk indicates the 42-kDa protein band whose tyrosine phosphorylation increases with decreasing hGrb14-IR interaction.

The quantity of IR was similar between the mock-transfected, hGrb14 R466Q, and hGrb14 R387Q samples, whereas the wild-type hGrb14 and hGrb14 R387Q R466Q samples showed slightly higher levels of IR protein capture (Fig. 30). Because IR protein levels were almost constant over the different hGrb14-IR immunocomplexes, we took the relative intensities of the $hGrb14_F$ probed bands to be accurate approximations of hGrb14-IR interaction. The wild–type protein appeared to have the strongest interaction with the IR followed by a reduced interaction for the hGrb14 R466Q mutant. The R387Q and R387Q/R466Q hGrb14 mutants showed very little and no interaction, respectively, with the IR. These findings are consistent with those from the yeast two-hybrid model that also showed reduced interactions in the presence of the BPS and SH2 mutations. Taken together these results suggest that if the function of the SH2 or BPS domains of the hGrb14 protein is destroyed by mutagenesis, the hGrb14-IR interaction is reduced. Furthermore, by mutating both domains in the hGrb14 molecule, the hGrb14-IR interaction is completely abolished, indicating that both the SH2 and BPS domains play important roles in the interaction between hGrb14 and the IR.

3.2.3. Tyrosine phosphorylation of proteins in CHO-IR cells overexpressing wild-type hGrb14

Previous findings by Hemming *et al* (2001) demonstrated that three proteins known to undergo insulin-stimulated tyrosine phosphorylation, Shc [73], IRS-1 [74], and Dok [75], showed a decrease in phosphorylation in CHO-IR cells also overexpressing the hGrb14 protein. Therefore we wanted to test the levels of insulin-stimulated tyrosine phosphorylation in CHO-IR cells overexpressing hGrb14 with BPS and/or SH2 domain mutations compared with cell expressing wild-type hGrb14. Using immunoprecipitation

with anti-IR antibodies and immunoblotting with anti-pTyr antibodies (Fig. 31), we measured the levels of tyrosine phosphorylation in CHO-IR cells expressing either the wild-type or mutant hGrb14 proteins. Consistent with previous findings, we observed an overall decrease in the levels of tyrosine phosphorylation for proteins from cell lysates overexpressing hGrb14 compared to untransfected cells (Fig. 31) [61]. Other studies have similarly shown a decrease in insulin-stimulated tyrosine phosphorylation of proteins from cell lysates overexpressing hGrb10 [44] or rGrb14 [56]. These results suggests that hGrb14 may be a negative regulator of insulin signaling, consistent with findings for the rGrb14 [56].

We found that, the levels of tyrosine phosphorylation of the β-subunit of the IR protein did not show a drastic change between Mock, wild-type and mutant hGrb14 transfected cells (Fig 32). However, the level of tyrosine phosphorylation of a 42-kDa protein was increased in cell lines transfected with mutant compared to wild-type hGrb14, with the greatest effect observed in cells overexpressing the hGrb14 protein encoding both the BPS (R387Q) and the SH2 (R466Q) domain mutations. Of the three trials that were carried out for this experiment, one trial did show no difference in the intensity of this band between wild-type and mutant hGrb14 samples. Overall, these results suggested that the mutations in the BPS and SH2 domains of the hGrb14 reduced the ability of hGrb14 to bind the IR, resulting in decreased tyrosine phosphorylation of downstream proteins. Therefore, it appears that BPS and SH2 domain mutations abolish the function of hGrb14 as a negative regulator in the insulin signaling pathway.

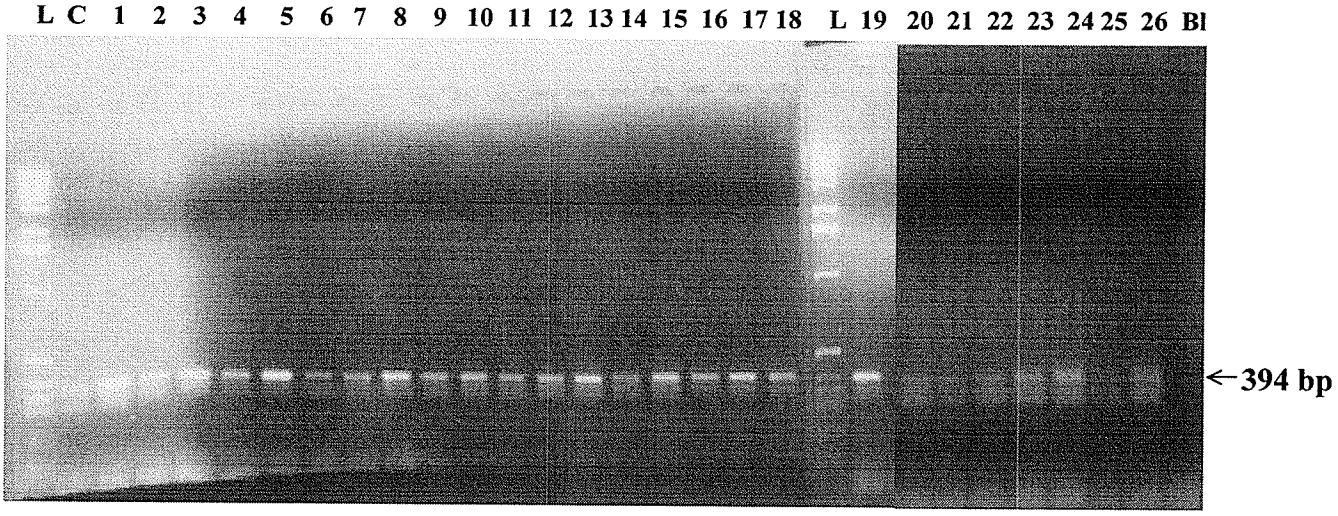

Figure 32. Assessment of DNA integrity in mouse-tail samples. The 394 bp PCR products were amplified from mouse-tail DNA using the *Hyal2* WPG164/WPG170 primers. Samples were labeled as follows: Ladder (L), control non-transgenic tail DNA (C), Lanes 1- sample I1980.1(F), 2- I1980.2(F), 3- I1980.3(M), 4- I1981.1(M), 5- I1981.2(M), 6- I1981.3(M), 7- I1982.1(F), 8- I1982.2(M), 9- I1982.3(M), 10- I1982.4(M), 11- I1983.1(F), 12- I1983.2(F), 13- I1983.3(F), 14- I1983.4(F), 15- I1983.5(M), 16- I1983.6(M), 17- I1983.7(M), 18- I1983.8(M), 19- I1983.9(M), 20- I1976.1(F), 21- I1976.2(M), 22- I1976.3(M), 23- I1978.1(F), 24- I1978.2(M), 25- I1978.3(M), 26- I1978.4(M). The sample designations were assigned at the Transgenic Core Facility; the numbers preceding the period (1980-1983) represent groups of pups from mothers 1980-1983, the numbers following the period are the numbers of litter mates (1-9), and the sex is designated male (M) or female (F). The blank water sample (Bl) served as a negative control.

3.3. hGrb14 transgenic mice

In these and previous studies using cell culture models [61] there is evidence that overexpression of the hGrb14 protein inhibits tyrosine phosphorylation of some downstream proteins in the insulin signalling pathway while stimulating the tyrosine phosphorylation of others. To further test the physiological relevance of these findings in an animal model, we endeavored to create a transgenic mouse that overexpressed hGrb14.

3.3.1. Strategy for creating hGrb14 transgenic mice

The hGrb14 gene was introduced into the mouse genome in the form of a 2.8 Kb *Mfe*I/*Bam*HI hGrb14 DNA fragment, which included an N-terminal CMV promoter and C-terminal FLAG tag (Fig. 8). The purified fragment was microinjected into mouse embryos as described in Sections 2.10.2-3. This procedure yielded twenty-nine pups, three of which were stillborn. Viable mice were screened using PCR and Southern blot analysis to identify the hGrb14 transgenic founders (Section 2.10.5.1-2).

Before testing for the presence of the transgenic *hGrb14* gene in the mouse genome, we wanted to verify the integrity of the genomic DNA extracted from mouse-tail clippings. A control PCR reaction was devised using WPG164/WPG170 oligonucleotides to amplify a 394 bp region of the mouse *Hyal2* gene. This PCR amplification revealed that the integrity of the mouse DNA was maintained during preparation for both the control and putative transgenic groups (Fig. 32).

In order to identify hGrb14 transgenic mice, we used two sets of primers (WPG246/WPG248 and WPG251/WPG252) that would specifically amplify only the human Grb14 transgene and not the mouse genomic Grb14, from mouse-tail DNA. In transgenic mice, we expected a 497 bp amplification product using the WPG246/WPG248 primer set, and a 241 bp fragment from the WPG251/WPG252 set (Fig. 33). In the PCR amplification using the WPG251/WPG252 primer set, a 400 bp band was observed in negative samples, this was likely amplification of mouse Grb14, because an additional intron likely present in the mouse genomic DNA would result in the larger PCR product. Although the PCR primers were designed to be specific for human and not mouse Grb14, the presence of this extra amplification band is not completely unexpected given the high degree of sequence conservation (86%) between human and mouse Grb14. Our screening experiments, carried out in duplicate, detected five mice, I1980.3(M), I1983.1(F), I1983.5(F), I1976.3(M), I1978.3(M) that showed positive results using PCR amplification with two different primer sets (WPG246/WPG248 and WPG251/WPG252).

To substantiate our results from PCR screening for hGrb14 transgenic founders, the five samples that showed positive results by PCR analysis were then tested for the presence of the transgene using Southern blot analysis (Fig. 34). Fifteen micrograms of DNA from each of the five mouse-tail DNA samples was digested with *Eco*RI and separated by gel electrophoresis. Copy number standards of *MfeI/Bam*HI-digested pRcCMV::hGrb14$_F$ at

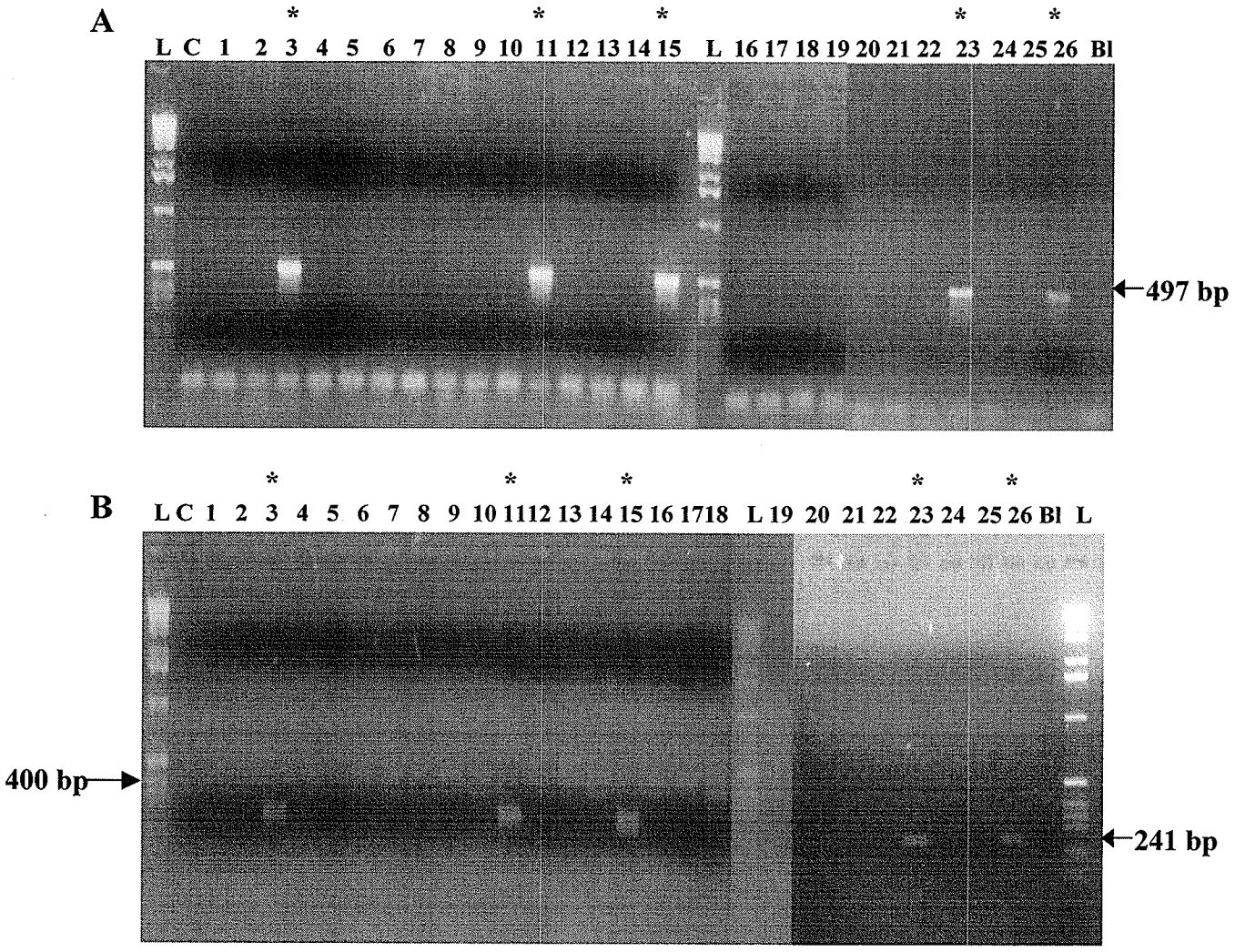

Figure 33. PCR screen of candidate hGrb14 transgenic mouse DNA samples. PCR amplification products from mouse-tail DNA using the hGrb14 WPG246/WPG248 primers (panel A) and the hGrb14 WPG251/WPG252 primers (panel B) are shown. The sample order and labeling is identical to Fig. 32. Successful amplification products 497 bp (A) and 241 bp (B) in lanes 3, 11, 15, 23, 26, indicated by asterisks above the lanes, correspond to putative transgenic amplification products. In panel B, the low abundance 400 bp amplification products correspond to genomic amplification from negative hGrb14 transgenic mouse samples.

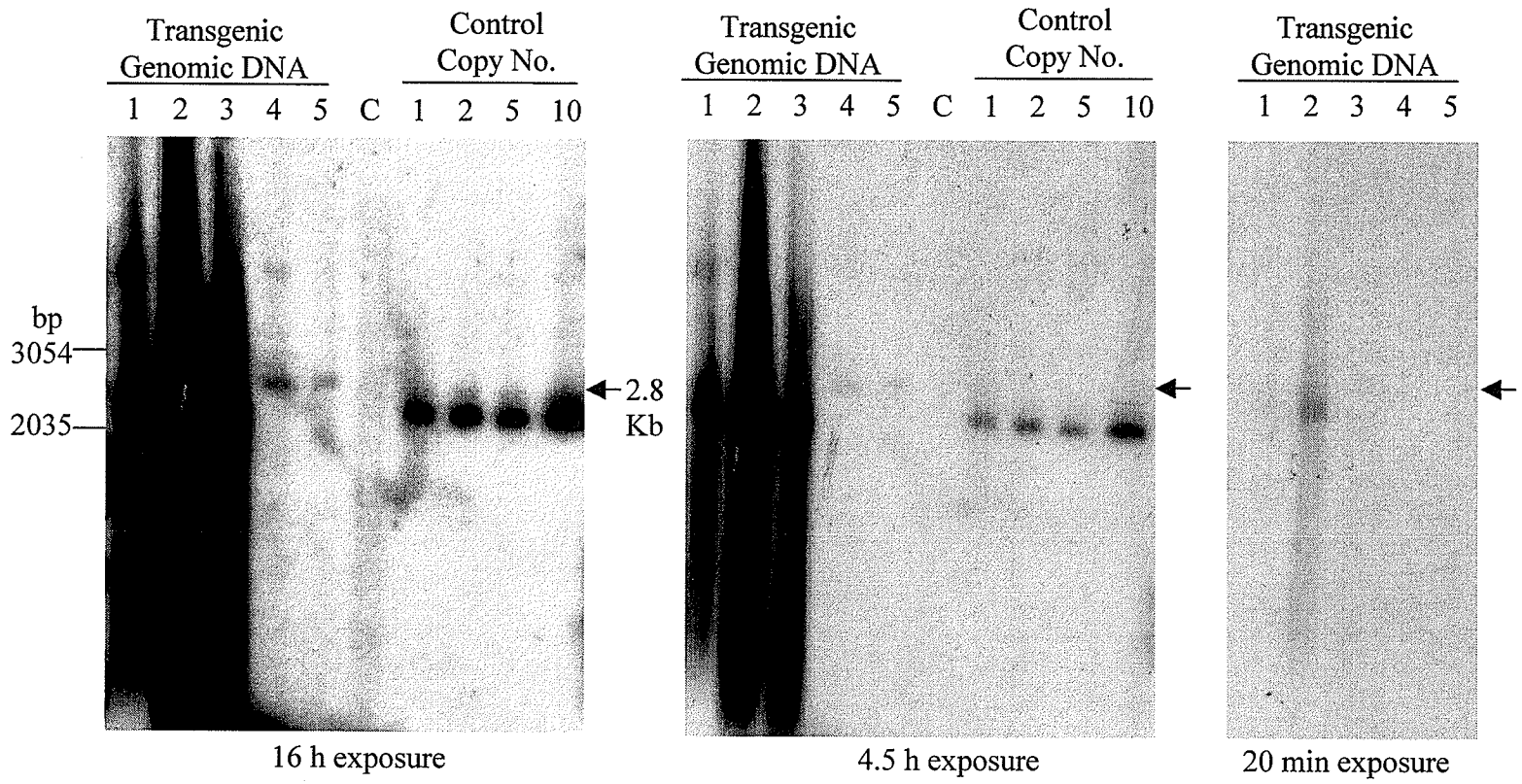

Figure 34. Southern blots of the hGrb14 transgenic mouse DNA samples that were positively identified by PCR analysis. Mouse-tail DNA was digested with *Eco*RI and separated on an agarose gel in the following order: Lane 1- I1980.3(M), 2- I1983.1(F), 3- I1983.5(F), 4- I1976.3(M), and 5- I1978.3(M). Copy number standards of the 2.8 Kb *Mfe*I/*Bam*HI-digested $hGrb14_F$ region were loaded on the gel, in 36 pg equivalents of (1), (2), (5) and (10) copies. The Southern blot was exposed to film for 16 h, 4.5 h, and 20 min.

estimated equivalents of (1), (2), (5) and (10) copies were loaded in separate wells on the gel alongside the positively identified DNA samples. A *Hind*III/*Eco*RI digested pRcCMV::hGrb14$_F$ fragment was labeled with [P^{32}] radioisotope and used to probe the Southern blot membranes. Results showed that the genomic DNA of the I1980.3(M), I1983.1(F), and I1983.5(F) mice contained high hGrb14 transgene copy numbers, whereas the I1976.3(M) and I1978.3(M) mice had low copy numbers. All five of these mice were therefore established as founders and were bred to produce F2 generation litters that could then be used to test for hGrb14 protein expression in various tissue samples.

3.3.2. hGrb14 protein expression in mouse tissues

Five hGrb14 transgenic founder mice were bred and the progeny were sacrificed in order to examine hGrb14 protein expression in the following tissues: liver, kidney, muscle, pancreas, brain, heart, fat, lung, spleen, large intestine, small intestine, blood, and gonads (Fig. 35, data not shown for the lung, spleen, large intestine, small intestine, blood, and gonad tissue). Using immunoblot analysis of the mouse tissue samples with anti-FLAG antibodies, no hGrb14 protein expression was detected from any of the progeny of founder mice that were initially positively identified by PCR and Southern blot screening. Since the FLAG epitope is not endogenously present in the mouse genome, the bands seen in the immunoblot in the control lanes must have represented cross-reacting proteins. Therefore, bands appearing at the same position in test samples were assumed to represent the same cross-reacting proteins. Expressed transgenic proteins, in contrast, would only have appeared in the test lanes and at positions different from those of the

A

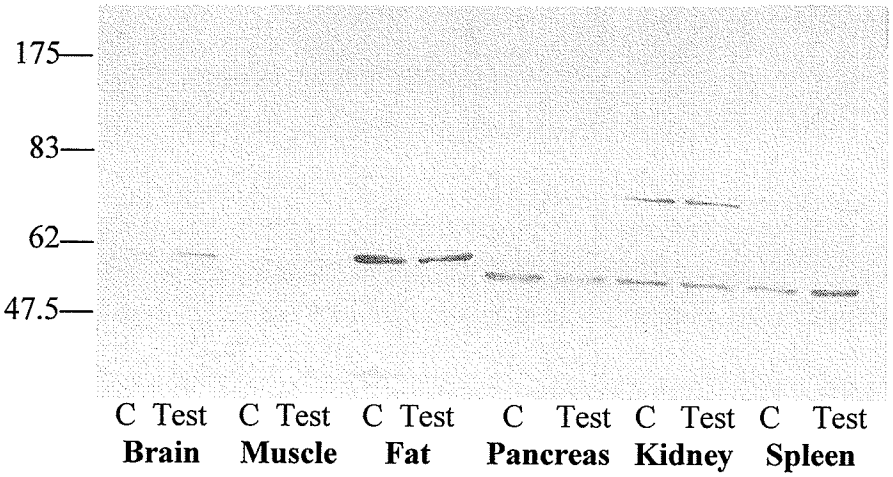

B

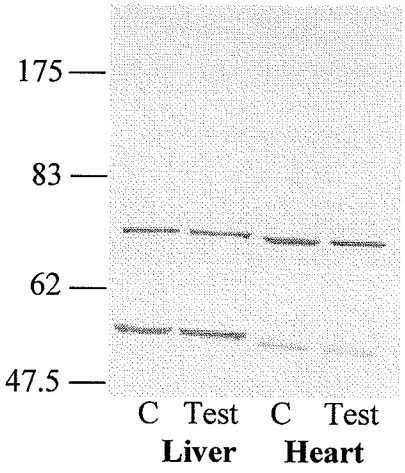

Figure 35. hGrb14 protein expression in mouse tissues. Proteins from founder mouse progeny tissues were separated on SDS-PAGE and detected using the anti-FLAG antibody. The control samples (C) were collected from non-transgenic mouse tissues. Blots were exposed to film for either 10 min (A) or 5 min (B). The identities of the mouse tissue samples are indicated below their respective lanes.

cross-reacting bands in the control lanes. One possible explanation for the lack of hGrb14 transgenic protein expression from mouse tissues could be that the hGrb14 gene may have been inserted in a silenced chromosomal region and thus was not expressed.

4. CONCLUSION

Using the yeast two-hybrid system and cell culture experiments we confirmed that hGrb14 interacts with the IR in a kinase dependent manner. We also confirmed that the SH2 domain of the hGrb14 protein played an important role in binding to the IR, as the R466Q SH2 domain mutation caused a reduction in binding to the IR.

Another domain of hGrb14, the BPS domain, was found to mediate the interaction with the active IR. Although, in the yeast two-hybrid system the BPS domain alone showed no interaction with the IR, we demonstrated its importance in the IR interaction using additional two-hybrid experiments. First, the hGrb14 protein with the deleted BPS domain showed a substantial reduction in IR binding. Further, the BPS plus SH2 domain fusion protein exhibited a much greater binding to the IR than the SH2 domain alone, indicating that the BPS domain played a key role in the hGrb14-IR binding. More striking was the yeast two-hybrid interaction finding that $hGrb14_F$ R387Q GAL4AD fusion protein that showed a 4-fold reduction in the interaction with the active IR compared to wild-type hGrb14, similar to that of the hGrb14 R466Q fusion protein. The interaction of hGrb14 encoding both the R387Q and R466Q mutations with the active IR was essentially abolished. Therefore, if you eliminate function of both the BPS and SH2 domains of hGrb14, you destroy the ability of hGrb14 to bind the IR, suggesting that the BPS and SH2 act cooperatively to facilitate the hGrb14-IR interaction.

The IR-hGrb14 immunocomplexes from CHO-IR cells stably overexpressing hGrb14 R387Q formed a very weak interaction compared to that with wild-type hGrb14. The

immunocomplexes formed between the IR and the hGrb14 protein encoding both the BPS, R387Q and R466Q mutations, in stably transfected CHO-IR cells, showed no interaction. This indicated that the BPS domain played an important role in the binding function of hGrb14 with the IR, as did the SH2 domain. These domains seemed to act in concert to bind to the IR, a finding that validated our original hypothesis. The conserved R387 residue also proved to be critical in interaction of hGrb14 with the active IR. These findings represent a novel discovery of a critical residue of the BPS domain, that when mutated abolishes the binding ability of the BPS domain.

Overexpression of hGrb14 in CHO-IR cells resulted in a decrease in tyrosine phosphorylation of proteins, which was consistent with previous findings. This effect was more pronounced with mutations of the hGrb14 BPS and/or SH2 domains, as these mutations led to decreased hGrb14-IR interaction. This observation was supported by results from R387Q BPS mutations and to an even greater extent when the R466Q SH2 mutation was combined with the R387Q BPS domain mutation.

Results from the mammalian cell culture experiments that showed that overexpression of the hGrb14 protein has a negative effect on downstream tyrosine phosphorylation of insulin-stimulated proteins, prompted us to examine the effects of overexpressing the hGrb14 protein in an animal model. Unfortunately, the putative hGrb14 transgenic founder mice we created did not appear to express the hGrb14 protein. One possible explanation for this was that the hGrb14 transgenic gene was inserted in a silenced chromosomal region and thus was not expressed. An hGrb14 transgenic mouse would be

beneficial to studying the effects of hGrb14 overexpression in an animal system and to study any effects on insulin signaling. Our results show that both the BPS and SH2 domains play important roles in hGrb14-IR binding, and these domains appear to act in concert in the hGrb14 protein.

A study conducted by the World Health Organisation in 2000, reported that 142 million people in the world suffer from diabetes mellitus, and this number is expected to double by the year 2025. Therefore, further understanding the malfunction of the IR and insulin signal transduction will aid in the discernment of diabetes, a major health concern.

5. FUTURE DIRECTIONS

Through mutagenesis studies using the yeast two-hybrid and cell culture models, we identified a residue of the BPS domain (R387) that was critical for binding of the hGrb14 protein to the IR. This finding suggests that the hGrb14 BPS mutant construct can be used to assess the role of the BPS domain in any similar model system studying other receptors such as IGFR-1 and FGFR to which hGrb14 has been shown to bind. As the BPS domain is unique to the Grb7 family of proteins, it is important to further analyze its function to understand the functional purpose of this conserved protein domain. Further studies might include introducing the R387Q mutation into other Grb7 protein family members and testing for changes in the binding of Grb7 proteins to receptor tyrosine kinases. In future work, CHO-IR cells stably transfected with hGrb14 BPS and SH2 mutant proteins can be used in studies to determine the effects of phosphorylation of other downstream insulin signaling proteins such as Shc, Dok, IRS-1, and PKB. This work would undoubtedly clarify the role of the BPS domain of hGrb14 in altering insulin signaling downstream of the receptor.

At present, solution of the X-ray crystal structure of the hGrb14 BPS domain is underway. If we could understand the structural interaction of the hGrb14 and the IR, we would be better equipped to study the effect the hGrb14-IR interaction on insulin signaling.

6. APPENDIX

6.1. Mutation Analysis

6.1.1. Electropherogram of pGAD424::hGrb14$_F$ R387Q using the GAL4AD reverse primer.

The R387Q substitution of the nucleotide sequence is as follows:

Forward strand	Reverse strand
AGA → **CA**A	TCT → T**TG**
Wild type → Substitutions	Wild type → Substitutions

Electropherogram of the reverse strand using the GAL4AD primer:

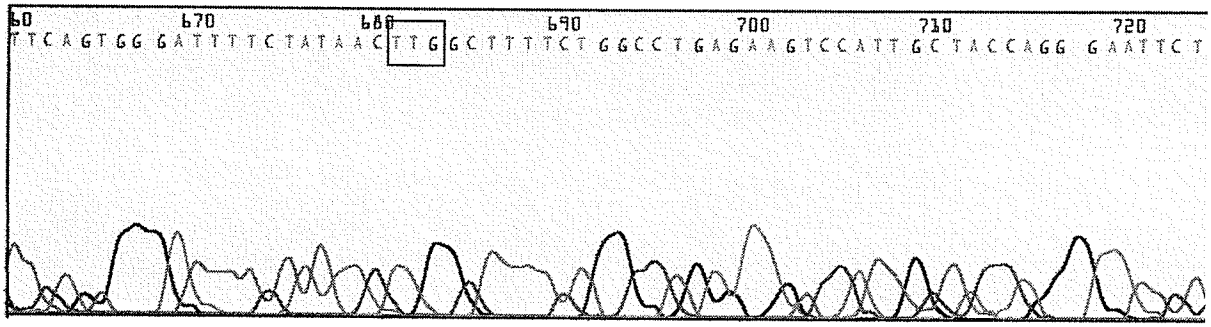

The boxed codon sequence in the diagram indicates the R387Q substitution from the complementary strand in the reverse direction.

The remainder of the automated sequencing sequence did not contain any unwanted substitutions.

6.1.2. Mutation analysis of pGAD424::hGrb14$_F$ R387Q R466Q using the GAL4AD reverse primer.

The R387Q substitution for the pGAD424::hGrb14$_F$ R387Q R466Q plasmid is the same as above. The R466Q substitution of the nucleotide sequence is as follows:

CGG → C**AG**
GCC → G**T**C
Wild type → Substitution

Electropherogram data not shown. The remainder of the automated sequencing sequence did not contain any unwanted substitutions.

6.2. Peptide mass analysis

Table 7. Peptide molecular weight* and pI values for the GAL4AD::hGrb14$_F$ fusion proteins

Protein sequences	pI	Molecular Weight (Da)	Molecular Weight (kDa)
GAL4AD + hGrb14 + FLAG	6.46	77892.80	78
GAL4AD + BPS Dropout + FLAG	6.32	69205.07	69
GAL4AD + BPS+SH2 + FLAG	5.76	38781.24	39
GAL4AD + SH2 + FLAG	5.20	28282.45	28
GAL4AD	4.42	15212.64	15
FLAG	3.97	1388.32	1.4

* Molecular weight values were generated using the Peptide Mass Tool from the Expasy web site. All mass values are average mass, not monoisotopic mass.

6.3. Media

6.3.1. Bacterial media

6.3.1.1. Luria Bertani (LB) medium

Difco bacto-tryptone 10 g/L
Difco bacto-yeast extract 5 g/L
NaCl 10 g/L
* Difco-bacto agar 16.7 g/L
Dissolve reagents in 800 mL deionized H_2O, adjust the pH to 7.0 with 5N NaOH, fill to a final volume of 1L, and sterilize by autoclaving.
*Omit agar for liquid medium

6.3.1.2. Low Salt LB medium

Difco bacto-tryptone 10 g/L
Difco bacto-yeast extract 5 g/L
NaCl 5 g/L
* Difco-bacto agar 16.7 g/L
Dissolve reagents in 800 mL deionized H_2O, adjust the pH to 7.0 with 5N NaOH, add water to a final volume of 1L, and sterilize by autoclaving.
*Omit agar for liquid medium.

6.3.1.3. SOC medium

Difco Bacto-tryptone 20 g/L
Difco Bacto-yeast 5 g/L
NaCl 0.5 g/L
Mix the above reagents in 1L of deionized H_2O, autoclave, allow to cool to 60°C, add 20 mM glucose, and sterilize by filtration through a 0.22-micron filter.

6.3.2. Yeast media

6.3.2.1. YPAD media

Difco bacto-peptone 20 g/L
Difco yeast extract 10 g/L
Glucose 20 g/L
Adenine hemisulphate 0.1 g/L
*Difco-bacto agar 16.7 g/L
Dissolve reagents in 800 mL deionized H_2O, adjust the pH to 6.0 with 5N NaOH, add water to a final volume of 1L, and sterilize by autoclaving.
*Omit agar for liquid medium

6.3.2.2. SC media

Difco yeast nitrogen base (minus aa) 6.68 g/L
Glucose 20 g/L
SC –TRP or SC-LEU or SC-HIS mix 0.668 g/L
*Difco-bacto agar 16.7 g/L
Dissolve reagents in 800 mL deionized H_2O, adjust the pH to 5.6 with 5N NaOH, add water to a final volume of 1L, and sterilize by autoclaving. If using solid medium, pour plates and allow drying 1-3 days in the dark, as this medium is light sensitive.
*Omit agar for liquid medium

6.3.3. Mammalian cell culture media

Ham's F12 medium was used for the culture and maintenance of the CHO-IR, and CHO-IR transfected cell lines. A prepared powder mixture was purchased from Invitrogen- and prepared according to manufacturer's specifications. The medium was sterilized by filtration through a 0.22-micron filter and stored at 4°C. Fetal-calf serum was added to a final concentration of 10% (v/v). Various antibiotics were used for selection.

6.3.3.1. Ham's F12 media

Amino Acids (mg/liter): l-Alanine 8.9, l-Arginine 211(HCl), l-Asparagine 13.2, l-Aspartic acid 13.3, l-Cysteine, l-Glutamic acid 14.7, l-Glutamine 146, Glycine 7.5, l-Histidine 19(HCl), l-Isoleucine 3.9, l-Leucine 13.1, l-Lysine 36.5(HCl), l-Methione 4.5, l-Phenylalanine 5, l-Proline 34.5, l-Serine 10.5, l-Threonine 11.9, l-Tryptophan 2, l-Tyrosine 5.4, l-Valine 11.7

Vitamins (mg/liter): Biotin (H) 0.0073, Choline 14(Cl), Cyanocobalamin(B12) 1.36, Folic acid(M) 1.32, Inositol 18, Nicotinamide 0.037, Pantothenic acid 0.477(Ca), Pyrodoxine(B6) 0.062(HCl), Riboflavin(B2,G) 0.038, Thiamine(B1) 0.337(HCl)

Salts (mg/liter): $CaCl_2$ 44($2H_2O$),$CuSO_4.5H_2O$ 0.0025, $FeSO_4.7H_2O$ 0.834, KCL 224, $MgCl_2$ 122(6H2O), NaCl 7597, $NaHCO_3$ 1176, Na_2HPO_4 268($7H_2O$), $ZnSO_4.7H_2O$ 0.863

Miscellaneous (mg/liter): Glucose 1800, Hypoxanthine 4.08, Linoleic acid, 0.084, Lipoic acid, 0.206, Phenolsulfophthalein 1.17, Putrecine dihydrochloride 0.161, Sodium pyruvate 110, Thymidine 0.726

6.4. Buffers

6.4.1. Cell lysis buffer

1% Triton X-100
25 mM Tris-HCl pH 7.5
150 mM NaCl
10 mM EDTA
1x protease inhibitor cocktail (Sigma)

6.4.2. Immunoprecipitation lysis buffer

1% Triton X-100
25 mM Tris-HCl pH 6.8
150 mM NaCl

6.4.3. PBS buffer

4.3 mM $Na_2HPO_4 \cdot 7H_2O$
1.47 mM KH_2PO_4
137 mM NaCl
2.7 mM KCl, pH 7.5

6.4.4. 4x SDS loading buffer

4% SDS
250 mM Tris, pH 6.8
0.1% Bromophenol blue
40% glycerol
2.8 M β-mercaptoethanol (or 20% v/v)

6.4.5. STE buffer

50 mM Tris-HCl, pH 8.0
10 mM EDTA
100 mM NaCl
0.1 % SDS

6.4.6. Tissue lysis buffer

250 mM sucrose
25 mM Tris-HCl, pH 6.8
1 mM EDTA
1x protease and phosphatase inhibitor cocktail (Sigma-Aldrich)

6.4.7. TAE buffer

40 mM Tris-acetate (pH 7.6)
1 mM Na_2EDTA

6.4.8. TBE buffer

89 mM Tris-borate (pH 8.3)
2 mM Na_2EDTA

6.4.9. TBS-T buffer
10 mM Tris-HCl, pH 7.4
150 mM NaCl
0.1% Tween 20

6.4.10. TCA buffer
20 mM Tris-HCl, pH 8.0
50 mM ammonium acetate
2 mM EDTA
1x protease inhibitor cocktail

6.4.11. TCA Laemmli loading buffer
20% β-mercaptoethanol (v/v)
80 mM Tris
8 mM EDTA
3.5% SDS
14% glycerol
40 mM Tris
1x protease inhibitor cocktail

6.4.12. Z buffer
$NaH_2PO_4 \cdot H_2O$ 13.79 g/L
KCl 0.75 g/L
$MgSO_4 \cdot 7H_20$ 0.246 g/L
Dissolve reagents in 800 mL deionized H_2O, adjust the pH to 7.0 with 5N NaOH, and add water to a final volume of 1L.

6.4.13. Z buffer/β-ME/X-gal
27 µL of β-mercaptoethanol
0.167 mL of 20mg/mL X-gal aqueous solution
10 µL Z-buffer

6.5. Sequencing gel
105 g Urea
37.5 mL (38% Acrylamide: 2% Bisacrylamide)
50 mL 10x TBE buffer
162.5 mL ddH_20
Dissolve by immersing solution in a 60°C water bath and mix by stirring. Solution is light sensitive.

6.6 Southern blotting analysis solutions

6.6.1. Denaturation solution
1.5 M NaCl
0.5 M NaOH

6.6.2. Neutralization solution
1 M Tris pH 7.4
1.5 M NaCl

6.6.3. 20 x Standard Saline Citrate (SSC)
3 M NaCl
0.3 M sodium citrate, pH 7.0

6.6.4. Hybridization buffer
6 x SSC
5 x Denhardt's Reagent
0.5% SDS
100 µg/mL single-stranded salmon sperm DNA (denatured by heating to 100°C for 5 min)

6.6.5. Wash #1
2 x SSC
0.5% SDS

6.6.6. Wash #2
2 x SSC
0.1% SDS

6.6.7. Wash #3
0.1 x SSC
0.5% SDS

REFERENCES

1. Kahn,B., Type 2 diabetes: when insulin secretion fails to compensate for insulin resistance., Cell, 92 (1998) 593-596.

2. Schell,U., Grun,M., and Hilgenfeld,R., Binding of Insulin to Its Receptor: Towards an Understanding in Three Dimensions, Chembiochem, 1 (2002) 37-40.

3. Taylor,S.I., Deconstructing Type 2 diabetes., Cell, 97 (1999) 9-12.

4. Steiner,D. and Oyer,P., The biosynthesis of insulin and a probable precursor of insulin by a human islet cell adenoma., Proc Nat Acad Sci, 57 (1967) 473-480.

5. Olefsky,J.M., The insulin receptor, Diabetes, 39 (1990) 1009-1016.

6. Shoelson,S., White,M., and Kahn,C., Tryptic activation of the insulin receptor. Proteolytic truncation of the alpha-subunit releases the beta-subunit from inhibitory control., J Biol Chem, 263 (1988) 4852-4860.

7. Sokol,L. and Prchal,J., Human genome--chromosome no. 19., Cas Lek Cesk, 134 (1995) 625-629.

8. White,M.F. and Kahn,C.R., The insulin signalling system, J. Biol. Chem., 269 (1994) 1-4.

9. Rhodes,C. and White,M., Molecular insights into insulin action and secretion, European Journal of Clinical Investigation, 32 (2002) 3-13.

10. Sheperd,P., Withers,D., and Siddle,K., Phosphoinositide 3-kinase: the key switch mechanism in insulin signalling, Biochem Journal, 333 (1998) 471-490.

11. Skolnik,E.Y., Batzer,A., Li,N., Lee,C.H., Lowenstein,E., Mohammadi,M., Margolis,B., and Schlessinger,J., The function of GRB2 in linking the insulin receptor to ras signaling pathways, Science, 260 (1993) 1953-1955.

12. Sasaoka,T., Braznin,B., Leitner,J.W., Langlois,W.J., and Olefsky,J.M., Shc is the predominant signaling molecule coupling insulin receptors to activation of guanine nucleotide releasing factor and p21ras-GTP formation, J. Biol. Chem., 269 (1994) 10734-10738.

13. Cantley,L., The phosphoinositide 3-kinase pathway, Science, 296 (2002) 1655-1657.

14. Hiles,I.D., Otsu,M., Volinia,S., Fry,M.J., Gout,I., Dhand,R., Panayotou,G., Ruiz-Larrea,F., Thompson,A., Totty,N.F., Hsuan,J.J., Courtneidge,S.A., Parker,P.J., and Waterfield,M.D., Phosphatidylinositol 3-kinase: structure and expression of the 110 kDa catalytic subunit., Cell, 70 (1992) 419-429.

15. Myers,M.G., Sun,X.J., and White,M.F., The IRS-1 signaling system, TIBS, 19 (1994) 289-293.

16. Dominici,F. and Turyn,D., Growth Hormone-Induced Alterations in the Insulin-Signaling System, Experimental Biological Medicine, 227 (2002) 149-157.

17. Tamemoto,H., Kadowaki,T., Tobe,K., Yagi,T., Sakura,H., Hayakawa,T., Terauchi,Y., Ueki,K., Kaburagi,Y., Satoh,S., Sekihara,H., Yoskioka,S., Horikoshi,H., Furuta,Y., Ikawa,Y., Kasuga,M., Tazaki,Y., and Aizawa,S., Insulin resistance and growth retardation in mice lacking insulin receptor substrate-1, Nature, 372 (1994) 182-186.

18. Withers,D.J., Gutierrez,J.S., Towery,H., Burks,D.J., Ren,J.-M., Previs,S., Zhang,Y., Bernal,D., Pons,S., Shulman,G.I., Bonner-Weir,S., and White,M.F., Disruption of IRS-2 causes type 2 diabetes in mice., Nature, 391 (1998) 900-904.

19. Liu,S., Wang,Q., Lienhard,G., and Keller,S., Insulin receptor substrate 3 is not essential for growth or glucose homeostasis, J Biol Chem, 274 (1999) 18093-18099.

20. Numan,S. and Russell,D., Discrete expression of insulin receptor substrate-4 mRNA in adult rat brain, Brain Res Mol Brain Res, 72 (1999) 97-102.

21. Riedel,H., Yousaf,N., Zhao,Y., Dai,H., Deng,Y., and Wang,J., PSM, a mediator of PDGF-BB-, IGF-1-, and insulin-stimulated mitogenesis, Oncogene, 19 (2000) 39-50.

22. Kotani,K., Wilden,P.A., and Pillay,T.S., SH2-Balpha is an insulin-receptor adapter protein and substrate that interacts with the activation loop of the insulin-receptor kinase., Biochem J, 335 (1998) 103-109.

23. Ahmed,S., Smith,B., Kotani,K., Wilden,P., and Pillay,T., APS, an adapter protein with a PH and SH2 domain is a substrate for the insulin receptor kinase, Biochemistry Journal, 341 (1999) 665-668.

24. Yokouchi,M., Wakioka,T., ,S.H., Yasukawa,H., Ohtsuka,S., Sasaki,A., Ohtsubo,M., Valius,M., Inoue,A., Komiya,S., and Yoshimura,A., APS, an adaptor protein containing PH and SH2 domains, is associated with the PDGF receptor and c-Cbl and inhibits PDGF-induced mitogenesis., Oncogene, 18 (1999) 759-767.

25. Skolnik,E., Margolis,B., Mohammadi,M., Lowenstein,E., Fischer,R., Drepps,A., Ullrich,A., and Schlessinger,J., Cloning of PI3 kinase-associated p85 utilizing a novel method for expression/cloning of target proteins for receptor tyrosine kinases., Cell, 65 (1991) 83-90.

26. Margolis,B., Silvenninen,O., Comoglio,F., Roonprapunt,C., Skolnik,E., Ullrich,A., and Schlessinger,J., High-efficiency expression/cloning of epidermal

growth factor-receptor-binding proteins with Src homology 2 domains, Proc. Natl. Acad. Sci. USA, 89 (1992) 8894-8898.

27. Ooi,J., Yajnik,V., Immanuel,D., Gordon,M., Moskow,J.J., Buchberg,A.M., and Margolis,B., The cloning of Grb10 reveals a new family of SH2 domain proteins, Oncogene, 10 (1995) 1621-1630.

28. Daly,R.J., Sanderson,G.M., Janes,P.W., and Sutherland,R.L., Cloning and characterization of GRB14, a novel member of the GRB7 Gene Family, J. Biol. Chem., 271 (1996) 12502-12510.

29. Daly,R.J., The Grb7 family of signalling proteins., Cell. Signal., 10 (1998) 613-618.

30. Wojcik,J., Girault,J.-A., Labesse,G., Chomilier,J., Mornon,J.-P., and Callebaut,I., Sequence analysis identifies a Ras-associating (RA)-like domain in the N-termini of band 4.1/JEF domains and in the Grb7/10/14 adapter family., Biochem. Biophys. Res. Commun., 259 (1999) 113-120.

31. Songyang,Z., Shoelson,S., Chaudhuri,M., Gish,G.D., Pawson,T., Haser,W.G., King,F., Roberts,T., Ratnofsky,S., Lechleider,R.J., Neel,B.G., Birge,R.B., Fajardo,J.E., Chow,M.M., Hanafusa,T., Schaffhausen,B., and Cantley,L. ΣH2 domains recognize specific phosphopeptide sequences. Cell 72, 767-778. 1993. Ref Type: Generic

32. Stein,D., Wu,J., Fuqua,S.A., Roonprapunt,C., Yajnik,V., D'Eustachio,P., Moskow,J.J., Bucherg,A.M., Osborne,C.K., and Margolis,B., The SH2 domain protein GRB-7 is coamplified, overexpressed and in a tight complex with HER2 in breast cancer, EMBO J., 13 (1994) 1331-1340.

33. Margolis,B., The Grb family of SH2 domain proteins, Prog. Biophys Molec Biol, 62 (1994) 223-244.

34. Pandey,A., Liu,X., Dixon,J.E., Di Fiore,P.P., and Dixit,V.M., Direct association between the ret receptor tyrosine kinase and the src homology 2-containing adapter protein Grb7, J. Biol. Chem., 271 (1996) 10607-10610.

35. Fiddes,R.J., Campbell,D.H., Janes,P.W., Sivertsen,S.P., Sasaki,H., Wallasch,C., and Daly,R.J., Analysis of Grb7 recruitment by heregulin-activated erbB receptors reveals a novel target selectivity for erbB3., J. Biol. Chem., 273 (1998) 7717-7724.

36. Kasus-Jacobi,A., Berezait,V., Perdereau,D., Girard,J., and Burnol,A.-F., Evidence for an interaction between the insulin receptor and Grb7. A role for two of its binding domains, PIR and SH2., Oncogene, 19 (2000) 2052-2059.

37. Keegan,K. and Cooper,J.A., Use of the two hybrid system to detect the association of the protein-tyrosine-phosphatase, SHPTP2, with another SH2-containing protein, Grb7, Oncogene, 12 (1996) 1537-1544.

38. Han,D., Shen,T., and Guan,J., The Grb7 family proteins: structure, interactions with other signaling molecules and potential cellular functions., Oncogene, 20 (2001) 6315-6321.

39. Tanaka,S., Mori,M., Akiyoshi,T., Tanaka,Y., Mafune,K., Wands,J.R., and Sugimachi,K., A novel variant of human Grb7 is associated with invasive esophageal carcinoma., J. Clin. Invest., 102 (1998) 821-827.

40. Jerome,C.A., Scherer,S.W., Tsui,L.C., Gietz,R.D., and Triggs-Raine,B.L., Assignment of growth factor receptor-bound protein 10 (GRB10) to human chromosome 7p11.2-p12, Genomics, (1997).

41. Dong,L.Q., Du,H., Porter,S.G., Kolakowski,L.F., Lee,A.V., Mandarino,J., Fan,J., Yee,D., and Liu,F., Cloning, chromosome localization, expression, and characterization of an Src homology 2 and pleckstrin homology domain-containing insulin receptor binding protein hGrb10γ, J. Biol. Chem., 272 (1997) 29104-29112.

42. Pandey,A., Duan,H., Paolo,D.F., and Dixit,V.M., The ret receptor protein tyrosine kinase associates with the SH2-containing adapter protein Grb10, J. Biol. Chem., 270 (1995) 21461-21463.

43. He,W., Rose,D.W., Olefsky,J., and Gustafson,T.A., Grb10 interacts differentially with the insulin receptor, insulin-like growth factor I receptor, and epidermal growth factor receptor via the Grb10 Src homology 2 (SH2) domain and a second novel domain located between the Pleckstrin homology and SH2 domains., J. Biol. Chem, 273 (1998) 6860-6867.

44. Liu,F. and Roth,R.A., Grb-IR: An SH2-domain-containing protein that binds to the insulin receptor and inhibits its function, Proc. Natl. Acad. Sci. USA, 92 (1995) 10287-10291.

45. O'Neill,T.J., Rose,D.W., Pillay,T.S., Hotta,K., Olefsky,J.M., and Gustafson,T.A., Interaction of a Grb-IR splice variant (a human Grb10 homolog) with the insulin and insulin-like growth factor I receptors, J. Biol. Chem., 271 (1996) 22506-22513.

46. Morrione,S., Valentinis,B., Li,S., Ooui,J., Margolis,B., and Baserga,R., Grb10: a new substrate of the insulin-like growth factor I receptor, Cancer Res., 56 (1996) 3165-3167.

47. Dong,L.Q., Porter,S., Hu,D., and Liu,F., Inhibition of hGrb10 binding to the insulin receptor by functional domain-mediated oligomerization., J. Biol. Chem, 273 (1998) 17720-17725.

48. Nantel,A., Mohammad-Ali,K., Sherk,J., Posner,B.I., and Thomas,D.Y., Interaction of the Grb10 adapter protein with the Raf1 and MEK1 kinases., J. Biol. Chem, 273 (1998) 10475-10484.

49. Morrione,A., Plant,P., Valentinis,B., Staub,O., Kumar,S., Rotin,D., and Baserga,R., mGrb10 interacts with Nedd4, J Biol. Chem., 274 (1999) 24094-24099.

50. Mano,H., Ohya,K., Miyazato,A., Yamashita,Y., Ogawa,W., Inazawa,J., Ikeda,U., Shimada,K., Hatake,K., Kasuga,M., Ozawa,K., and Kajigaya,S., Grb10/Grb-IR as an in vivo substrate of Tec tyrosine kinase, Genes to Cells, 3 (1998) 431-441.

51. Bai,R.Y.J.T., Schrem,S., Munzert,G., Weidner,K.M., Wang,J.Y.J., and Duyster,J., The SH2-containing adapter protein GRB10 interacts with BCR-ABL, Oncogene, 17 (1998) 941-948.

52. Wang J, Dai,H., Yousaf,N., Moussaif,M., Deng,Y., Boufelliga,A., Swamy,O.R., Leone,M.E., and Riedel,H., Grb10, a positive, stimulatory signaling adapter in platelet-derived growth factor BB-, insulin-like growth factor I- and Insulin-mediated mitogenesis., Mol Cell Biol, 19 (1999) 6217-6228.

53. Langlais P., Dong,L.Q., Hu,D., and Liu,F., Identification of Grb10 as a direct substrate for members of the Src tyrosine kinase family., Oncogene, 19 (2000) 2895-2903.

54. Stein,E.G., Gustafson,T.A., and Hubbard,S.R., The BPS domain of Grb10 inhibits the catalytic activity of the insulin and IGF1 receptors, FEBS Lett., 493 (2001) 106-111.

55. Baker,E., Sutherland,G.R., Sutherland,R.L., and Daly,R.J., Assignment of the human GRB14 gene to chromosome 2q22-q24 by fluorescence in situ hybridization, Genomics, 36 (1996) 218-220.

56. Kasus-Jacobi,A., Perdereau,D., Auzan,C., Clauser,E., Van Obberghen,E., Mauvais-Jarvis,F., Girard,J., and Burnol,A.-F., Identification of the rat adapter Grb14 as an inhibitor of insulin actions., J. Biol. Chem, 273 (1998) 26026-26035.

57. Wyant,K. Grb14: A Novel Signalling Protein that Interacts with the Insulin Receptor and the Insulin-like Growth Factor-1 Receptor. Dissertation at the University of Manitoba (unpublished), 154-160. 1999.
Ref Type: Thesis/Dissertation

58. Reilly,J., Mickey G, and Maher,P., Association of fibroblast growth factor receptor 1 with the adaptor protein Grb14, J Biol. Chem., 275 (2000) 7771-7778.

59. Jones,N., Master,Z., Jones,J., Bouchard,D., Gunji,Y., Sasaki,H., Daly,R., Alitalo ,K., and Dumont,D.J., Identification of Tek/Tie2 binding partners, J Biol. Chem., 274 (1999) 30896-30905.

60. Lyons,R., Deane,R., Lynch,D., Ye,Z.-S., Sanderson,G., Eyre,H., Sutherland,G., and Daly,R., Identification of a novel human Tankyrase through its interaction with the adapter protein Grb14, J Biol Chem, 276 (2001) 17172-17180.

61. Hemming,R., Agatep,R., Badiani,K., Wyant,K., Arthur,G., Gietz,R.D., and Triggs-Raine,B., Human growth factor receptor bound 14 binds the activated insulin receptor and alters the insulin-stimulated tyrosine phosphorylation levels of multiple proteins., Biochem. Cell Biol., 79 (2001) 21-32.

62. Bereziat,V., Kasus-Jacobi,A., Perdereau,D., Cariou,B., Girard,J., and Burnol A-F, Inhibition of insulin receptor catalytic activity by the molecular adapter Grb14, J Biol Chem, 277 (2002) 4845-4852.

63. Sherman,F., Getting started with yeast. In: Guthrie,C., Fink,G.R. (Eds.), Meth Enzym, Acad Press, NY, 1991, pp. 3-21.

64. Woods RA and Gietz RD. High-efficiency transformation of plasmid DNA into yeast. Meth Mol Biol 177, 85-97. 2001.

65. Gary S Coombs and David R.Corey, Site Directed PCR Mutagenesis and Protein Engineering. In: Proteins: Analysis and Design, Academic Press, 1998, pp. 268-271.

66. Higgins,D., Thompson,J., Gibson,T., Thompson,J., Higgins,D., and Gibson T.J., CLUSTAL W: improving the sensitivity of progressive multiple sequence alignment through sequence weighting, position-specific gap penalties and weight matrix choice., Nucl. Acids. Res., 22 (1994) 4673-4680.

67. Gietz,R.D., Schiestl,R.H., Willems,A.R., and Woods,R.A., Studies on the transformation of intact yeast cells by the LiAc/SS-DNA/PEG procedure, Yeast, 11 (1995) 355-360.

68. Miller,J.F., Assay of ß-galactosidase. In: Experiments in Molecular Genetics, Cold Spring Harbor Laboratory, Cold Spring Harbor, New York, 1972, pp. 352-355.

69. Sambrook,J., Fritsch,E.F., and Maniatis,T., Molecular Cloning : a Laboratory Manual, (1989), Cold Spring Harbour Laboratory Press, 2nd edition, 9.31

70. Rigby,P., Dieckmann,M., Rhodes,C., and Berg,P., Labeling deoxyribonucleic acid to high specific activity in vitro by nick translation with DNA polymerase I, J. Mol. Biol., 113 (1977) 237-251.

71. Zhang,B., Tavare,J.M., Ellis,L., and Roth,R.A., The regulatory role of known tyrosine autophosphorylation sites of the insulin receptor kinase domain. An assessment by replacement with neutral and negatively charged amino acids, J. Biol. Chem., 266 (1991) 990-996.

72. Pawson,T., Protein modules and signalling networks, Nature, 373 (1995) 573-580.

73. Pronk,G.J., McGlade,J., Pelicci,G., Pawson,T., and Bos,J.L., Insulin-induced phosphorylation of the 46 and 52-kDa Shc proteins, J. Biol. Chem., 268 (1993) 5748-5753.

74. White,M.F., The insulin signalling system and the IRS proteins, Diabetologia, 40 (1997) S2-S17.

75. Hosomi,Y., Shii,K., Ogawa,W., Matsuba,H., Yoshida,M., Okada,Y., Yokono,K., Kasuga,M., Baba,S., and Roth,R., Characterization of a 60-kilodalton substrate of the insulin receptor kinase., J Biol Chem, 269 (1994) 11498-11502.